N° Ordre...../FSI/UMBB/2017

REPUBLIQUE ALGERIENNE DEMOCRATIQUE ET POPULAIRE

MINISTERE DE L'ENSEIGNEMENT SUPERIEUR ET DE LA RECHERCHE SCIENTIFIQUE

UNIVERSITE M'HAMED BOUGARA-BOUMERDES

Faculté des **S**cience de l'**I**ngénieur

Thèse de Doctorat

Présentée par :

YAMANI Noureddine

En vue de l'obtention du diplôme de **DOCTORAT** en **:**

Filière :Génie Mécanique

Option : Modélisation et Simulation en Mécanique

Comparative study of receiver performance in solar power tower

Devant le jury composé de :

BOUALI Elahmoune	Professeur	UMBB	Président
AKNOUCHE Hamid	MC/A	UMBB	Examinateur
BOUDRIES Rafika	Maitre de recherche A	CDER	Examinatrice
KHELLAF Abdellah	Directeur de recherche	CDER	Directeur de thèse
MOHAMMEDI Kamal	Professeur	UMBB	Co-directeur de thèse

Année Universitaire 2016/2017

Acknowledgements

I express my most sincere gratitude to my advisors, Prof. Abdellah Khellaf and Prof. Kamal Mohammedi for their guidance, encouragement and understanding throughout this work.

Special thanks to Dr. Omar Behar who with their advice and kindness were great help for me.

I would like to thank the University of Boumerdes (UMBB) for the academic support.

I would like to give special thanks to my mother, my father, my sister and my brothers for giving me strength in moments of weakness, without their help this thesis would not have been written.

Table of Contents

List of tables iv

List of Figures vii

List of symbols viii

Abstract x

Introduction: A review of studies on central receiver solar thermal power plants 1

CHAPTER I: Overview of solar thermal technologies

1. Introduction 9
2. Historic and Current status 11
3. Concentrating Solar Power (CSP) 14
3.1. Parabolic trough 14
3.2. Central Receiver Systems (Solar Power Tower) 16
3.3. Linear Fresnel 17
3.4. Parabolic dish systems 19
4. A comparison of different technologies 19
5. Cost Versus Value 23
6. Conclusion 24

References 25

CHAPTER II: Background of the Central receiver system

1. Introduction 27
2. Current status 28
3. Main components of solar power tower 32
3.1. Heliostats 33
3.1.1. Heliostat Field Performance Background 34
3.1.2. Field Layout Configuration 34
a. Radial Configuration 34
b. Straight field Configuration 35
3.1.3. Losses from the Heliostat Field 36
a. Cosine effects 37
b. Shading efficiency 38
c. Reflectivity 39
d. Blocking effects 39
e. Attenuation 40

f. Spillage efficiency 41
3.2. Solar receiver 42
3.2.1. Volumetric Receivers 44
3.2.2. Tubular Receiver 45
3.1.power cycle 47
3.2.3. Rankine Cycle review 47
3.2.4. Brayton Cycle review 49
3.2.5. Combined Cycle review 50
3.3. Heat Transfer Fluid 50
3.3.1. Air 51
3.3.2. Water/Steam 51
3.3.3. Molten salt 51
4. Conclusion 52
Reference 53
CHAPTER III: Solar thermal power in Algeria
1. Introduction 58
2. Algeria Energy Status 59
3. Renewable energies potentials 61
4. Solar energy characterization 62
4.1. Temperature 64
4.2. Sunshine duration 65
4.3. Global irradiation 67
4.4. Direct Normal Irradiation 68
5. Conclusion 72
Reference 72
CHAPTER IV: Assessment of solar thermal tower technology under Algerian climate
1. Introduction 74
2. What is TRNSYS? 74
3. Simulation and Parameters of the Installation 75
3.1. System configuration 76
3.1.1. Solar field 76
3.1.2. Solar receiver 79
a. Open air volumetric receiver 79

b. water/steam Tubular receiver 80
3.1.3. The power block 81
3.1.3.1.Brayton cycle 81
a. Description 81
b. Main modules used 84
3.1.3.2.Rankine cycle 86
a. Description 86
b. Main modules used 89
3.2. Results and discussion 90
3.2.1. Solar field 91
3.2.2. First configuration: Brayton cycle with volumetric air receiver 93
a. Receiver 93
b. Combustion chamber fuel 95
3.2.3. Second configuration : Rankine cycle with water/steam receiver 97
a. Receiver 97
b. Heat recovery steam generator performance 99
c. Turbine 101
4. Economic assessment 105
4.1. The Total Capital Requirement 106
4.2. Operation and Maintenance Cost 107
4.3. Fuel price 107
4.4. Capital charge factor 107
4.5. Results 108
4. Conclusion 110
Reference 111
Conclusion 113

List of Figures

Fig.1.1. Basic concept of the four CSP families: (a) parabolic trough collector (b) linear Fresnel collector (c) central receiver system with dish collector (d) central receiver system with distributed reflectors 10

Fig.1.2. Flow diagram for a typical CSP 11

Fig.1.3. CSP Projects Around the 14

Fig.1.4. Parabolic-trough collector field coupled to a steam cycle 15

Fig1.5. Basic concept of solar power tower 17

Fig.2.1. The three main subsystems of central receiver solar thermal power plant 28

Fig.2.2. Examples of Solar Power Tower Projects 31

Fig.2.3. Worldwide solar tower thermal power plants [google Mape] 32

Fig.2.4. Representation of optimized fields for latitude of 360° with surround field 35

Fig.2.5. Representation of optimized fields for north field configurations. 35

Fig.2.6. Heliostat field Straight Configuration 36

Fig.2.7. Optical losses in a power tower plant 37

Fig.2.8. Nomenclature of optical efficiency in heliostat fields 37

Fig.2.9. The cosine effect as seen on two heliostats A and B; A is placed in the North and B in the South 38

Fig.2.10. 'No-blocking' effect between two heliostats 40

Fig.2.11. Slant distance between the heliostat and the 41

Fig.2.12. Spillage efficiency 42

Fig.2.13. Principle of volumetric receivers 45

Fig.2.14. External cylindrical tubular receiver 47

Fig.3.1. Evolution of energy generation in Algeria 62

Fig.3.2. Economic potential of most active countries in CSP in MENA 63

Fig.3.3. Algeria map showing the different locations 64

Fig.3.4. Temperature variation in the various site 65

Fig.3.5. Average monthly of the daily sunshine duration: a) Hassi R'Mel b) Algiers c) Adrar d) Tamanrasset 67

Fig.3.6. Daily global radiation a) Hassi R'Mel b) Tamanrasset c) Algiers 68

Fig.3.7. Evolution of Monthly DNI (KWh/m²) over the year for selected sites in Algeria 69

Fig.3.8. Yearly DNI compared in the in different locations 70

Fig.3.9.Direct normal irradiation at the 4th sites during the 2st June 70

Fig.3.10. Direct normal irradiation at the 4th sites during January 29 71
Fig.4.1. Heliostat field coordinate in relation to the sun and the receiver position 77
Fig.4.2.Design of solar power tower with Brayton configuration 82
Fig.4.3.TRNSYS model for simulation of solar power tower Brayton based configuration case 83
Fig.4.4. Design of solar power tower with a Rankine configuration 86
Fig.4.5.TRNSYS model for simulation of solar power tower Steam Rankine case 87
Fig.4.6. Zenith angle a) case of January 29; b) case of June 2 91
Fig.4.7. Azimuth angle a) case of January 29; b) case of June 2 91
Fig.4.8. The incident power flux a) case of January 29; b) case of June 2 92
Fig.4.9. Daily incident power flux 93
Fig.4.10. Variation of Receiver temperature a) case of January 29; b) case of June 2 94
Fig.4.11. Receiver thermal efficiency a) case of January 29; b) case of June 2 94
Fig.4.12. Hourly fuel needs for the combustion chamber a) case of January 29; b) case of June2 96
Fig.4.13. Daily fuel needs for the combustion chamber a) case of January 29; b) case of June2 97
Fig.4.14. Variation of the flow rate in Receiver a) case of January 29; b) case of June 2 98
Fig.4.15. Variation of temperature in the super heater a) case of January 29; b) case of June 2 99
Fig.4.16. Variation of temperature in the evaporator a) case of January 29; b) case of June 2 100
Fig.4.17. Variation of temperature in the economizer a) case of January 29; b) case of June 2 100
Fig.4.18.Variation of the turbine inlet enthalpy a) case of January 29; b) case of June 2 101
Fig.4.19.Variation of the turbine outlet enthalpy a) case of January 29; b) case of June 2 101
Fig.4.20.Variation of , the difference between enthalpy $h_{out} - h_{in}$ a) case of January 29; b) case of June 2 102
Fig.4.21. Variation of turbine power a) case of January 29; b) case of June 2 103
Fig.4.22.Steam turbine Efficiency a) case of January 29; b) case of June 2 103
Fig.4.23.TRNSYS model for simulation of solar power tower Steam Rankine case with thermal storage 104
Fig.4.24. Variation of turbine power a) case of January 29; b) case of June 2 105

Fig.4.25. The deferent value of the LCOE 110

List of tables

Table.1.1 Comparison of the four CSP families 20

Table.1.2. Pros and cons of different CSP technology 22

Table.2.1 Operational Solar Power Tower Projects 30

Table.2.2. advantage & disadvantage of deferent heat transfer fluid 52

Table.3.1. Monthly Sunshine duration in different locations (hour) 65

Table.4.1 Heliostats field input parameters 78

Tabale.4.2 Reported Receiver characteristics of Power Plant Jülich (DLR) 80

Table.4.3 Reported water/steam Receiver characteristics 81

Table4.4 Input parameters value of SPT with air receiver 84

Table.4.5 Input parameters value of SPT with water/steam receiver 87

Table.4.6. Available Gross Costs of power Rankine generation 106

Table4.7. Available Gross Costs of power Brayton generation 106

Table.4.8. Main features economic parameters 108

Nomenclature

A_f	Reflective field Area
A_r	Receiver area
c_{fuel}	fuel price
C_P	Specific heat
H	Enthalpy
h_{eq}	Yearly equivalent operating hours
h_{cv}	Coefficient of convection transfer
h^s	Enthalpy isentropic
I	direct normal irradiation
$\dot{m}$	Mass flow
P	pressure
$\dot{Q}$	Power
q_{fuel}	Specific fuel consumption
q_{CO2}	Specific CO2 emission
$SC\text{-}CO_2$	The social cost of carbon
T	Temperature
V	wind speed

Greek letters

ρ_M	Reflectivity of the mirror
σ	Stefan Boltzmann constant (=5.6696.10-8 W/m² K4)
ε	Absorber emissivity
γ	Specific heat ratio
M	Efficiency
Γ	control parameter for describing the fraction of the field in track

Abbreviations

CCF	capital charge factor
CSP	Concentrating solar power
DNI	direct normal irradiation
CRS	Central receiver system
HRSG	heat recovery steam generation

HTF	heat transfer fluid
LCOE	levelized cost of electricity
O&M	operating and maintenance costs
STEC	Solar Thermal Electric Components
TCR	total capital requirement

Subscripts

A	Air
Ac	Air compressor
At	Atmosphiric
Co	Convection
Eco	Economizer
Eva	Evaporator
Ex	External
F	Field
G	Gas
In	Interior
R	Receiver
Ra	Radiation
Sh,blk	Shad,block
Sup	Super heater
T	Turbine

ملخص

من بين جميع تقنيات الطاقة الشمسية المركزة المتاحة لتوليد الطاقة، برج الطاقة الشمسية، المعروف أيضا باسم نظام الاستقبال المركزي،الذي اخذ يجتذب الكثير من الاهتمام يوما بعد يوم. ويرجع ذلك إلى أدائه الجيد مقارنة مع التقنيات الاخرى المستعملة.

في هذا العمل، اجرينا مقارنة لأداء محطتين مركزيتين للطاقة الشمسية الحرارية ، هما دورة "رانكين" مع مستقبل أنبوبي للمياه / البخار ودورة "برايتون" مع جهاز مستقل حجمي للهواء . وقد قمنا بهذه الدراسة في ظل المناخ الجزائري حيث تم اختيار مناطق مختلفة لتقديم تحليل شامل. وقد استخدمت حزمة برامج "ترنسيس-ستيك" لمحاكاة الأداء الحراري في حين يتم تطبيق "ميتونورم" للحصول على بيانات المناخ دقيقة للمناطق المختارة.

وأظهرت النتائج أنه من الناحية الاقتصادية مستقبل الحجمي للهواء بتكنولوجيا دورة برايتون يعتبر الحل الامثل ، الا انه مستقبل المياه / البخار بتكنولوجيا دورة رانكين هو أكثر ملاءمة خاصة عند الاشعاع الشمسي الضعيف. وكذالك تتطلب التوربينات الغازية درجات حرارة تشغيل أعلى يصعب عادة الوصول إليها طوال العام.

مفاتيح : برج الطاقة الشمسية، نظام الاستقبال المركزي للطاقة الشمسية، محطة للطاقة الشمسية الحرارية، ترنسيس

Résumé

Parmi toutes les technologies de concentration solaire disponibles pour la génération d'énergie, la tour solaire ou également appelée système à récepteur central, attire beaucoup d'attention. Ceci est dû à leur meilleure performance par rapport à d'autres familles telles que les centrales cylindro_parabolique et Les centrales solaires à miroir de Fresnel.

Dans le présent travail, on effectue une comparaison de la performance thermique de deux centrales thermiques La premier configuration avec un récepteur tubulaire eau / vapeur en utilisant le cycle de Rankine et la deuxième avec un récepteur d'air volumétrique intégré au cycle de Brayton.

L'étude a été menée sous les donné météorologique algérien selon laquelle diverses régions ont été sélectionnées pour fournir une analyse complète. Le logiciel TRNSYS-STEC a été utilisé pour simuler la performance thermique, tandis que Meteororm est appliqué pour obtenir des données climatiques précises pour les déférentes régions sélectionnées.

Les résultats montrent que la technologie de cycle Rankine de l'eau / vapeur est plus adaptée Bien que économiquement légèrement pas aussi compétitif que le récepteur volumétrique d'air du cycle de Brayton, en particulier sous une intensité de rayonnement solaire plus faible. La turbine à gaz nécessite des températures de fonctionnement plus élevées, généralement difficiles à atteindre tout au long de l'année.

Mots-clés: Tour solaire, système solaire de récepteur central, centrale solaire thermique, TRNSYS, CSP

Abstract

Among all Concentrating Solar Power technologies available for power generation, the solar power tower, also known as central receiver system, is attracting a lot of interest day to day. This is due to their better performance over other options such as parabolic trough and parabolic dish.

In the present work, a thermal performance comparison of two mature central receiver solar thermal power plants namely the Rankine cycle with a tubular water/steam receiver and the Brayton cycle with volumetric air receiver is carried out. The investigation has been carried out under the Algerian climate whereby various regions have been selected to provide a comprehensive analysis. TRNSYS-STEC software package has been used for simulating the thermal performance while Meteororm is applied to get accurate climate data for the selected regions.

The results show that , though economically slightly not as competitive as the volumetric air receiver Brayton cycle technology, the water/steam receiver Rankine cycle technology is more suitable particularly under lower solar radiation intensity. The gas turbine requires higher operating temperatures which are usually difficult to reach throughout the year.

Keywords: Solar power tower, Solar central receiver system, Solar thermal power plant, TRNSYS, CSP

Introduction

A review of studies on central receiver solar thermal power plants

From all Concentrating Solar Power (CSP) technologies available for power generation, the solar power tower is moving to the forefront and it is attracting a lot of interest day to day. A typical solar power tower plant consists of a heliostat field, a solar receiver and a thermodynamic power conversion block. Research and development activities on central receiver solar thermal power plants have shown significant advances in recent years. These activities have been mostly aimed at a detailed analysis and development of the three main parts of the power plant including the heliostat field, the solar receiver and the power block. O. Behar et al [1] have reviewed the most important studies on the three main components of the central receiver solar thermal power plants.

For the heliostat field many published papers have been interested on the design of the heliostat field layout. Indeed, the heliostat field is used to concentrate and focus direct solar radiation into the solar receiver that is located on the top of a tower. This interest stems from the fact that the heliostat field is the most expensive part of the solar power plant. Effort is then carried out to optimize the heliostat filed in an effort to reduce the costs [2,3]

Zhang et al. [4] have optimized the heliostats position of 1 MW solar power plant using the available land efficiency factor. Collado [5] has developed a simple method for heliostat field layout and results have shown good agreement with Solar Tres field. Noone et al [6] have introduced a spiral field layout. When compared with current PS10 field that is arranged in radial staggered layout, the proposed spiral layout has shown higher efficiency with significant reduction in land area. Wei et al. [7] have developed a

new method for positioning the heliostats based on the receiver geometrical aperture. Sanchez and Romero [8] have proposed a new technique in which the heliostats position is calculated based on the yearly solar radiation They have compared the performance of the proposed layout method with those of WinDelsol and SOLVER codes and found that the method is time consuming. Siala and Elayeb [9] have suggested a graphical method for no-blocking radial stagger heliostats layout. For positioning the heliostats, the method is first divide the field into certain groups of heliostats to increase its density. This method is simpler than that proposed by Sanchez and Romero [8]. Danielli et al [10] have examined the micro-tower configuration and found that this concept offer better performance than larger configuration since it enhances the optical efficiency by about 15%.

The solar receiver is a heat exchanger where the solar radiation is concentrated and converted into heat and then transferred, by means of a heat transfer fluid, to the power block. There are various types of solar receivers. Each type has a specific geometrical configuration, absorber materials and heat transfer fluid. Among all the solar receivers that have been developed and successively tested the volumetric receiver and the tubular receiver are up to now the most mature technology.

The volumetric receivers are basically made up of porous materials such as ceramic and metal of high thermal conductivity. Intensive R&D activities have been carried out on the volumetric receiver during the last three decades. As a result several prototypes have been developed and successively tested. The Phoebus-TSA, SOLAIR, DIAPR and REFOS are good examples [11]. Due to their performance, this latter receiver has been installed at large scale in the Jülich power plant [12]. After that, significant studies have been conducted to evaluate and to improve the performance of volumetric receiver. Villafán-Vidales [13] has focused on the heat transfer in volumetric receiver. Fend et al [14] have compared the thermal proprieties of six porous materials that might be used in volumetric solar receivers. In these two studies, it has been found that ceramic is the most suitable material due to their higher porosity and higher thermal performance. Wu [15] has analyzed the distribution of temperature in a ceramic foam receiver. The author has found that suitable temperature distribution is obtained for thin ceramic foam sizes.

Several simulation studies on volumetric receiver have been carried out. Becker et al. [16] have been interested in the fluid flow into porous material. Fend et al. [17] have evaluated the porosity of various materials that are widely used in volumetric receivers. Lenert and Wang [18] have studied the performance of volumetric receiver with nano-fluid as a heat transfer medium. Veeraragavan [19] has evaluated the effect of design parameters on the performance of volumetric receiver with nano-fluid. Wu et al. [20] have focused on the pressure drop in ceramic foam taking into account various configurations of the volumetric receiver The combination of experimental and numerical studies has allowed driving a more accurate pressure drop correlation. Buck et al. [21] have introduced a novel solar receiver that combines a volumetric configuration with a tubular receiver. The simulation results of all these studies have shown that the proposed concept can offer better advantages than the tubular receiver.

Whereas the volumetric receiver employs air as a heat transfer fluid, the tubular receiver is commonly used with water/steam as heat transfer fluid. The tubular receiver is a heat exchanger in which the water is circulated to absorb the concentrated solar radiation. This receiver is the most mature and the widely used in current solar power tower plants. For instance, it has been installed at the PS10 and PS20 power plants in Spain, and also in several central receiver power plants in the US. Research on tubular receiver has been dramatically increased in recent years. Many authors have focused on the modeling and performance prediction. Others have proposed some improvements and some others have conducted experiments for better understanding of the thermal behaviors. Hischier et al. [22] have developed a 2-D model for a tubular receiver that employs air as a heat transfer fluid. They found that the air outlet temperature could reach 1000°C at 10 bars with a thermal efficiency of 78%. Wu et al. [23] have proposed 3-D model to evaluate the effect of geometric configuration on the performance of tubular receiver A new correlation for Nusselt number for the case of natural convection heat losses has been derived. Melchior et al. [24] have experimentally analyzed a small scale tubular receiver that is used to power a chemical reactor. During the tests, a solar-to-chemical efficiency of 28.5% has been achieved. Wu et al. [25] have experimentally investigated the heat transfer mechanism in a molten salt tubular receiver. Yang et al.

[26] have carried out a heat transfer analysis of a molten salt tube receiver and found that the higher the heat flux the higher is the velocity of the heat transfer fluid.

As solar radiation is concentrated on the receiver, it is transformed into heat which is in its turn converted into electricity in the power conversion block. For the central receiver technology two thermodynamic cycles are used, i.e., the Brayton cycle and the Rankine cycle. Indeed, the Brayton cycle is commonly coupled with a volumetric air receiver while the Rankine cycle is combined with a water/steam tubular receiver.

A central receiver system with a Rankine cycle is typically consisted of a large heliostat field, tubular receiver and a steam cycle. Solar energy that is collected in the tubular receiver is used to generate steam that is in its turn used to drive the steam turbine. This concept has been successively tested during the 1980s. Thus, many authors have studies, analyzed and suggested some improvements to bring this concept to become more competitive. Yebra et al. [27] have developed a model for simulating the CESA-I power plant thermal performance while Moon et al. [28] have proposed a new model to simulate the performance of Dahan solar thermal power plant. Zoschak and Wu [29] have analyzed various schemes of central receiver Rankine cycle and found that the use of solar energy for evaporating water is the most efficient. Different softwares have also been used to simulate the feasibility and performance of central receiver power plants. Xu [30] has used STAR-90 software to simulate the performance of Dahan central receiver power plant. Hu et al. [31] have introduced new simulation software named THERMOSOLV to evaluate the feasibility solar thermal power plants. Yao et al. [32] have used TRNSYS software to predict the thermal performance of a solar power tower. Ahlbrink et al. [33] have combined STRAL, LabView and Dymola software to analyze a solar power tower plant.

Regarding the Brayton cycle, the solar central receiver consists basically of a heliostats field, a high tower with volumetric air receiver atop and an adapted gas turbine. The gas turbine is usually installed close to the receiver in order to reduce additional energy losses at interconnections [1].

This concept has been tested within the framework of SOLGATE project. Heller et al. [34] have highlighted the operation experiences of SOLGATE project that has aimed at the development of a solar hybrid gas turbine with a volumetric air receiver. Schmitz et

al. [35] have proposed a hybrid solar gas turbine with a secondary concentrator and an elliptic heliostat field design. Behar et al. [36] have simulated the performance of commercial solar hybrid gas turbine under Algerian climate.

The literature survey has indicated that R&D activities on the central receiver solar thermal power plants are increasing. As reviewed above, most published studies have been focused on the three main components including the heliostat field, the solar receiver and the power block. However, for implanting this promising technology at large scale, the selection of the most suitable configuration is an important issue.

For instance, Algeria has planned to install about 7 GW of concentrating solar power plants by 2030 [37]. During the period of 2021-2030, an annual capacity of 500 MW would be installed by 2023, then 600 MW per year after that. These important investments require accurate selection of the most suitable technology that would be installed. To the best of our knowledge [38].

There is a lack of comparative studies on solar thermal power plants to find out the most efficient one. Therefore, a detailed thermal performance comparison of two configurations of central receiver solar thermal power plants has been carried out in the present work. These two configurations concern the Rankine cycle with a tubular water/steam receiver and the Brayton cycle with volumetric air receiver. The aim is to determine the most suitable configuration under the Algerian climate conditions. Therefore the present dissertation has been organized as follow, The first chapter represents an overview of solar thermal technologies (concentrating solar power), a Background of the Central receiver system is the aim of chapter 2, chapter 3 highlights of solar thermal power in Algeria in chapter4 two configurations of of solar power tower have been analyzed to find out the most suitable for Algeria. The most important findings of the dissertation have been summarized in the conclusion.

Reference

[1] O. Behar, A. Khellaf, K. Mohammedi, A review of studies on central receiver solar thermal power plants, Renew. Renewable and Sustainable Energy Reviews 23 (2013) 12–39.

[2] Hongli Zhang, Zhifeng Wang, Xiudong Wei, Zhenwu Lu. Design of Heliostats Field for Scale of 1MW Solar Power Tower Plant. Procedia Environmental Sciences 11 (2011) 1164 – 1170.

[3] Francisco J. Collado. Preliminary design of surrounding heliostat fields. Renewable Energy 34 (2009) 1359–1363
[4] Corey J. Noone, Manuel Torrilhon, Alexander Mitsos. Heliostat field optimization: A new computationally efficient model and biomimetic layout. Solar Energy 86 (2012) 792–803.
[5] Xiudong Wei, Zhenwu Lu, Zhifeng Wang, Weixing Yu, Hongxing Zhang, Zhihao Yao. A new method for the design of the heliostat field layout for solar tower power plant. Renewable Energy 35 (2010) 1970–1975.
[6] Marcelino Sa´nchez, Manuel Romero. Methodology for generation of heliostat field layout in central receiver systems based on yearly normalized energy surfaces. Solar Energy 80 (2006) 861–874
[7] F.M.F. Siala, M.E. Elayeb. Mathematical formulation of a graphical method for a no-blocking heliostat field layout. Renewable Energy 23 (2001) 77–92
[8] Amos Danielli, Yossi Yatir, Oded Mor. Improving the optical efficiency of a concentrated solar power field using a concatenated micro-tower configuration. Solar Energy 85 (2011) 931–937
[9] Maolong Zhang, Lijun Yang, Chao Xu, Xiaoze Du. An efficient code to optimize the heliostat field and comparisons between the biomimetic spiral and staggered layout. Renewable Energy 87 (2016) 720-730.
[10] Pasha Piroozmand, Mehrdad Boroushaki. A computational method for optimal design of the multi-tower heliostat field considering heliostats interactions. Energy 106 (2016) 240e252
[11] H.I. Villafán-Vidales, Stéphane Abanades, Cyril Caliot, H. Romero-Paredes. Heat transfer simulation in a thermochemical solar reactor based on a volumetric porous receiver. Applied Thermal Engineering 31 (2011) 3377-3386
[12] Thomas Fend, Bernhard Hoffschmidt, Robert Pitz-Paal, Oliver Reutter,Peter Rietbrock. Porous materials as open volumetric solar receivers: Experimental determination of thermophysical and heat transfer properties. Energy 29 (2004) 823–833
[13] Zhiyong Wu, Cyril Caliot, Gilles Flamant, Zhifeng Wang. Coupled radiation and flow modeling in ceramic foam volumetric solar air receivers. Solar Energy 85 (2011) 2374–2385
[14] M. Becker, Th. Fend, B . Hoffschmidt, R. Pitz-Paal, O. Reutter, V. Stamatov, M. Steven, D. Trimis. Theoretical and numerical investigation of flow stability in porous materials applied as volumetric solar receivers. Solar Energy 80 (2006) 1241–1248
[15] T. Fend, R.-P. Paal, O. Reutter, J. Bauer, B. Hoffschmidt. Two novel high-porosity materials as volumetric receivers for concentrated solar radiation. Solar Energy Materials & Solar Cells 84 (2004) 291–304
[16] Andrej Lenert, Evelyn N. Wang. Optimization of nanofluid volumetric receivers for solar thermal energy conversion. Solar Energy 86 (2012) 253–265
[17] Ananthanarayanan Veeraragavan, Andrej Lenert, Bekir Yilbas, Salem Al-Dini, Evelyn N.Wang. Analytical model for the design of volumetric solar flow receivers. International Journal of Heat and Mass Transfer 55 (2012) 556–564
[18] Zhiyong Wu, Cyril Caliot, Fengwu Bai, Gilles Flamant, Zhifeng Wang, Jinsong Zhang, Chong Tian. Experimental and numerical studies of the pressure drop in ceramic foams for volumetric solar receiver applications. Applied Energy 2010; 87:504–513.

[19] Reiner Buck, Christian Barth, Markus Eck, Wolf-Dieter Steinmann. Dual-receiver concept for solar towers. Solar Energy 80 (2006) 1249–1254.
[20] Qing Li, Fengwu Bai, Bei Yang, Zhifeng Wang, Baligh El Hefni, Sijie Liu, Syuichi Kubo, Hiroaki Kiriki, Mingxu Han. Dynamic simulation and experimental validation of an open air receiver and a thermal energy storage system for solar thermal power plant. Applied Energy 178 (2016) 281–293
[21] Raffaele Capuano, Thomas Fend, Peter Schwarzbözl, OlenaSmirnova, Hannes Stadler, Bernhard Hoffschmidt, RobertPitz-Paal. Numerical models of advanced ceramic absorbers for volumetric solar receivers. Renewable and Sustainable Energy Reviews 58 (2016) 656–665.
[22] I. Hischier, D. Hess, W. Lipiński, M. Modest, A. Steinfeld, Heat Transfer Analysis of a Novel Pressurized Air Receiver for Concentrated Solar Power via Combined Cycles, ASME Journal of Thermal Science and Engineering Applications, 1 (2009) 041002.
[23] Shuang-Ying Wu, Lan Xiao, You-Rong Li. Effect of aperture position and size on natural convection heat loss of a solar heat-pipe receiver. Applied Thermal Engineering 31 (2011) 2787-2796
[24] Tom Melchior, Christopher Perkins, Alan W. Weimer, Aldo Steinfeld. A cavity-receiver containing a tubular absorber for high-temperature thermochemical processing using concentrated solar energy. International Journal of Thermal Sciences 47 (2008) 1496–1503
[25] Wu Yu-ting, Liu Bin, Ma Chong-fang, Guo Hang. Convective heat transfer in the laminar–turbulent transition region with molten salt in a circular tube. Experimental Thermal and Fluid Science 33 (2009) 1128–1132
[26] Xiaoping Yang, Xiaoxi Yang, Jing Ding, Youyuan Shao, Hongbo Fan. Numerical simulation study on the heat transfer characteristics of the tube receiver of the solar thermal power tower. Applied Energy 90 (2012) 142–147
[27] Pyong Sik Pak, Yutaka Suzuki, Takanobu Kosugi. A CO2-capturing hybrid power-generation system with highly efficient use of solar thermal energy. Energy 22(1997), 295-299
[28] Pyong Sik Pak, Takeshi Hatikawa, Yutaka Suzuki A hybrid power generation system utilizing solar thermal energy with CO2 recovery based on oxygen combustion method. Energy Conversion and Management 36(1995) 823-826
[29] Mark Schmitza, Peter Schwarzbözl, Reiner Buck, Robert Pitz-Paal. Assessment of the potential improvement due to multiple apertures in central receiver systems with secondary concentrators. Solar Energy 80(2006)111-120
[30] Pierre Garcia, Alain Ferriere, Gilles Flamant, Philippe Costerg, Robert Soler and Bruno Gagnepain. Solar Field Efficiency and Electricity Generation Estimations for a Hybrid Solar Gas Turbine Project in France. journal of solar energy engineering. 130 (2008),014502
[31] Maya Livshits, Abraham Kribus. Solar hybrid steam injection gas turbine (STIG) cycle. Solar energy 86(2012) 190-199
[32] L.V. Griffith, H. Brandt. Solar-fossil HYBRID system analysis: Performance and economics. Solar Energy 33(1984) 265-276
[33] Chao Xu, Zhifeng Wang, Xin Li, Feihu Sun. Energy and exergy analysis of solar power tower plants. Applied Thermal Engineering 31 (2011) 3904-3913

[34] Ronan K. McGovern , William J. Smith. Optimal concentration and temperatures of solar thermal power plants. Energy Conversion and Management 60 (2012) 226–232
[35] Bruno Coelho, Peter Schwarzbozl , Armando Oliveira , Adélio Mendes. Biomass and central receiver system (CRS) hybridization: Volumetric air CRS and integration of a biomass waste direct burning boiler on steam cycle. Solar Energy 86 (2012) 2912–2922
[36] L.J. Yebra, M. Berenguel, S. Dormido, M. Romero. Modelling and Simulation of Central Receiver Solar Thermal Power Plants.In: Proceedings of the 44th IEEE Conference on Decision and Control, and the European Control Conference 2005; 7410-7415.
[37] Myung-Hoon Moon, Yong Kim, Kyung-Moon Kang, Jo Han Ko, Tae Beom Seo. System performance estimation for a solar tower power plant. Chapter Proceedings of ISES World Congress 2007, 5: 1899-1903
[38] R.J. Zoschak, S.F. Wu. Studies of the direct input of solar energy to a fossil-fueled central station steam power plant. Solar Energy,1975 Vol. 17, pp. 297-305.

CHAPTER I

Overview of solar thermal technologies

1. Introduction

For deferent reasons (Political, Economic development, Climate change) many countries are mandating that a part of the electric power be from renewable origin, in particular solar energy. According to IEA, 50% of the new power infrastructures will base on clean-sustainable energies. As a result, renewable energy will become the world's second-largest source of power generation by 2015; delivering about 30% of the electricity needs by the year 2035. Nowadays, Concentrating Solar Power (CSP) technology implantation is growing faster than any other renewable technology. This is because, as shown in (fig 1.1), it offers an integrated solution to the coming decade's global problems, i.e., climate change and associated shortage of energy, water and food. For instance, a one megawatt of installed CSP avoids the emission of 688 tonne of CO_2 compared to a combined cycle system and 1360 tonne of CO_2 compared to a coal/steam cycle power plant. A one square mirror in the solar field produces 400 kWh of electricity per year, avoids 12 tonne of CO_2 emission and contributes to a 2.5 tonne savings of fossil fuels during its 25-year operation lifetime.

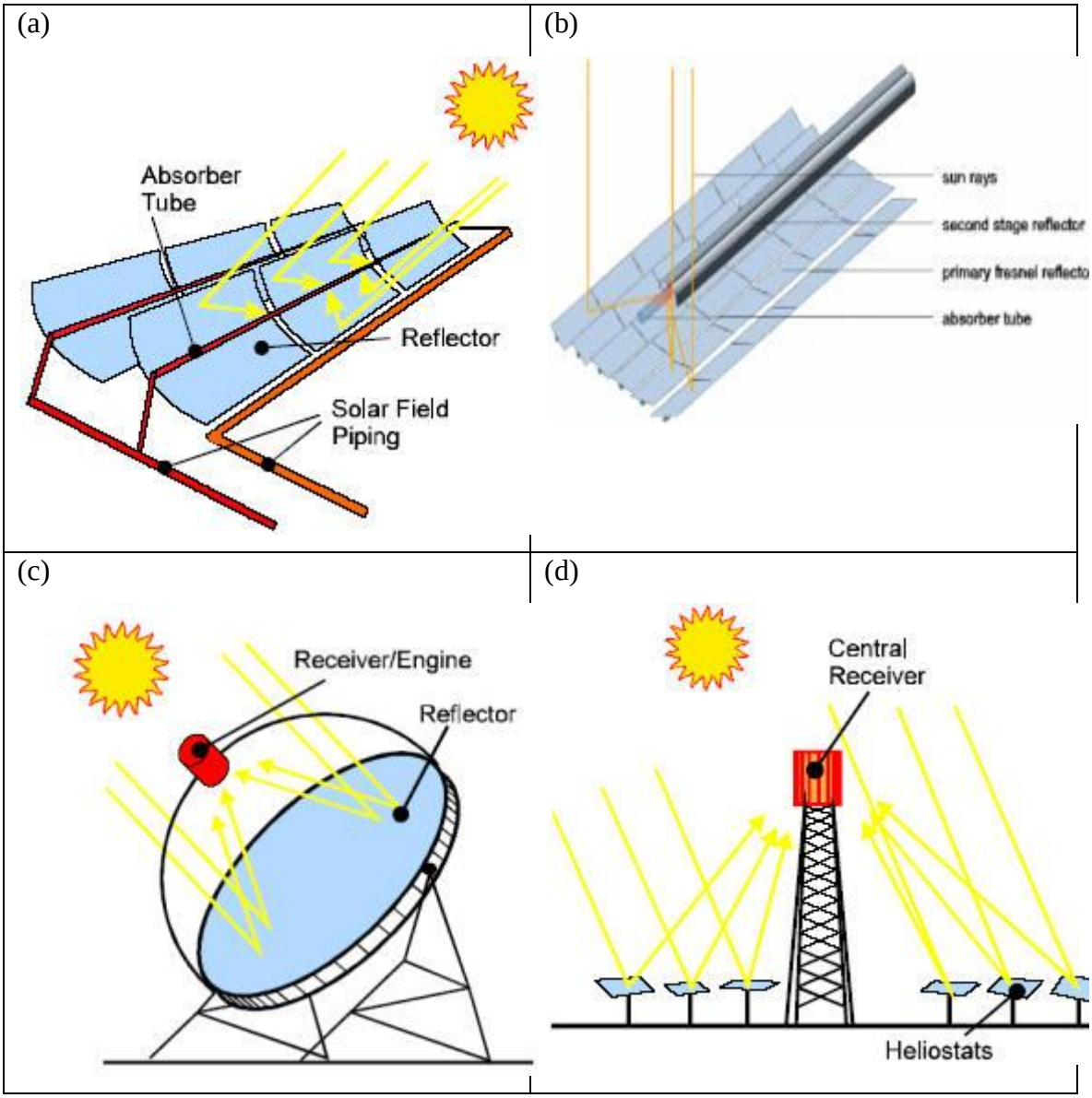

Fig.1.1.Basic concept of the four CSP families: (a) parabolic trough collector (b) linear Fresnel collector (c) central receiver system with dish collector (d) central receiver system with distributed reflectors [1]

Concentrating solar thermal power plants produce electric power by converting the sun's energy into high temperature heat using various mirror or lens configurations. a typical CSP-plant consists of three main subsystems(fig.1.2): solar collector field, solar receiver and a power conversion system Solar thermal systems (trough, dish-Stirling, power tower, Fresnel), transfer heat to a turbine or engine for power generation. They are classified according to the manner they focus the sun's rays and the receiver

technology. Because of the variable nature of solar radiation, it is necessary to design the collector field to generate more energy than the turbine can accept under normal conditions. This excess of energy is used to charge the storage system, which provides the required energy to the turbine during periods when there is insufficient solar radiation

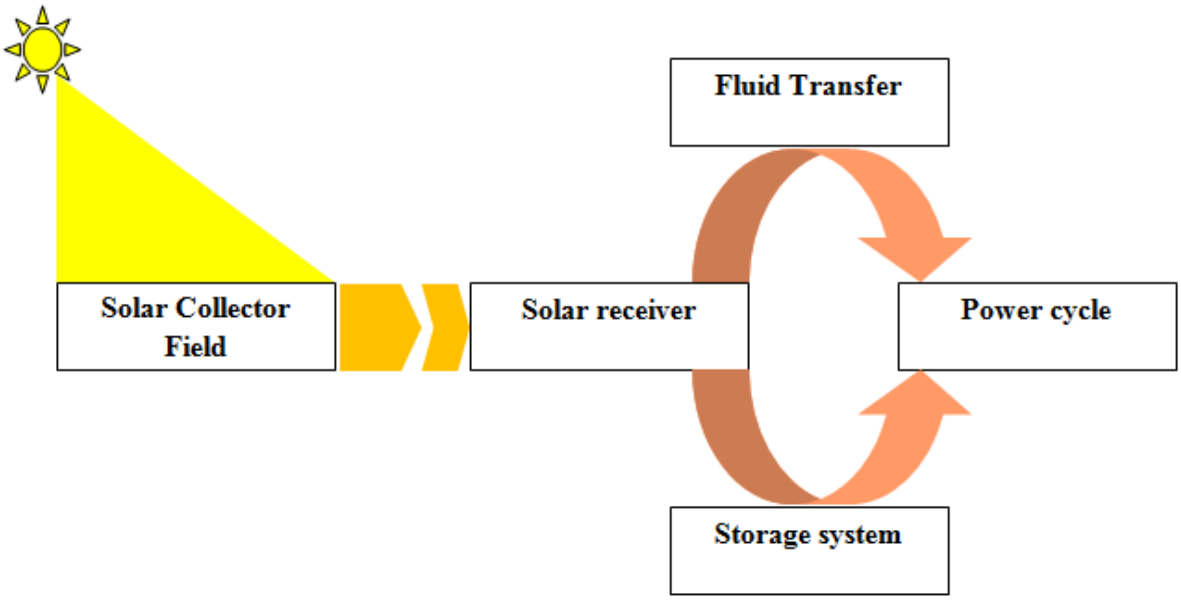

Fig1.2. flow diagram for a typical CSP[2]

2. Historic and Current status

Concentrating Solar Power (CSP) is not an innovation of the last few years. Records of its use date as far back as 212 BC when Archimedes used mirrors for the first time to concentrate the Sun's rays [1]. In the early seventeenth century, Salomon De Caux developed in 1615 a small solar powered motor consisting of glass lenses and an airtight metal vessel containing water and air [3]. More than a century later, in 1774, Lavoisier and Joseph Priestley developed the theory of combustion by concentrating solar radiation on a test tube for gas collection [4]. Next, Augustin Mouchot has devised a solar steam machine to run a printing press [5]. After that, in 1878, a small solar power plant made up of a parabolic dish concentrator connected to an engine was exhibited at the World's Fair in Paris [6]. In the early 1900s, although interest in solar power was

then lost due to advances in internal combustion engines and increasing availability of low cost fossil fuel, the first CSPplant, powered by a parabolic trough solar field, was installed at Al Meadi (Egypt)[7, 8]. This first CSP-plant, installed in 1913, was used for pumping water for irrigation [9]. In the 1960s, with the focus on photovoltaic for the space program, interest in solar energy began to arise again. During 1970s the oil crisis boosted R&D activities on CSP and numerous pilot plants were built, tested and bringing CSP technology to the industrial and commercial level [10]. As a result, the first commercial plants had operated in California (USA) over the period of 1984-1991, spurred, more particularly, by federal and state tax incentives and mandatory long-term power purchase contracts. A drop in oil and gas prices has though driven many countries to retreat from the policy that had supported the advancement of CSP, and thus, no new plants have been built between 1990 and 2000. It wasn't until 2006 that interest was once again rekindled for the development of large scale CSP-plants. The market re-emerged more particularly in Spain and the United States, again in response to government measures such as the feed-in tariffs (Spain) and the policies requiring a share of solar power in their energy mix. As of 2011, have been worldwide 1.3 GW of CSP plants in operation, 2.3 GW under construction, and 31.7 GW in the planning stage [1]. Nowadays, in 2013, 2.136 GW are operating, 2.477 GW under construction and 10.135 GW are announced mainly in the USA followed by Spain and China [11]. According to reference [12], about 17 GW of CSP projects are under development worldwide, and the United States leads with about 8 GW. Spain ranks second with 4.46 GW in development, followed by China with 2.5 GW.

The overall experience in CSP technology development has been positive and new opportunities are opening. At the R&D and demonstration level, many projects have been carried out. At the configurations and component development projects, one can name DISS, SOLAIR, EURODISH and ECOSTAR projects. SOLGATE, SOLASYS and SOLHYCO are among the projects that have been carried out for the hybrid concepts implementation. DISTOR is a project worth citing for storage systems development [15]. At the pilot and demonstration level, the projects PS10, PS20 and SOLAR TRES among others have provided valuable information for the development of the CSP technology. They have offered excellent pattern to move CSP technology

forwards [16]. Building on this experience, new pilot projects are underway or in the planning stage (ALSOL in Algeria). At the industrial and commercial plants of 50 MW to 400 MW power are underway or in operation in Spain, USA, Algeria, Egypt, Morocco, Mexico, Greece, Iran, India and China. The exploitations of these plants have been conclusive that there is a move to the deployment of large scale CSP plants [2]. Up to the year 2030, the market potential is estimated at least at 7 GW in the EU-MENA. This offers the opportunity to CO2 reduction prospective of up to 12 million tons per year. These plants represent also a cost fall potential of 20% compared to the last built 80 MWe SEGS IX plant in USA. According to ECOSTAR, there are three main drivers for cost reduction: scaling up, volume production and technology innovations. About 50% of the intended reductions in costs of CSP-plants will be from technology developments, and the other half from scale up and volume production [15]. In this context solar thermal power plants will be capable of delivering efficiently more than 3% of the EU's electricity by 2020, and at least 10% by 2030 [18]. Moreover, it offers the opportunity to generate about 50% of the electricity needs of the EU-MENA region [19,20] and supply over 10% of the world's electricity by 2050 [21]. Advanced scenario by IEA, EU and DLR has anticipated that global CSP capacity will reach 1.5 TW at this year. The (fig1.3) show a data on concentrating solar power (CSP) projects around the world that have plants that are either operational, under construction, or under development. CSP technologies include parabolic trough, linear Fresnel reflector, power tower, and dish/engine systems

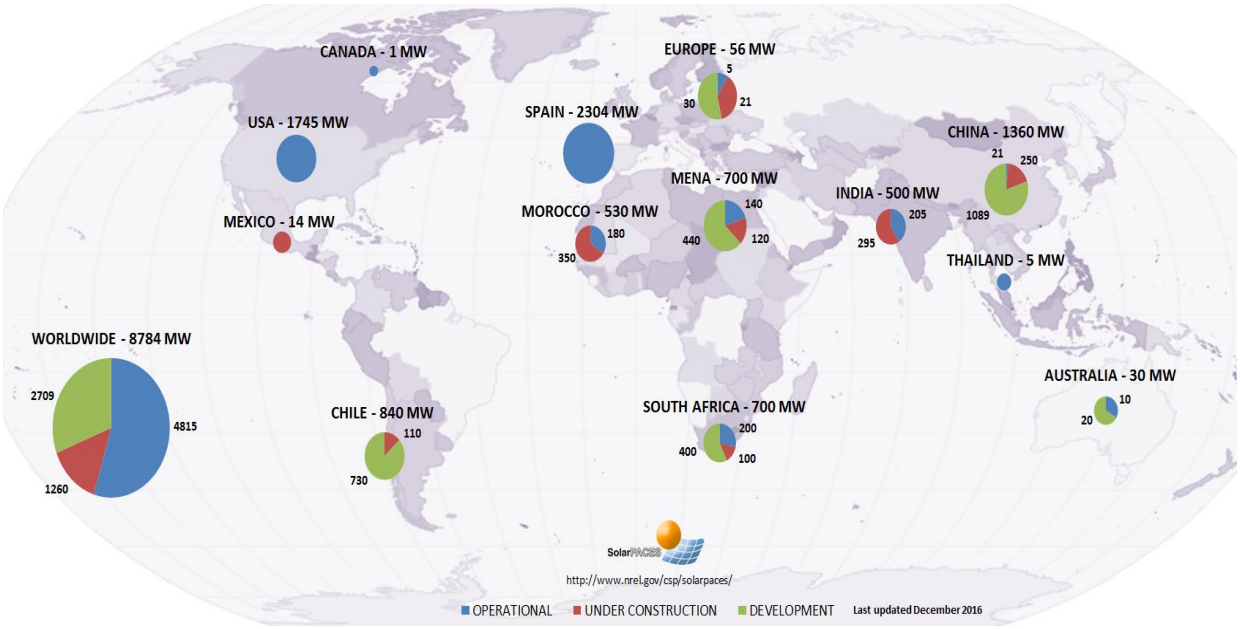

Fig.1.3. CSP Projects Around the World [22]

3. Concentrating Solar Power (CSP)

3.1. Parabolic trough

The parabolic trough is the most commons systems comprise rows of trough-shaped mirrors hitch direct solar insolation to a receiver tube along the focal axis of each trough. The focused radiation raises the temperature of heat transfer fluid , This fluid is heated to 390 °C and pumped through a series of heat exchangers to produce superheated steam which powers a conventional turbine generator to produce electricity. The storage systems in the first parabolic trough plants were based on two storage tanks, in which the heat transfer fluid also served as the storage medium. This concept was demonstrated successfully in the first of the solar electric generating systems (SEGS) plants 1990. However, the heat transfer fluid used in these parabolic trough plants was very expensive, greatly increasing the total cost of scaling up the storage capacity. For this reason, a study was carried out to evaluate the concept of molten salts as the thermal storage medium in parabolic trough plants, using data from the solar tower plant “Solar Two”. The study concluded that, given its characteristics and cost, this type of storage could also be used in parabolic trough plants, with indirect storage in two molten salt tanks. It is an efficient, low-cost storage medium and, moreover, the molten

salts are neither flammable nor toxic Sandia National Laboratories 2008. This is the system currently used in commercial plants, such as ANDASOL, the first commercial plant with such technology in Spain Solar Millennium 2009. The basic system consists of circulating the HTF through the collector solar field, then transferring its thermal energy through a heat exchanger to the thermal storage medium, in this case molten salts (fig1.4)

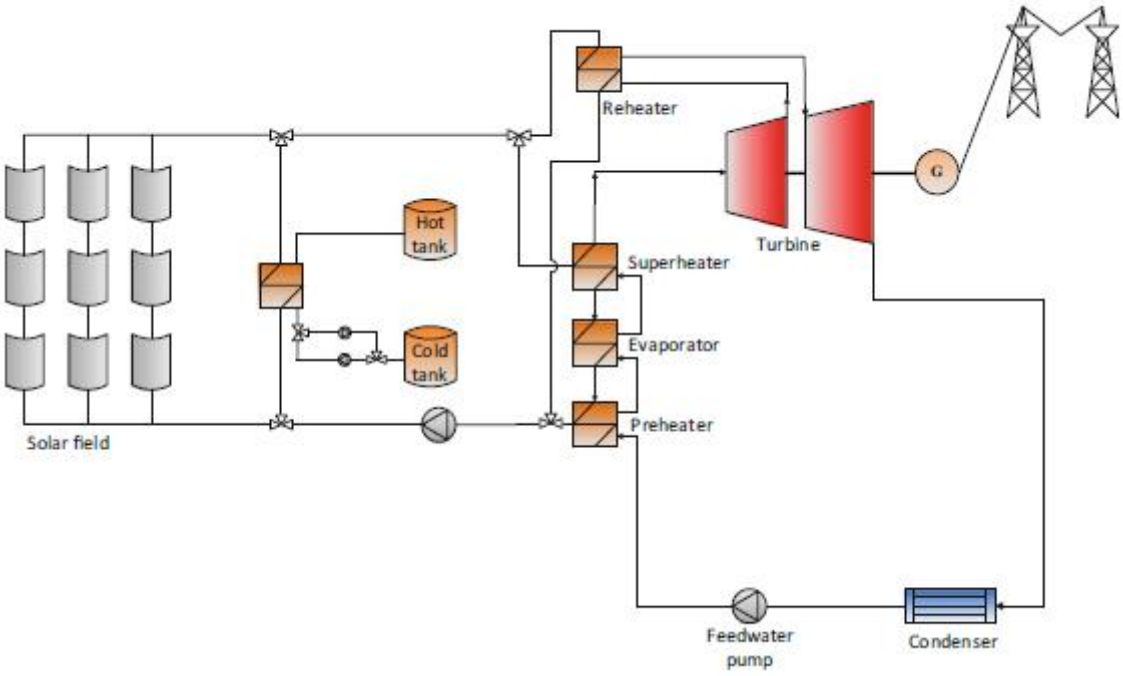

Fig.1.4 Parabolic-trough collector field coupled to a steam cycle [15]

One of the tanks is used to store the hot molten salts (the hot tank) and the other to receive the cold molten salts (the cold tank). During the thermal storage charging cycle, part of the oil coming from the solar collector field is sent to the oil–salt heat exchanger. In this way, thermal energy is transferred from the oil to the salt stored in the hot tank. During the discharge cycle, the salt and oil pathways in the oil–salt heat exchanger are inverted and, therefore, the thermal energy is transferred from the salt to the oil on its way to the cold tank. Direct steam generation in parabolic-trough absorber tubes is seen as a promising option for increasing the economic efficiency of CSP plants 2005 as they can reach higher temperatures and thus achieve greater efficiencies 2009. Furthermore,

the environmental risks from oil are avoided, as well as the heat exchanger between the collector field and the power cycle unnecessary. Within an European project framework carried out at the Plataforma Solar de Almerı´a (PSA), the operation and control of this new technology has been successfully proven under transitory and steady-state conditions. For this purpose, a loop 700 m length was constructed with a 5.70 m parabolic-trough aperture, in which steam temperatures of up to 400°C and pressures of 100 bar have been achieved. The long-term objective is to heat steam to a temperature of 550 °C and 120 bar and to develop a thermal storage system that matches this technology, based on phase-change storage. Parabolic-trough systems dominate the global market in CSP plants. The first to be installed using this technology were the SEGS plants in the Mojave Desert in California. This was at the beginning of the 1980s when plants with more than a 350 MWe capacity were put into operation. By the middle of 2009, 95 % of the 560 MWe produced by CSP plants in the world corresponded to plants whose technology was based on parabolic-trough collectors. Currently, parabolic-trough technology for the CSP plants is the one most widely installed in the world (90 % of the total). These systems achieve solar–electric conversion efficiencies of between 10 and 15 %, but have the potential of reaching 18 % in the medium-term . Solar–electric efficiency includes the conversion of solar energy to thermal energy by means of a solar collector field and the conversion of thermal energy to electricity using a power block. A maximum solar–electric efficiency of 21.5 % was measured in a 30 MWe plant in California .

3.2. Central Receiver Systems (Solar Power Tower)

The power tower systems (Fig.1.5) consist of a field of thousands of sun-tracking mirrors which direct insolation to a receiver atop a tall tower. A heat-transfer fluid is heated in the receiver and is piped to a ground based steam generator. The steam drives a steam turbine-generator to produce electricity. Because trough and power tower systems collect heat to drive central turbine generators, they are best suited for large-scale plants: 50 MW or larger. Trough and tower plants, with their large central turbine generators and balance of plant equipment, can take advantage of economies of scale for cost reduction, as cost per kW goes down with increased size. Additionally, these plants

can make use of thermal storage or hybrid fossil systems to achieve greater operating flexibility and dispatch ability. This provides the ability to produce electricity when needed by the utility system, rather than only when sufficient solar insolation is available to produce electricity, for example, during short cloudy periods or after sunset. This capability has significantly more value to the utility and potentially allows the owner of the CSP plant to receive additional credit, or payment, for the electric generating capacity of the plant.

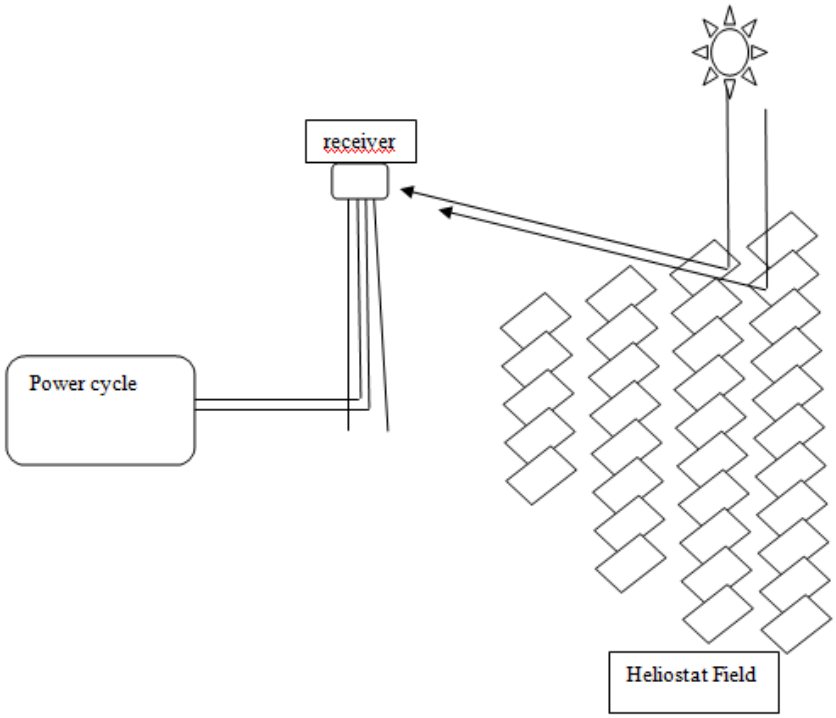

Fig1.5. basic concept of solar power tower

3.3. Linear Fresnel

In linear Fresnel systems, as with parabolic-trough collector systems, solar radiation is concentrated onto a line and can be coupled to steam cycles for electricity generation. These systems have been developed with the aim of attaining a simpler design and at less cost than the parabolic-trough systems. The first prototypes have shown promise and the first CSP plants that include this technology are currently in the construction phase. The collectors in a linear Fresnel system are made up of a large number of mirror segments that can individually follow the path of the sun (see Fig.1.1). Unlike parabolic-trough collectors, the absorber tubes in the Fresnel systems are in a fixed

position above the mirrors in the centre of the solar field and, therefore, do not move together with the mirrors as they follow the sun. The system can operate with oil, water or molten salts. Current designs use water directly in the receiver tubes at 50 bar pressure and 280 °C, or alternatively molten salts. The storage methods applicable for these systems are similar to those used for parabolic trough collector systems. The steam cycle efficiency of linear Fresnel systems is less than that of parabolic-trough collector systems because the steam temperature is lower. However, the Fresnel systems have certain advantages over parabolic-trough systems. The Fresnel collectors have a lighter structure; those designed by Novatec-Biosol are 80 % lighter per square metre (Trieb 2007). Consequently, such systems require less investment and have lower operation and maintenance costs than parabolic trough collectors. Regarding the disadvantages, the simple optical design of the Fresnel system means that the optical efficiency of a field formed by these mirrors is less; therefore, approximately 33 % more aperture area is necessary for the same thermal energy production compared with parabolic-trough collectors 2007. In terms of integrating the solar field into the environment, the Fresnel system has considerable advantages over parabolic-trough collectors. The land use is far better because less distance is required between mirrors. The aperture area of the collectors covers between 80 and 95 % of the land required, compared with only 30 % covered by parabolic-trough mirrors as a result of the considerable distance needed between the collector rows to avoid shadowing. Therefore, the land-use efficiency of linear Fresnel collectors is approximately three times greater than for parabolic trough collectors. Taking into account that the Fresnel system has less optical efficiency (about 67 % of that for a parabolic trough), the production per square metre of land from this type of solar field is twice that of a parabolic-trough field. This fact might be of little importance in isolated desert areas where land use is not limited, but could be of relevance when it is integrated into a CSP plant in industrial or tourist complexes, or near urban centres. However, this technology is not as mature as parabolic-trough technology and it remains in the demonstration phase. Two plants are currently in operation, with a total capacity of 6.4 MWe.

3.4. Parabolic dish systems

Systems use an array of parabolic dish-shaped mirrors (stretched membrane or flat glass facets) to focus solar energy onto a receiver located at the focal point of the dish (Fig2.1). Fluid in the receiver is heated to 750 °C and used to generate electricity in a small engine attached to the receiver. Engines currently under consideration include Stirling and Brayton cycle engines.

Dish systems are modular in nature, with single units producing power in the range of 10 kW to 35 kW. Thus, dish systems could be used for distributed or remote generation applications, or in large arrays of several hundred or thousand units to produce power on a utility scale. Dish systems have the potential advantage of mass production of individual units, similar to the mass production of automobiles or wind turbines. At this time, neither the dish Stirling system use storage or hybrid fossil capabilities to provide a firm resource.

4. A comparison of different technologies

A brief comparison between these families is illustrated in [Table 1.1]. For each technology the overall efficiency of the whole system varies with the location, the time of day and the day of the year. Towers and troughs are best suited for large, grid-connected power projects in the 30-200 MW size, whereas, dish/engine systems are modular and can be used in single dish applications or grouped in dish farms to create larger multi-megawatt projects. Parabolic trough plants are the most mature solar power technology available today and the technology most likely to be used for near-term deployments. Power towers, with low cost and efficient thermal storage, promise to offer dispatch able, high capacity factor, solar-only power plants in the near future. The modular nature of dishes will allow them to be used in smaller, high-value applications. Towers and dishes offer the opportunity to achieve higher solar-to-electric efficiencies and lower cost than parabolic trough plants, but uncertainty remains as to whether these technologies can achieve the necessary capital cost reductions and availability improvements. Parabolic troughs are currently a proven technology primarily waiting for an opportunity to be developed.

Table1.1 Comparison of the four CSP families

characteristics	Concentration method			
	Line concentrating system		Point concentrating system	
Solar field type	Parabolic trough	Linear Fresnel	Central receiver	Parabolic dish
State of the art	Commercial	Recently commercial	Commercial	Demonstration projects
Cost of the solar field(€/m²)	300-350	200-250	300-400	>350
Investment costs (€/m²)	3500-6500	2500-4500	4000-6000	6000-10000
Typical unit size(MW)	10-250	5-200	10-100	0.1-1
Peak solar efficiency (%)	21	15	<20	31.25
Annual solar efficiency (%)	10-16 (18 projected)	8-12 (15 projected)	10-16 (25projected)	16-29
Concentration ratio	50-90	35-170	600-1000	Up to 3000
Operating temperature (°C)	350-450 (550 projected)	270-450 (550 projected)	550-1000	750-900
Solar receiver	Mobil	Fixed	Fixed	Mobil
Heat transfer fluid	Synthetic oil, water/steam	Synthetic oil, water/steam	Air, molten salts,water/steam	Air
Thermodynamic power cycle	Rankine	Rankine	Brayton/rankine	Stirling,Brayton
Power unit	Steam turbine	Steam turbine	Gas, steam turbine	Stirling engine
Reliability	Long-term proven	Recently proven	Recently proven	Moderate
Thermal storage media	Molten salts, concrete, phase-change material	Molten salts, concrete, phase-change material	Molten salts, concrete, ceramics, phase-change material	No storage available
Combination with desalination	Simple	Simple	Simple	Simple
Integration into the environment	Demanding	Simple	Moderate	Moderate
Land requirements	High	Low	High	Moderate
Typical capacity (MW)	10-300	10-200	10-200	0.01-0.4

In each CSP family, a variety of options is possible for solar field layout, tracking system, receiver type, heat transfer fluid (HTF), storage technology and power conversion system. North-South and East-West orientations equipped with single tracking mechanism are usually applied in trough solar field. For central receiver, surrounded and North field configurations are the most proven technologies, while MTC (Micro Tower Configuration) is now under development .Whereas linear receivers are used for parabolic trough and Fresnel technologies, various configurations exist for power tower concept. These configurations, for some of them under design, test or improvement, include the volumetric receiver, the particle receiver and the cavity receiver. Concerning heat transfer fluids (HTF), molten salt is widely used as HTF in commercial plants. Synthetic oil and saturated steam are also currently used as HTF's in commercial plants. Superheated steam has been recently introduced as HTF. Pressurized air and other gases, in particular CO_2 and N_2, nano-fluids, concrete and circulating particles are under development for both trough and tower, while helium or hydrogen is used in dish Sterling. The [table.1.2] summarizes the advantages and disadvantages associated with each technique

Table.1.2. Pros and cons of different CSP technology

	Advantages	Disadvantages
Trough	• Commercially available –over 12 billion kWh of operational experience operating temperature potential up to 500°C(400°C commercially proven) • commercially proven annual net plant efficiency of 14% (solar radiation to net electric output) • commercially proven investment and operating costs • modularity • best tand-use factor of all solar technologies • lowest materials demand • hybrid concept proven • storage capability	• the use of oil-based heat transfer media restricts operating temperatures today to 400°C resulting in only moderate steam qualities
Central receiver	• good mid-term prospects for high conversion efficiencies, operating temperature potential beyond 1000°C (565°C proven at 10 MW scale) • Storage at high temperatures • hybrid operation possible	• projected annual performance values investment and operating costs still need to be proven in commercial operation
Dish strling	• very high conversion efficiencies peak solar to net electric conversion over 30% • Modularity • hybrid operation of first demonstration projects	• Reliability needs to be improves • projectd cost goal of mass production still need to be achieved
Linear Fresnel	• Steam as heat transfer fluid allows higher temperatures because there is no danger of thermo oil cracking.	• The parallel mirror rows shade each other at high transversal incidence angles. They also block parts of the reflected radiation at high transversal incidence angles.

5. Cost Versus Value

Through the use of thermal storage and hybridization, solar thermal electric technologies can provide a firm and dispatchable source of power. Firm implies that the power source has a high reliability and will be able to produce power when the utility needs it. Dispatchability implies that power production can be shifted to the period when it is needed.

As a result, firm dispatchable power is of value to a utility because it offsets the utility's need to build and operate new power plants. This means that even though a solar thermal plant might cost more, it can have a higher value.

The cost of electricity from solar thermal power systems will depend on a multitude of factors. These factors, discussed in detail in the specific technology sections, include capital and O&M cost, and system performance. However, it is important to note that the technology cost and the eventual cost of electricity generated will be significantly influenced by factors "external" to the technology itself.

As an example, for troughs and power towers, small stand-alone projects will be very expensive.

In order to reduce the technology costs to compete with current fossil technologies, it will be necessary to scale-up projects to larger plant sizes and to develop solar power parks where multiple projects are built at the same site in a time phased succession. In addition, since these technologies in essence replace conventional fuel with capital equipment, the cost of capital and taxation issues related to capital intensive technologies will have a strong effect on their competitiveness.

6. Conclusion

Solar thermal power technologies are in different stages of development. Trough technology is commercially available today, with 1000 MW currently operating in the world wide. Power towers are exceeded the demonstration phase, with the 500 MW currently undergoing after 15 years of testing and power production Though most of the installed CSP is of parabolic trough technology, the central receiver system technology is gaining ground and is under consideration worldwide for many projects. Dish/engine technology has been demonstrated. Several system designs are under engineering development, a 25 kW prototype unit is on display in Golden, CO,USA. Solar thermal power technologies have distinct features that make them attractive energy options in the expanding renewable energy market worldwide.

For these reasons, more and more countries are mandating that a part of the electric power be from renewable origin, in particular solar energy. [10-28]. According to IEA, 50% of the new power infrastructures will base on clean-sustainable energies. As a result, renewable energy will become the world's second-largest source of power generation by 2015; delivering about 30% of the electricity needs by the year 2035

Nowadays, Concentrating Solar Power (CSP) technology implantation is growing faster than any other renewable technology. This is because it offers an integrated solution to the coming decade's global problems, i.e., climate change and associated shortage of energy, water and food. For instance, a one megawatt of installed CSP avoids the emission of 688 tonne of CO_2 compared to a combined cycle system and 1360 tonne of CO_2 compared to a coal/steam cycle power plant. A one square mirror in the solar field produces 400 kWh of electricity per year, avoids 12 tonne of CO_2 emission and contributes to a 2.5 tonne savings of fossil fuels during its 25-year operation lifetime.

References

[1] Concentrating solar power: its potential contribution to a sustainable energy future. The European Academies Science Advisory Council (EASAC) policy report 16, November 2011.

[2] O. Behar, A. Khellaf, K. Mohammedi, A review of studies on central receiver solar thermal power plants, Renew. Renewable and Sustainable Energy Reviews 23 (2013) 12–39.

[3] European Research on Concentrated Solar Thermal Energy. Directorate-General for Research Sustainable Energy Systems.European Union (EU) 2004.

[4] Goswami, D. Yogi, Kreith, Frank, and Kreider, Jan F., Principles of Solar Engineering, 2nd edition. Taylor and Francis, Philadelphia, PA, 2000.

[5] Pifre, A. 1882. A solar printing press. Nature, 21, 503–504.

[7] Kryza, Frank, the Power of Light. McGraw-Hill, New York, 2003.

[8] Duffie, John A., and Beckman, William A., Solar Engineering of Thermal Processes, 2nd edition. Wiley, New York, 1991

[9] Samir Rafaat, Maadi 1904-1962, Society and Historic in a Cairo Suburb, Using the Sun's Force, Al alhram Newspaper, Julay 9,1913, Maadi Introduces Solar energy to the World in 1913, htpp://www.egy.com/maadi/

[10] Winter, C. J., Sizmann, R. L., and Vant-Hull, L. L. eds. 1991. Solar Power Plants, pp. 21–27. Springer, Berlin.

[11] http://www.cspworld.com/ Visited 10/06/2016

[12] http://www.renewableenergyworld.com/index.html Visited 10/06/2016

[13] Concentrating Solar Power: From Research to Implementation. European Communities, 2007

[14] Pitz-Paal, R., Dersch, J. and Milow, B. (2005). European Concentrated Solar Thermal Road-Mapping (ECOSTAR): roadmap document. SES6-CT-2003-502578.

[15] Concentrating Solar Power: From Research to Implementation. European Communities, 2007

[16] Pitz-Paal, R., Dersch, J. and Milow, B. (2005). European Concentrated Solar Thermal Road-Mapping (ECOSTAR):

[17] Evaluating policies in support of the deployment of renewable power, IRENA 2012
[18] EUROPEAN Solar Thermal Electricity Association Solar Thermal Electricity European Industrial Initiative (Ste-Eii) Implementing Plan 2010-2012.
[19] Steffen Erdle, the DESERTEC Initiative-Powering the development perspectives of Southern Mediterranean countries? Discussion paper, December 2010.
[20] An Overview of the Desertec Concept, Red paper, 3ed Edition.
[21] Technology Roadmap Concentrating Solar Power, IEA 2010. http://www.iea.org/papers/2010/csp_roadmap.pdf
[22] http://www.solarpaces.org/csp-technology/csp-projects-around-the-world

CHAPTER II

Background of the Central receiver system

1. Introduction

As shown in (Fig.2.1), a typical central receiver system, also known as a solar tower power, consists of three major subsystems, namely the heliostat field, the receiver and the power conversion system. The solar field consists of numerous computer-controlled mirrors that track the sun individually in two axes and reflect the solar radiation onto the receiver located on the top of the tower. The receiver absorbs the heliostat reflected solar radiation and converts it into heat at high temperature levels. Depending on the receiver design and the heat transfer fluid nature, the upper working temperatures can range from 250°C to 1 000°C [1,2],. A power conversion system is used to shift thermal energy into electricity in the same way as conventional power plants [3,4]. The heliostat field is the main subsystem and its optical efficiency has a significant impact on the performance of the power plant; it represents about 50% of the total cost [5] and its annual energy losses are around 47% [6].The receivers are made up of material which withstands high temperature changes and high energy density such as ceramic and metal alloys. There are different types of receivers that can be classified into three groups depending on their functionality and geometric configurations. The three groups are the volumetric receivers, the cavity receivers and the particle receivers. In a power conversion system thermal energy can be converted into electricity with higher efficiency in Rankine cycle, Brayton cycle or combined cycle.

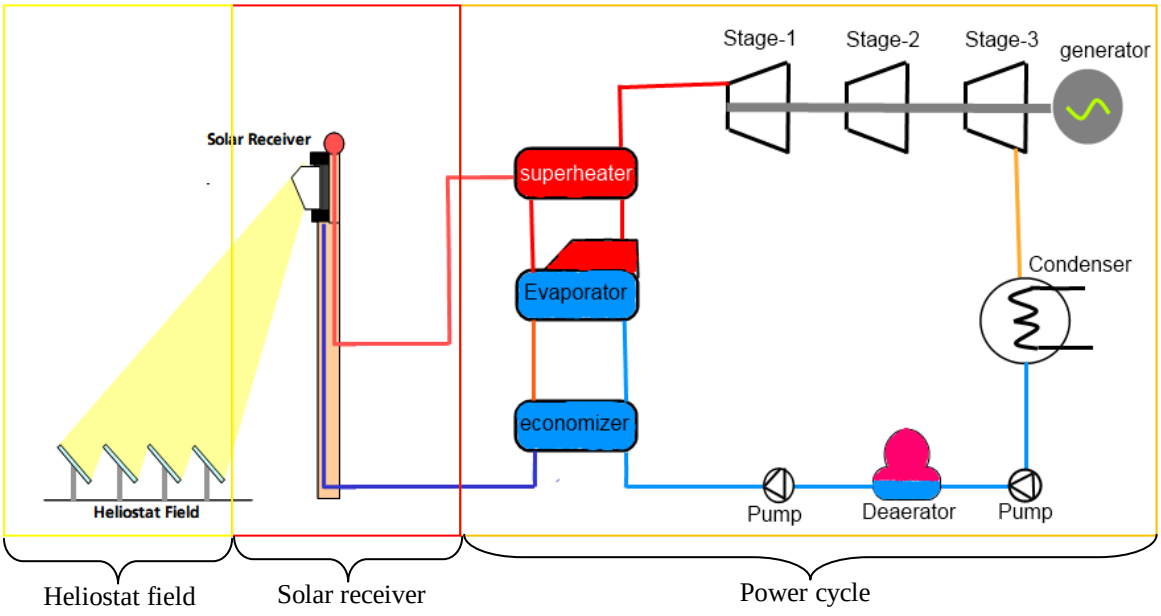

Fig.2.1. the three main subsystems of central receiver solar thermal power plant

2. Current status

The central receiver solar power technology has show a fast development during recent years. The number of power plants that have been installed is a good indication of that. In [Table.2.1]. [7], the most important power stations that have been implanted in the last decade are highlighted. As we can see the installed capacity is increasing day by day. This is due to the intensive R&D activities that have significantly improved the solar tower technology. Reducing initial costs and project risks, and improving components performance are the major factors that have favored this deployment. The solar tower power components are mainly the heliostat field, the receiver and the power block. also is illustrated the technical data of the three main components of the power plants. It has been observed that most of the power plants are equipped with a steam tubular receiver that power a Rankine thermodynamic cycle.

Concerning the heat transfer fluids (HTF), water/steam has initially been adopted in some solar towers such as PS10, PS20, Beijing Balading, Sierra and Yanqing. Molten salt is also a very commonly used HTF. It has been used for example in Gemasolar thermo-solar plant. Lately, there has been a big interest in developing air as a HTF.

Jülich solar tower is an example of this case. Depending on the receiver design and the heat transfer fluid, the working temperatures of the power conversion system range from 250°C, for water/steam cycles, to around 600°C with current molten salt design. The development of Direct Steam Generation (DSG), which is currently in its early stage, as HTF is very promising for reducing costs and enhancing thermal efficiency by eliminating the heat exchangers network [8] In 2006, the 11MWe CRS power plant PS10 was built by Abengoa Solar in Sevilla Spain. It has been followed by the 20 MWe power tower plants PS20 in the same location, the 5 MW Sierra Sun Tower (in Lancaster, USA) and the 1.5 MW in Jülich Germany in 2009. Since 2011, the Gemasolar power plant, built in Spain as large as the PS 20 power plant, but with surrounded heliostat field and15 h storage, has been operating and delivering power around the clock [9]. After the three pioneer CSP countries, i.e., the USA, Germany and Spain, Chin

Table.2.1 Operational Solar Power Tower Projects [7]

	Ivanpah solar	**Crescent Dunes Solar**	**khi solar one**	**Supcon solar**	**Gema solar**	**Planta solar 20**	**Planta solar 10**	**Dahan**	**Sierra sun tower**	**Lake cargelligo**	**Acme Solar tower**	**Jülich solar tower**
Country	usa	usa	south africa	china	spain	spain	Spain	china	usa	australia	india	germany
Solar Resource kWh/m²/yr	2 717	2 685	_	_	2 172	2 012	2 012	1 290	2 629	_	_	902
Start Production	2014	2015	2014	2013	2011	2009	2007	2012	2009	2011	2011	2008
Land Area(m²)	14163 998	6474970	3000000	3300000	1950000	800 000	550 000	52 609	90 000	50 300	48 562	170 000
Reflective field Area (m²)	260 000	1071361	576 800	434 880	304 750	150 000	75 000	10 000	27 670	6 080	16 222	17 650
Heliostat Area (m²)	15	62.4	140	2	120	120	120	100	1.13	9.8	1.136	8.2
number of Heliostats	173 500	17 170	4 120	217 440	2 650	1 255	624	100	24 360	620	14 280	2153
Tower Height (m)	140	164.6	200	80	140	165	115	118	55	_	46	60
Receiver type	steam receiver	External cylindri-cal	steam receiver	External cylindri-cal	External cylindri-cal	cavity receiver	cavity receiver	cavity receiver	External cylindri-cal	steam receiver	steam receiver	open-volumetri c
Receiver Outlet Temp (°C)	565	565	_	_	565	300	300	400	440	500	440	680
power cycle Type	Steam Rankine	Steam Rankine	Steam Rankine	Steam Rankine	Steam Rankine	Steam Rankine	Steam Rankine	Steam Rankine	Steam Rankine	Steam Rankine	Steam Rankine	Brayton
Heat-Transfer Fluid Type	Water/ Steam	molten salt	Water/ Steam	molten salt	molten salt	water/ Steam	water/ Steam	water/ Steam	water/ Steam	water/ Steam	water/ Steam	Air
Turbine Capacity (Net) (MW)	377	100	50	50	20	20	11	10	5	3	2.5	1.5
Electricity Generation MWh/yr	**1 079 323**	**485 000**	**180 000**	**120 000**	**110 000**	**48 000**	**23 400**	**1 950**	_	_	_	_

Ivanpah solar electric generating system

crescent Dunes Solar Energy Project

Khi solar one

Supcon solar project

Gema solar thermo solar plant

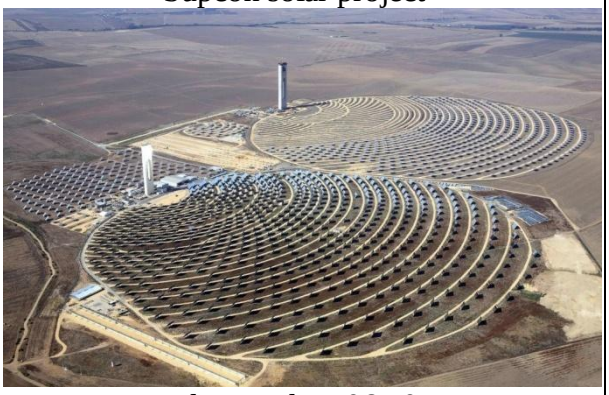

Planta solar 20&10

Jülich solar tower

Sierra sun tower

Fig.2.2. Examples of Solar Power Tower Projects [google maps]

It is interesting to note that the most of these plants are located at nearly the same latitude (28°11’ N to 38°14’ N) (fig.2.3) but the layouts are different because different types of receivers are used. At these latitudes the sun is due south throughout the year.Therefore in the PS 10, PS 20, ACME, Dahan and Solugas plants, using single cavity receivers, it is appropriate to locate all heliostats to the North of the tower. The Gemasolar plant uses an external cylindrical receiver, consequently the heliostats are located all around the tower (surround field), but higher number of heliostats are on the northern side.

Fig.2.3. worldwide solar tower thermal power plants [google Maps]

3. Main components of solar power tower

Central Receiver uses a large number of heliostats, having dual axis control system (one about the vertical axis and the other about the horizontal axis). These heliostats reflect the solar radiation (impinging on their surface) to a stationary receiver located at the top of a tower. This concentrated solar energy incident on the receiver is converted to thermal energy, which is carried by the HTF passing through the receiver. The thermal

energy of the HTF is transferred to the working fluid of the power cycle, thereby generating electricity.

The advantage of solar power tower is that a high geometrical concentration ratio ranging from 200 to 1000 can be achieved. Consequently, temperatures of the order of 1000°C can be reached with suitable HTF's. The high temperature leads to an increase in the power cycle efficiency. As a result of this, potentially, an overall solar to electric conversion efficiency of around 28% can be achieved. The major components involved in the solar power tower system are explained below

3.1.Heliostats

A noted advantage of the concentrating solar power (CSP) tower technology compared to other CSP technologies such as parabolic trough or linear Fresnel is that the receiver operates at a higher thermal efficiency due to the high incident flux concentration on the receiver surface. But unlike other CSP technologies, the power tower concept requires reflected solar radiation from the sun-tracking mirrors (heliostats) to travel significant distances to a tower-mounted receiver. This distance can be on the magnitude of 1 km or more for large plants [10]

Since the average distance between a heliostat and the receiver is considerable, precise construction, installation, and control of the heliostats is required to ensure that optical losses are minimized. This requirement results in the heliostat field capital cost being disproportionately large with respect to the overall plant cost. [11] Note the heliostat field capital costs ranges from 30-40% of the total plant capital costs. As a result, careful optimization of the capital-intensive heliostat field is essential for an economically viable power tower system.

A thorough understanding of the mechanisms affecting heliostat field performance is beneficial in achieving an optimized heliostat field layout (where the power reflected to the receiver is optimized in terms of capital cost per unit area of mirror surface).

3.1.1. Heliostat Field Performance Background

The performance of solar power tower depends strongly on the solar field efficiency which in its turn is related to the heliostat design, the field layout, the tracking system and control system. The central receiver system heliostat field contains a varying but generally large number of individual heliostats. The number of heliostats is dependent on the size of individual heliostats and the desired system thermal power. Heliostat geometry can also vary widely with height, width both circular and rectangular variations are possible.

Regardless of heliostat geometry, the heliostat is subject to a number of optical losses that result in a reflected image on the receiver surface that is somewhat less than the amount of solar energy originally incident on the surface of the heliostat.

The following subsections discuss loss mechanisms and demonstrate layout techniques designed to overcome the losses to the greatest possible extent. Certain layout patterns emerge as a result, and these common field configurations are also presented.

3.1.2. Field Layout Configuration

a. Radial Configuration

In this configuration, the heliostats are arranged such that they form circles around the tower. For this configuration there are two technology the first one shown in (Fig.2.4) This configuration surround field applied in the heliostat field of the Gema solar plant.(fig.2.2). the second is the north field configurations shown in (fig 2.5) the heliostats are arranged such that a heliostat immediately behind another one is offset circumferentially by a small distance so that they are not in a line. this field used for the PS 10 and PS 20 towers (fig2.2.)

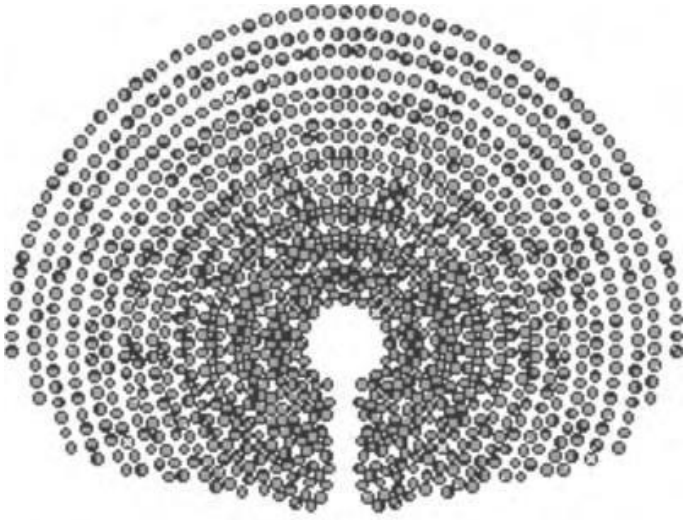

Fig.2.4. Representation of optimized fields for latitude of 360° with surround field[12]

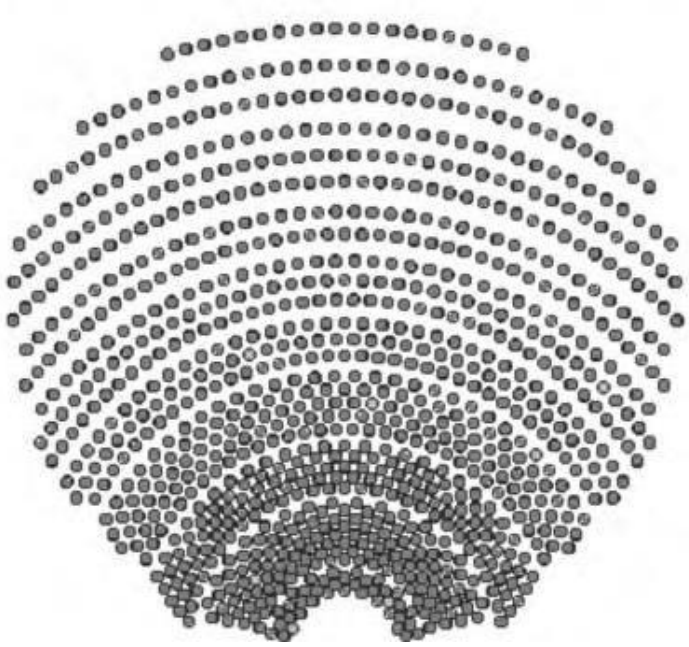

Fig.2.5. Representation of optimized fields for north field configurations.[12]

b. Straight field Configuration

Or the cornfield layout, as the name suggests, refers to a configuration where the heliostats are arranged in straight rows, one behind the other. This is used in julich power tower (fig2.2) it is a single field where in this case the field is only on one side of the tower a cavity receiver is used with a single side aperture. the same configuration in sierra sun tower (fig2.2) the field of heliostat are arranged in strainght tows

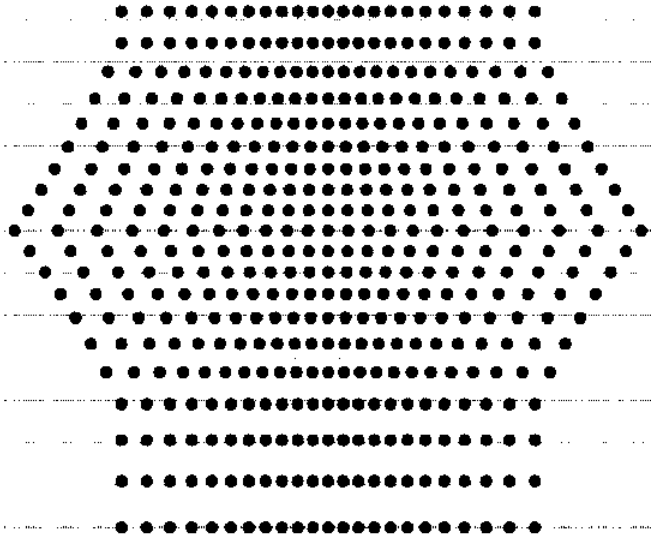

Fig.2.6. Heliostat field Straight Configuration

3.1.3. Losses from the Heliostat Field

A number of losses can adversely affect the performance of the heliostat field as shown in the figure below (fig.2.7) an illustration of the losses that must be considered while evaluating the optical performance of a power tower. There are several quantities that control the thermal power transferred to the top of a receiver in a power tower plant. These quantities can be categorized as enrgetical, geometrical, and material Among these quantities, geometrical quantities can be estimated and summarized into one 'characteristic function' without major approximations. This characteristic function can be defined for a specific sun position as the effective surface area of all the heliostats, in a given field, that reflects the beam radiation onto the receiver. The geometrical quantities could relate to heliostat area or to ground area. (Fig.2.8) shows the nomenclature of the factors to be considered while evaluating at the optical performance of a power tower plant.

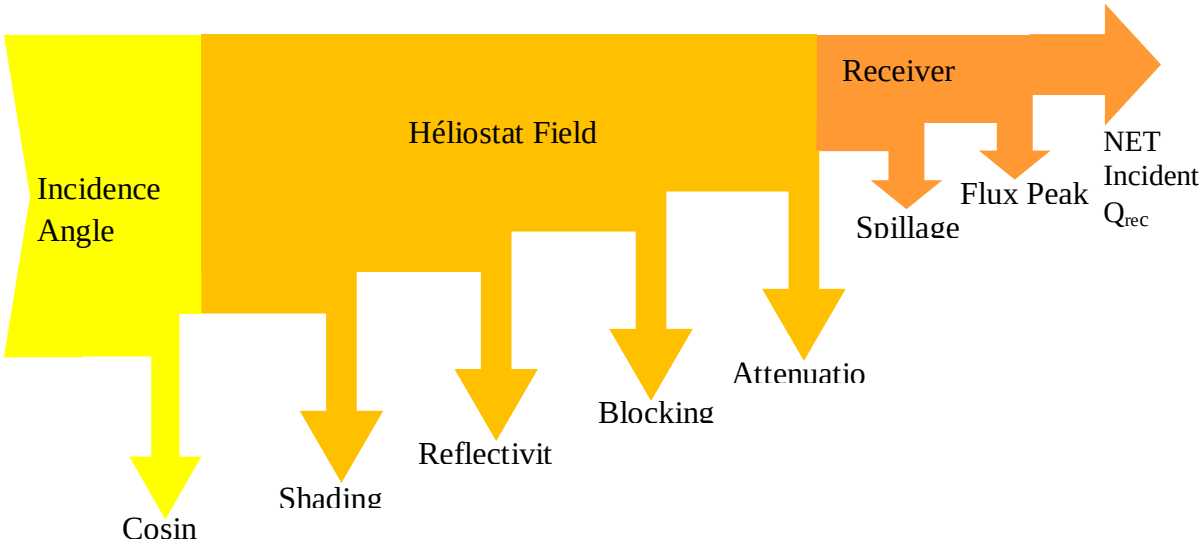

Fig.2.7. Optical losses in a power tower plant

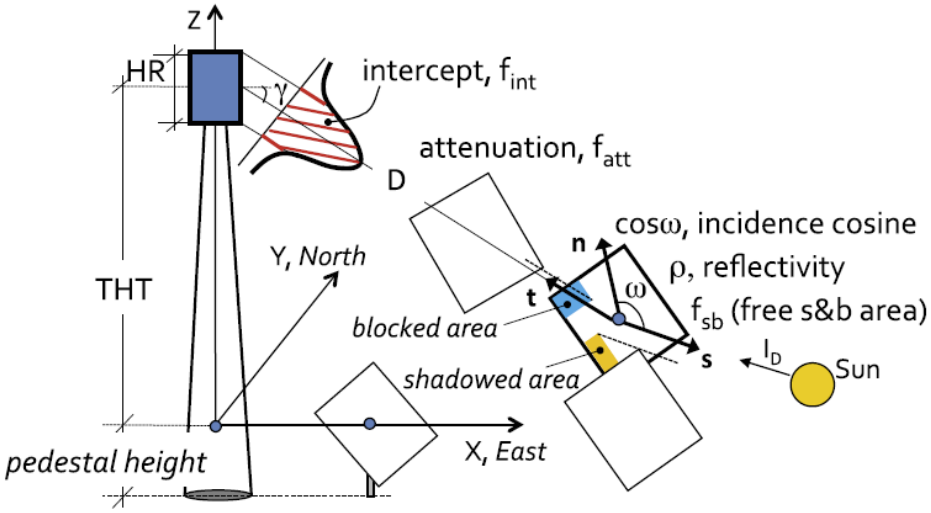

Fig.2.8. Nomenclature of optical efficiency in heliostat fields [13]

a. Cosine effects

A heliostat facet which is not normal to the sun, will not be able to reflect all the beam radiation falling on it and this radiation is reduced by the cosine of the angle between the collector normal and the sun. This effect is known as the cosine effect and is one of the major factors in the calculation of the annual optical heliostat field efficiency.

The cosine efficiency of the heliostat field depends on the position of the sun and the relative position of each heliostat in the field with respect to the receiver (fig.2.9)

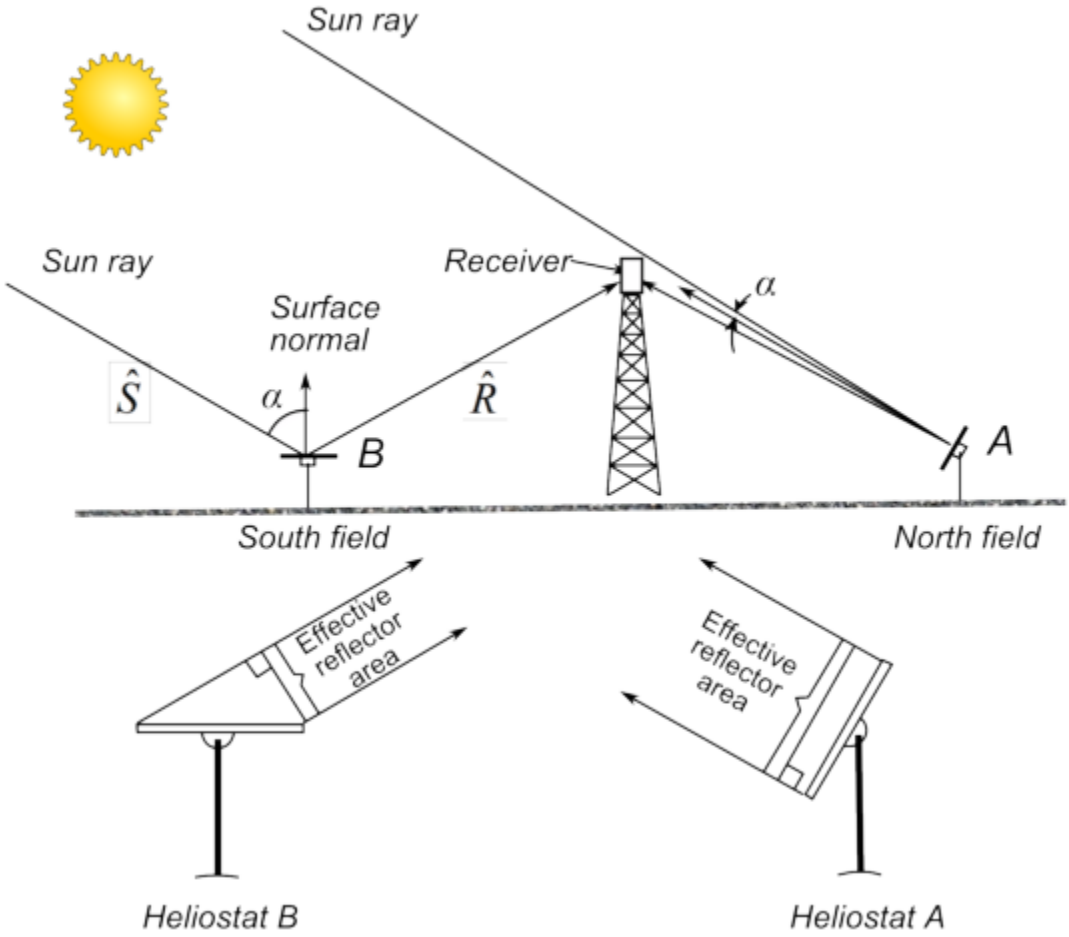

Fig.2.9. The cosine effect as seen on two heliostats A and B; A is placed in the North and B in the South [12]

b. Shading efficiency

Shading losses occur when one or more heliostats cast their shadow on a neighbouring heliostat. These losses, like blocking losses, are dependent on the placement of heliostats in the field and occur before the beam radiation hits the heliostat. These losses are highest when the sun is very low in the sky: in the early morning or in the late evening. These losses can be obtained by projecting the polygons of the nearby heliostats on the heliostat considered in the direction of the sun [14], However, a few studies are of the opinion that shading losses are negligible as they occur during low sun angles and the plant is not in operation during these hours [15]. Blocking efficiency is sufficient to get an idea about the annual efficiency trends and the final heliostat field layout. Furthermore, including shading losses could lead to a 'cascaded' loss in

efficiency, where heliostats that would otherwise be excluded due to high blocking losses, shadow 'productive' heliostats and cause their removal from the field layout.

c. Reflectivity

In a power tower plant, mirrors are the first link in the conversion of energy from the sun to the electrical energy delivered to the grid. The shape of the mirror and the solar reflectance are of primary importance to estimate how beam radiation is concentrated and the amount of radiation reflected [16], According to Snell's law, the angle of incidence and the angle of reflection are equal for specular reflection and are measured from the surface normal at the reflected point. For heliostats, the surface normal on a point on the facet can deviate due to the optical errors like slope errors and improper tracking. This has an effect on the reflected image of the heliostat. Astigmatic aberrations and accumulated dust on the mirrors [17] also have an effect on specular reflectance. A value of 0.95 is assumed for solar reflectance of the mirror and a soiling factor of 0.95 . Hence the total optical reflectance of the mirror facets is taken as 0.9025.[18]

d. Blocking effeects

Blocking occurs when a heliostat blocks a neighbor's reflected beam radiation to the receiver [19] Blocking is exclusively a function of the placement a heliostat with respect to the others in a given field. With increasing heliostat sizes, the effects of blocking increases and a trade-off between packing density and blocking effects must be the deciding factor [20].

a graphical method for 'no-blocking' heliostat field layout has been described by Siala and Elayeb (2001). According to this method, the minimum azimuthal distance between two heliostats in a row is twice the heliostat width. With an increase in the radial distance between the rows, the azimuthal distance continues to increase till a certain value is reached when it is reset again to twice the heliostat width. The position of the rows, are then determined so that heliostats that lie directly behind the next row are placed properly to ensure the 'no-blocking' effect. (fig.2.10) shows that the beam radiation reflected by the lowermost part of the distal heliostat is not blocked by the uppermost part of the proximal heliostat. Each intermediate row does not contribute to

the blocking losses. In this study, blocking losses are eliminated in the heliostat field layout using this method

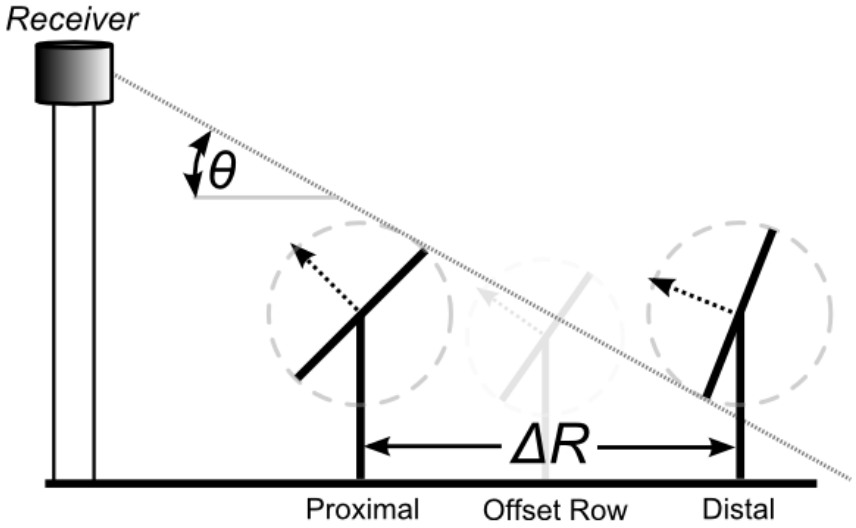

Fig.2.10. 'No-blocking' effect between two heliostats (Wagner, 2015)

e. Attenuation

The beam radiation reflected by the heliostat to the top of the receiver gets attenuated as the slant distance between the heliostat and the tower increases. (Fig.2.11) illustrates this slant distance.With increasing heliostat field sizes, attenuation losses are estimated to be as high as 10 % when the heliostats are placed more than a kilometre away from the tower [21]. Atmospheric transmittances of the direct beam radiation and the losses have been approximated for clear and hazy days in several studies, and more recently in [22].These studies study the effect of atmospheric attenuation as a function of the distance between the heliostat and the receiver An analytical model has recently been proposed by NREL to account for the effects of atmospheric attenuation as a function of the measured direct beam radiation. However, since different sites have various weather conditions, there is a difference between these models and the actual attenuation losses. these analytical models should be validated by actual experiments at the site as it was found that a heliostat field could be 4 % larger due to the water vapour in the atmosphere. However, this is difficult as obtaining ground measured data for a particular location for more than one year can sometimes be difficult.

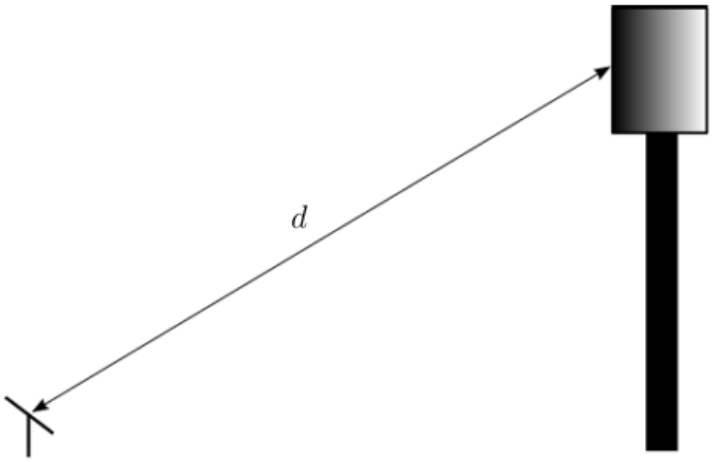

Fig.2.11. Slant distance between the heliostat and the receiver

f. Spillage efficiency

A part of the reflected beam radiation that falls outside the perimeter of the receiver aperture area is lost into the atmosphere and cannot be used for power generation. These losses, known as spillage losses, depend on the type of the receiver: external or cavity type. As shown (Fig.2.12) Image aberration for the heliostat as a function of errors and the sun shape. The resulting reflected image on average is larger than the ideal reflected image.

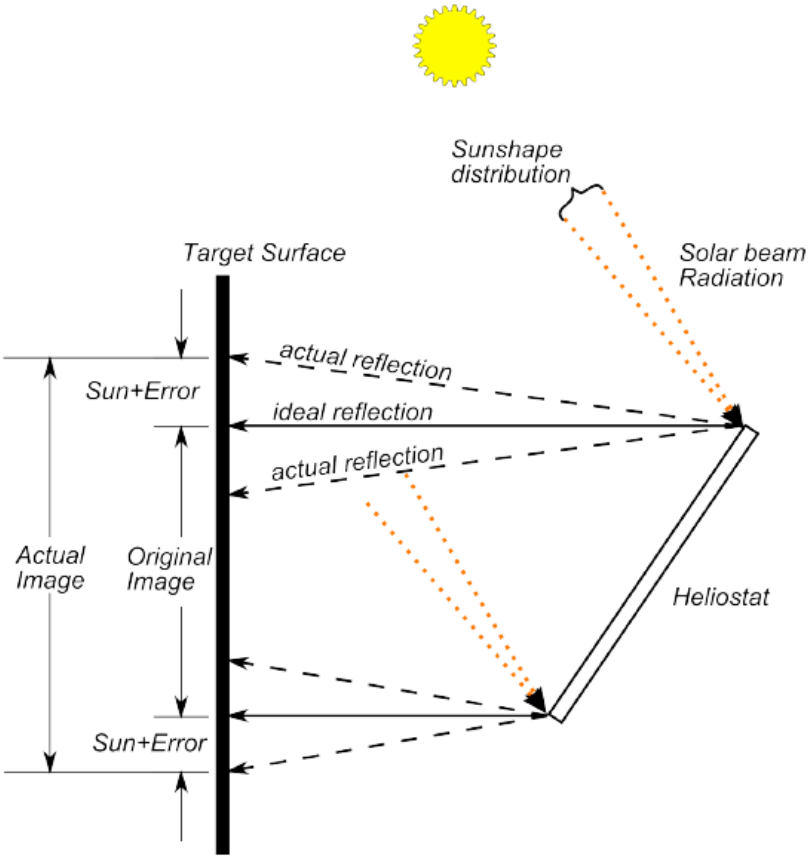

Fig.2.12. Spillage efficiency [18]

3.2.Solar receiver

In power tower systems, the irradiance incident on the heliostat field is reflected at all times on a receiver located at the top of a tower. The incoming energy can have up to several hundreds of MW, depending on the size of the receiver and the size of the heliostat field. The receiver absorbs the solar radiation and heats a HTF (thermal energy conversion) at temperatures that may be over 1000°C and can be used in industrial facilities as process heat, converted into electricity, or used in chemical reactions. This thermal energy is then sent to a steam generator or stored in a storage system. This takes place at high temperatures and high incident solar flux, so it must be done with the least possible loss of energy absorbed (radiation, convection), with the least consumption of electricity and avoiding loss or degradation of the transfer fluid, keeping in mind the long distances it has to cover to go up and down the 50–150 m tower. Many solar

receivers with different configurations and adapted to different HTF There are direct exchange receivers (in which the fluid is exposed directly to the solar radiation) and indirect exchange (when a component converts the solar radiation into heat which is the convectively yielded to the HTF). Receivers can be classified by their configuration into flat and cavity systems and by their technology as tube, volumetric, panel/film and direct absorption. The heat exchange process can take place in the following basic ways:

- Through tubes that receive the irradiance on the outside, absorb the energy through their walls and transmit it to the heat fluid circulating through them. These receivers in turn may be cavity or flat and operate as an indirect recovery heat exchanger.
- Converting the heat and transferring the thermal energy by convection to the air that flows through the volume of a metal or ceramic absorber which may have different shapes. These volumetric receivers operate like a convective heat exchanger.
- Through the use of particles in fluids or jets that receive the irradiance directly in their volume or on their surface. This type of receiver operates like a direct heat exchanger.

Solar receiver designs are thus closely related to the type of plant and thermodynamic cycle. Flat receivers are absorbent surfaces directly exposed to the solar irradiance. In cavity receivers, the solar irradiance passes through an aperture to a box type structure before being absorbed by the receiver surface. Both types have different
thermal loss mechanisms (spillage, convective, reflective, radiative and conductive). In tube and panel receivers, the working fluid circulates through them and is heated by conduction.

Tube technologies make high temperatures or high pressures possible, but not both at the same time. In volumetric receivers, the fluid (usually air) flows through a metal or ceramic mesh and is heated convectively. Volumetric receivers can achieve the highest temperatures at pressures up to 30 bar. Finally, in direct absorption receivers, the solar irradiance is absorbed directly by the working fluid and the receiver is merely a support for it. Working fluids used up to now and at present are: air, water/steam, molten salt

and liquid sodium. The receiver is the real core of a power tower system and the most technically complex component, because it has to absorb the incident irradiance with the least loss and under very demanding concentrated solar flux conditions. A large number of configurations have been tested around the world, most of them at the PSA, with liquid sodium, molten salt, saturated steam, superheated steam, atmospheric air and pressurized air as the coolant

3.2.1. Volumetric Receivers

Volumetric receiver's (fig.2.13) consist of a set of different-shaped metal or ceramic structures, prepared to fill a volume. They may be open to the outside or have a front window. They can work at outlet temperatures of 700°C to 850°C with metal absorbers and over 1000°C with ceramic absorbers. The volumetric receiver works by causing a fluid, usually air, to flow through the absorber volume. The radiation incident on the absorber heats it to high temperatures and the air is heated convectively as it flows through. Usually, the air that flows through the absorber is adjusted to the incident flux density distribution, so that the outlet temperature of the absorber does not form a steep gradient between two different points. When air is sucked through the volumetric matrix, the convective loss is practically nil. As the gas flows through the absorber volume, its temperature increases at the same time as the temperature of the material also increases with depth. Thus the highest temperatures are in the interior of the absorber matrix, thereby minimizing loss. An additional advantage of the volumetric receivers is that since heat is exchanged throughout the internal volume of the matrix, working incident radiation flux can be similar to and even higher than conventional receivers. Maximum flux of 1000 kW/m2 has been surpassed, so that receiver design sizes can be equivalent to salt or steam receivers, even though the thermal properties of air are worse.

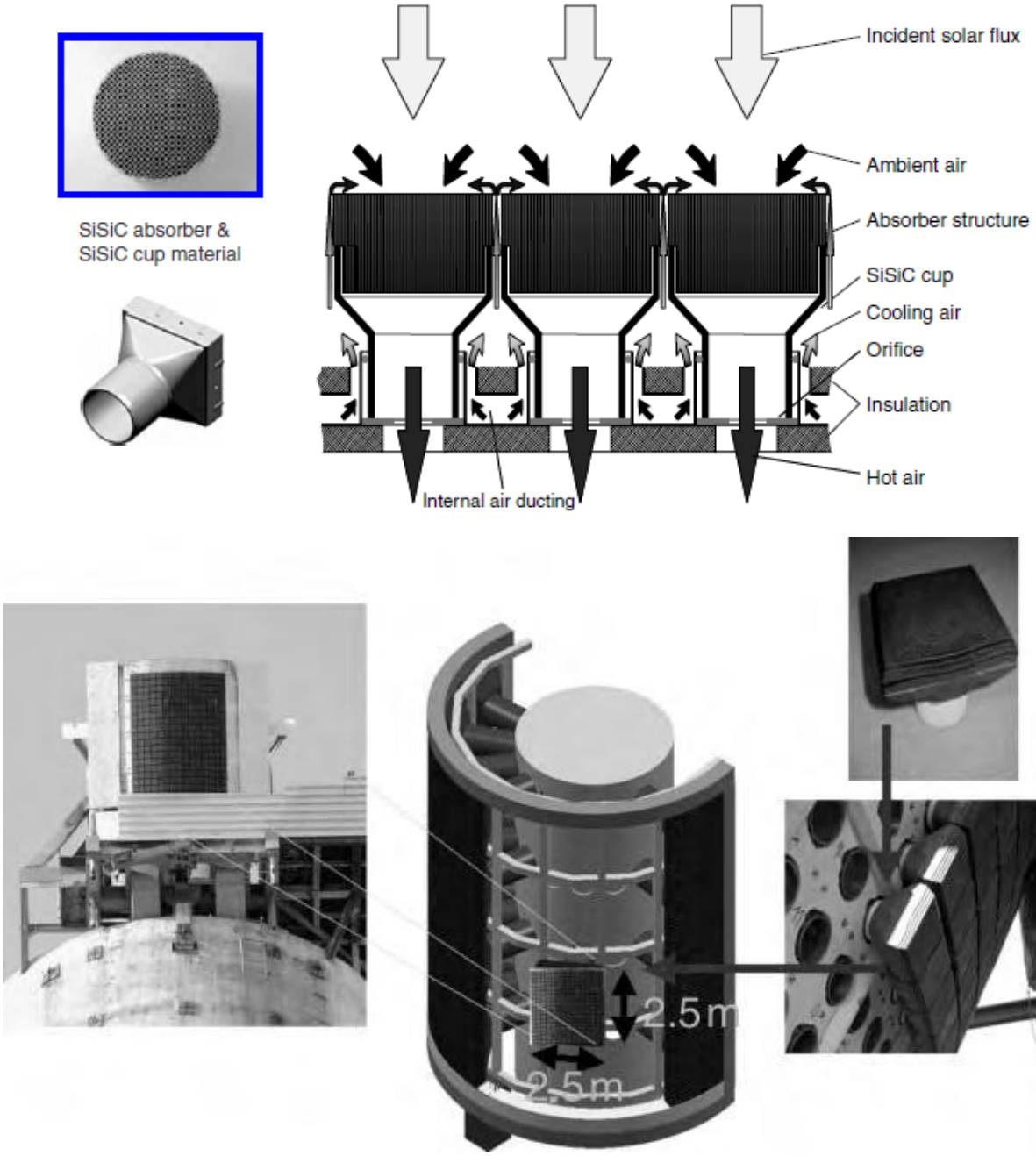

Fig.2.13 Principle of volumetric receivers [23]

3.2.2. Tubular Receiver

The first pilot solar plants had tube receivers in which the heat transfer medium (gas or liquid) flows through the tubes to extract the solar power absorbed on the outside of the tubes. Therefore, the physical processes in this receiver are related to the use of two

transfer surfaces: the solar radiation is absorbed on the outside of the tubes and the heat is extracted on the inside. The heat is transferred from the tube walls by conduction, which is intrinsically associated with a difference in temperature between two surfaces. In these receivers, there is a wide temperature difference between the front (which is exposed to the irradiance) and the back, so the materials are subjected to strong thermal stress which often leads to their deformation or even breakage. Some solutions employed to minimize this problem consist of introducing auxiliary fossil energy on the back (gas burner, etc.) to equalize the temperatures on both sides of the tube.

The configuration may be flat or cavity, but the trend is to manufacture cavity receivers since due to the large surfaces exposed to radiation, there is higher thermal loss in the flat receivers and this loss is minimized in the cavity receivers, which may even be constructed with movable doors so they can be closed when the receiver is not in use to keep the temperature inside and minimize radiation and convection losses.

Depending on which working fluid is used, they operate in a range of up to 120 bar pressure and temperatures up to 550°C for flat receivers and 1000°C for cavity receivers, while average incident flux hardly surpasses 0.5 MW/m^2. This flux is limited by the low heat transfer coefficient between the tube and the coolant, which impedes high temperatures being reached. Its use is limited to generating steam, either directly in the receiver or introducing the working fluid in a steam generator for integration in Rankine cycles.

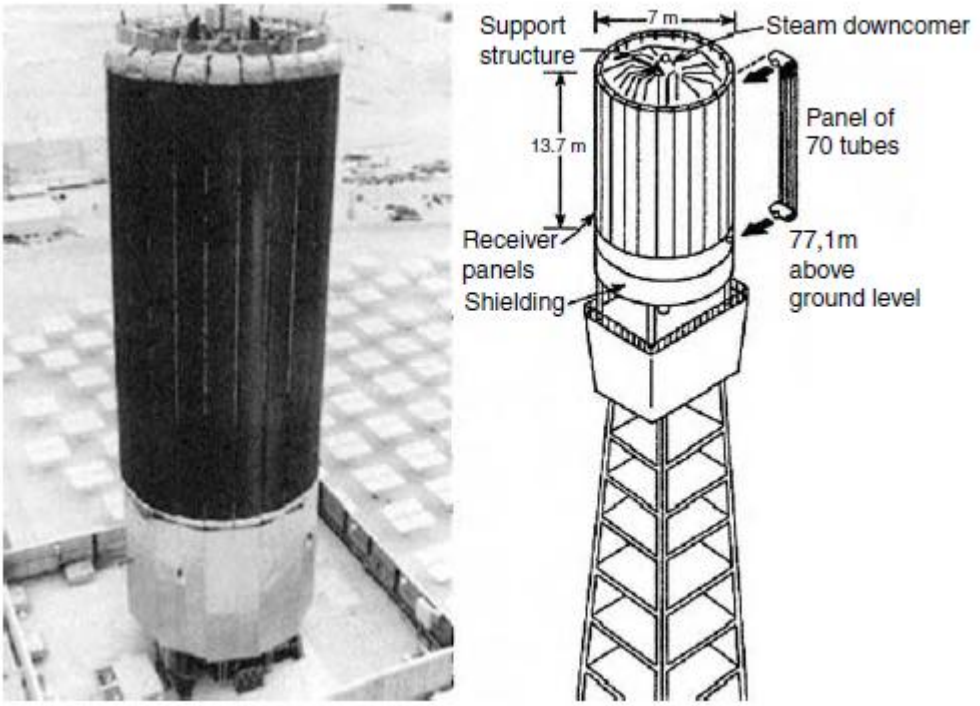

Fig.2.14. External cylindrical tubular receiver [24]

3.3.Power cycle

In the power conversion system thermal energy produced at the receiver is converted into electricity with an efficiency that depends on the thermodynamic cycle and components performance. The three mostly used thermodynamic cycles are: the Brayton cycle the Rankine cycle and the combined cycle.

3.3.1. Rankine Cycle review

The thermal power from the central receiver system is used to drive an electric power generation cycle. The most common generation cycle for this application is the steam Rankine cycle. As with any steam Rankine power generation cycle, the central receiver power cycle can include any variety of configurations to ease implementation and boost efficiency.

R.J. Zoschak and S.F. Wu [25] have examined seven configurations that integrate concentrated solar radiation by CRS into solar hybrid steam cycle of 80 MW, including feed-water heating, water evaporation, steam superheating, combined evaporation and superheating, steam reheating, air preheating, and combined air preheating and feed-

water heating, and the energy balance for each hybrid cycle. Applying the energy balance, they have found that the scheme that uses solar heat for both evaporation and superheating is the most suitable for converting solar energy into electricity. G.Q. Chen et al. [26] have reported the design and the engineering of 1.5MWsolar tower plant in China. They have anticipated that such a solar system is able to save about 3.92E+08 GJ and reduce greenhouse gas emissions by 4.17E+04 tonne of CO2 compared to conventional power plants Z. Yao et al. [27] have described the basic flow calculation of the key components in CRS and their integration to be a whole plant model. In this work the heliostat field has been designed using HFLD code and the total power plant simulated using TRNSYS software. K. Hennecke et al. [28] have reported the technical data about the engineering and the development of the Solar Power Tower Jülich. The Jülich central receiver is used atmospheric air as the heat transfer fluid to generate a steam that used to drive a Rankine cycle. R.K. McGovern and W.J. Smith [29] have investigated the effect of thermal conductance and receiver irradiance on the optimal receiver temperature and the solar conversion efficiency of five power cycles, i.e., Rankine cycle, solar parabolic-trough, solar central-receiver, direct-steam and molten-salts power plant. they have concluded that, for maximum efficiency and optimum receiver temperatures, sub-critical Rankine cycles is preferred for parabolic trough power plants, while super-critical Rankine cycles is suitable for central receiver systems. Z. Wang and Z. Yao [30] have reported the design and data of DAHAN power plant. L.J. Yebra et al. [31] have developed a dynamic model for the simulation and the control of the CESA-I power plant taking into consideration typical operation cycle with a real perturbation introduced by start-up, shutdown and passing cloud. M.H. Moon et al. [32] have developed a program using Visual Basic 6.0 to predict the performance of Dahan solar thermal power plant. S. Alexopoulos and B. Hoffschmidt [33] have overviewed the solar tower technologies. They have indicated that such technology offers many benefits for both power generation and environment. They have then suggested the implantation of central receiver system in Greece and Cypru

3.3.2. Brayton Cycle review

The basic concept of SCR-Brayton cycle consists of a heliostats field, a high tower with volumetric air receiver atop and an adapted gas turbine that is usually installed close to the receiver to reduce additional energy losses at interconnections (at the compressor outlet and combustor inlet). The concentrated solar radiation in the receiver will heat the air, which flows at high pressure coming from the compressor of a gas turbine, up to 100 ºC. This air feeds the combustion chamber of the gas turbine, which increases the temperature to more than 1000 ºC. The main advantages of this technology are a greater efficiency due to the high operating temperature and an efficient hybridization. Using both TRANSYS-STEC and Thermoflex softwares, G. Barigozzi et al. [34] have simulated the real off design performance of a commercial solar hybrid gas turbine. They have come to the conclusion that the hybridization increases pressure losses and reduces compression ratio, and thus, lowering then the overall performance. R. Buck et al. [35] have tested and modified a hybrid GT with a pressurized volumetric air receive. They have examined the concept at several configurations and the potential of such technology to become competitive with conventional plants. U. Fisher et al. [36] have experimentally examined the performance of CRS- hybrid GT in both hybrid and fossil fuel only modes. They concluded that solar hybrid gas turbine operation is technically ready for commercial applications. M. Bhon et al [37] have introduced the technique of solar preheating-Brayton cycle and evaluated its effects on the system performance. They have found that the proposed design provides higher efficiency. The solar fraction is has nevertheless to be limited if higher performance to be attained. P.S. Pak et al. [38] have suggested a hybrid solar fossil system that employs a CO2 as working fluid. This CO2 has been recovered using the method of oxygen combustion. They have found that solar conversion efficiency becomes significantly higher than that of conventional hybrid solar gas turbines that utilize air as working fluid. P.S. Pak et al. [39] have introduced a solar hybrid GT that recovers the CO2 resulting from burning fossil fuel in the combustor. They have then recommended CO2-capturing power process to energy saving and for reducing carbon dioxide emissions.

3.3.3. Combined Cycle review

However the other two cycles combined cycle has a wide interest by the researcher and developers but until now no experiments existing .G.J. Kolb [40] has economically compared various configurations of hybrid and solar only CRS- power plants. He has found that CRS-CC and CRS-Coal- fired plants are more competitive than solar only systems. M. Horn et al. [41] have technically and economically compared two technologies of CSP for integration into CC: HTF-trough and volumetric air receiver. Their findings have been that the hybrid CC with air tower is as efficient as hybrid plant with trough technology. They have also indicated that such a concept presents an attractive option for renewable electricity in Egypt. P. Garcia et al. [42] have compared six simulation environments for solar tower power investigation: UHC, DELSOL, HFLCAL, MIRVAL, FIAT LUX and SOLTRACE. They have then classified them into two groups. The first one comprises optimization codes HFLCAL, UHC-RCELL, and DELSOL. The second group includes performance analysis codes such as FIAT LUX, MIRVAL, UHC-NS, and SOLTRACE. J. Spelling et al. [43] have focused on the thermodynamic and economic performance of solar only SCR-CC with volumetric receiver. They have used a population-based evolutionary algorithm for optimization, and obtained that the combined cycles ranging from 3-18 MWe can achieve efficiencies in the range of 18-24%, with Levelized electricity costs in the order of 12-24 UScts/kWhe. H.W. Price et al. [44] have proposed the use of Air-CRS to power a combined cycle. Their results have been indicated the solar energy can be converted into electricity, at higher exergy level into a Brayton cycle, especially, when high concentration ratio and high temperature are possible.

3.4.Heat Transfer Fluid

Different types of HTFs can be used in solar power tower based on the type of receiver and power cycle employed in the system. The HTF used in the operational plants are water, molten salt and air. Other possible candidates are liquid sodium, Hitec salt and synthetic oil.

3.4.1. Air

Air is used as a HTF when the receiver used is a volumetric receiver, as discussed in the previous section. However, the receiver design is rather complex and also one disadvantage is that air has poor heat transfer properties (thermal conductivity, film coefficient etc) and therefore, the efficiency of heat transfer to the power block is not very high. However, when a CO_2 Brayton cycle is being used, this is minimised to some extent. Compressed air has better heat transfer properties as compared to uncompressed air as it is denser. Air at higher temperatures of the order of 1000°C gives rise to better heat transfer properties but the material constraints of the HTF carrying pipes will have to be considered. Also air does not require cooling water and hence is advantageous especially in locations where water availability is a problem.

3.4.2. Water/Steam

When water is used as HTF, the solar field generates steam directly (Direct Steam Generation) and the Rankine steam cycle is used for power generation. As the HTF is itself water, it eliminates the need of a heat exchanger in order to transfer the heat from the HTF to water (or steam) which is used to drive the turbine in the power block. The minimum temperature at inlet is around 250°C while the maximum possible temperature that has been achieved with water is 566°C.

3.4.3. Molten salt

In the case of molten salt as HTF, a heat exchanger is used to transfer the thermal energy from the HTF to water in order to generate steam. Rankine steam cycle is used for power generation. Use of molten salt as HTF allows easy thermal storage. When the plant is not in operation, HTF from the receiver has to be drained out as the freezing temperatures of the molten salt are relatively high, around 238°C. It can be noted that using molten salt as the HTF is preferred in a solar power tower system rather than a parabolic through system as gravity helps aid the draining of the molten salt at the end of the day in order to prevent it from freezing in the pipes in a parabolic through system, this HTF will have to be pumped out to drain the pipes and this is not very convenient as some auxiliary power source will be required for this purpose.

The advantages and disadvantages of these HTF's are given in Table 2.2

Table.2.2. advantage & disadvantage of deferent heat transfer fluid

	advantages	disadvantages
Air	➢ High temperatures of the order of 1000°C can be utilized.	➢ Poor heat transfer properties (conductivity and film coefficient etc.) compared to other fluids ➢ Complex receiver design
Water Steam	➢ For steam Rankine cycle, water being the working fluid, the need for heat exchanger is eliminated. ➢ Eliminates the costs associated with the salt or oil based HTFs	➢ Dissimilar heat transfer coefficients in liquid, saturated vapor and superheated gas phases. Consequent problems with temperature gradient and thermal stress to be tackled. ➢ Flow control problems with varying solar flux. ➢ Thermal Storage for long hours difficult
Molten salt	➢ Stable and non-toxic and environmentally benign. ➢ High thermal onductivity and thermal capacity. ➢ Operating temperatures can go up to 560°C.	➢ High melting point (~222°C); Needs auxiliary heating to prevent solidification ➢ Highly corrosive at elevated temperatures

4. Conclusion

Solar power tower technology has been lately attracting a lot of attention. A sustainable effort is underway to develop its technology. Tough it has been reached the commercial maturity. As seen from the existing plants, most of the tower plants are employing either the external cylindrical or the cavity type receiver. By using molten salt one can achieve high temperatures along with thermal storage for a long duration. The main advantage of using molten salt is that it can be used both as the HTF as well as the storage medium. there are still a lot of activities at different levels to improve its performance. Examination of the available data has shown that there has been an exponential increase in the installed power. At this level Spain and the USA followed

by China are setting the place for a viable development of a CSP economy. At the regional level, Desertec initiative has been recently advocating and taking steps for the development of CSP in the Mediterranean region.

To see the growth potential of solar tower technology in the next few years the operating plant capacity was calculated The total installed capacity of the power plants worldwide is 1600 MW compared with the Parabolic Trough technology as 2400 MW We can note that power tower capacity is almost comparable to that of Parabolic Trough technology and therefore it needs to be explored and will certainly prove to be a very useful form of energy conversion (solar to electric), in the years to come.

Reference

[1] O. Behar, A. Khellaf, K. Mohammedi, A review of studies on central receiver solar thermal power plants, Renew. Renewable and Sustainable Energy Reviews 23 (2013) 12–39.

[2] Renewable energy technologies: cost analysis series, volume 1: power sector issue 2/5, concentrating solar power. IRENA, June 2012.

[3] Xiong Yaxuan, Wu Yuting, Ma Chongfang, Modibo Kane Traore, Zhang Yeqiang. Numerical investigation of thermal performance of heat loss of parabolic trough receiver. Sci China Tech Sci February 2010; 53(2): 444-452.

[4] Manuel Romero-Alvarez and Eduardo Zarza. Concentrating Solar Thermal Power. Energy conversion (19), Taylor & Francis Group, LLC, 2007

[5] Kolb,G.J., Jones, S.A.,Donnelly,M.W., et al., 2007.Heliostat cost reduction study, SAND2007-3293

[6] William, B.S., Micheal, G., 2001. Power from the sun. Available from: <http://www.powerfromthesun.net/book.htm>.

[7] NREL Web site “http://www.nrel.gov/csp/solarpaces/power_tower.cfm” accessed july 2016

[8] Steinmann, W.-D., Eck, M. Buffer storage for direct steam generation. Solar Energy 2006; 80: 1277–1282.

[9] Y. Tian, C.Y. Zhao. A review of solar collectors and thermal energy storage in solar thermal applications. Applied Energy 2013;
104: 538–553.
[10] Xiudong Wei, Zhenwu Lu, Zhifeng Wang A new method for the design of the heliostat field layout for solar tower power plant in Renewable Energy 35(9):1970–1975 · September 2010
[11] Mehdi Aghaei Meybodi, Andrew C. Beath Impact of cost uncertainties and solar data variations on the economics of central receiver solar power plants: An Australian case study Renewable Energy, Volume 93, August 2016, Pages 510-524
[12] Guillermo Ortega , Antonio Rovirab, Proposal and analysis of different methodologies for the shading and blocking efficiency in central receivers systems; Solar Energy Volume 144, 1 March 2017, Pages 475–488
[13] Francisco J. Collado, , Jesús Guallar , A review of optimized design layouts for solar power tower plants with campo code Renewable and Sustainable Energy Reviews, Volume 20, April 2013, Pages 142–154
[14] Germain Augsburger, E-mail author, Daniel Favrat , Modelling of the receiver transient flux distribution due to cloud passages on a solar tower thermal power plant , Solar Energy
Volume 87, January 2013, Pages 42–52
[15] Francisco J. Collado, , Jesús Guallar, A review of optimized design layouts for solar power tower plants with campo code , Renewable and Sustainable Energy Reviews Volume 20, April 2013, Pages 142–154
[16] M.montecchi et al ,Simplified analysis of solar-weighted specular reflectance for mirrors with high specularity, AIP Conference Proceedings 1734 May 2016
[17] Annie Zirkel-Hofera, Stephen Perrya, Sven Fahra, Korbinian Kramera, Anna Heimsatha, Stephan Schollb, Werner Platzera, Improved in situ performance testing of line-concentrating solar collectors: Comprehensive uncertainty analysis for the selection of measurement instrumentation , Applied Energy Volume 184, 15 December 2016, Pages 298–312
[18] Arvind Sastry Pidaparthi book ”Heliostat Cost Reduction for Power Tower Plants”

[19] Zhiwei Huang1, 6, 8, Kaifu Chen3, 4, 8, Jianhuai Zhang1, 8, Yongxiang Li1, 8, Hui Wang2, 5, Dandan Cui1, Jiangwu Tang7, Yong Liu7, Xiaomin Shi1, Wei Li3, 4, Dan Liu1, Rui Chen2, 5, Richard S. Sucgang1, A Functional Variomics Tool for Discovering Drug-Resistance Genes and Drug Targets, Cell Reports Volume 3, Issue 2, 21 February 2013, Pages 577–585

[20] Gopalakrishnan Srilakshmi , Challenges and opportunities for Solar Tower technology in India, Renewable and Sustainable Energy Reviews 45(May 2015):698–709 February 2015

[21]Manajit Sengupta and Michael J. Wagner , Impact of Aerosols on Atmospheric Attenuation Loss in Central Receiver Systems; solarpaces sptember 20-23 2011

[22] Z. Tahboub.A.oumbe.Z Hassar Modeling of Irradiance Attenuation from a Heliostat to the Receiver of a Solar Central Tower . Energy Procedia Volume 49, 2014, Pages 2405-2413.

[23] B. Hoffschmidt, R. Pitz-Paal, P. Rietbrock and M. Boehmer,solar receiver, US patent number 6003508, DLR , December 1999

[24] William B. Stine and Michael Geyer, book "Power From The Sun" 2001 Available from: http://www.powerfromthesun.net/book.html

[25] Zoschak RJ, Wu SF. Studies of the direct input of solar energy to a fossil-fueled central station steam power plant. Solar Energy 1975; 17:297–305.

[26] G.Q. Chena, Q. Yanga, Y.H. Zhaob, Z.F. Wang. Nonrenewable energy cost and greenhouse gas emissions of a 1.5MW solar

power tower plant in China. Renewable and Sustainable Energy Reviews 2011; 15: 1961–1967.

[27] Zhihao Yao, Zhifeng Wang, Zhenwu Lu, Xiudong Wei. Modeling and simulation of the pioneer 1 MW solar thermal central

receiver system in China. Renewable Energy 2009; 34: 2437–2446.

[28] Hennecke, K., Schwarzbözl, P., Hoffschmidt, B., Göttsche, J., Koll, G., Beuter, M., Hartz, T. The solar power tower jülich1a olar thermal power plant for test and demonstration of air receiver technology. In: Proceedings of ISES Solar World Congress 2007: Solar Energy and Human Settlement, 2007; 5: 1749-1953.

[29] Ronan K. McGovern, William J. Smith. Optimal concentration and temperatures of solar thermal power plants. Energy Conversion and Management 2012; 60: 226–232.
[30] Zhifeng Wang, Zhihao Yao, Jun Dong, Hongguang Jin, Wei Han, Zhengwu Lu, Xiudong Wei. The design of a 1MW solar thermal tower plant in beijing, china. In: Proceedings of ISES Solar World Congress 2007: Solar Energy and Human Settlement, 2007; p.1729-1732
[31] L.J. Yebra, M. Berenguel, S. Dormido, M. Romero. Modelling and Simulation of Central Receiver Solar Thermal Power Plants. In: Proceedings of the 44th IEEE Conference on Decision and Control, and the European Control Conference 2005; 7410-7415.
[32] Myung-Hoon Moon, Yong Kim, Kyung-Moon Kang, Jo Han Ko, Tae Beom Seo. System performance estimation for a solar tower power plant. In: Proceedings of ISES Solar World Congress 2007: Solar Energy and Human Settlement, 2007; 5: 1899-1903.
[33] Spiros Alexopoulos, Bernhard Hoffschmidt. Solar tower power plant in Germany and future perspectives of the development of the technology in Greece and Cyprus. Renewable Energy 2010; 35: 1352–1356.
[34] G. Barigozzi, G. Bonetti, G. Franchini, A. Perdichizzi, S. Ravelli. Thermal performance prediction of a solar hybrid gas turbine.
Solar Energy 2012; http:// dx.doi.org/10.1016/j.solener.2012.04.014, in press.
[35] Buck R, Brauning T, Denk T, Pfander M, Schwarzbozl P, Tellez F. Solar-hybrid gas turbine-based power tower systems (REFOS).Journal of Solar Energy Engineering 2002;124:2–9.
[36] Fisher U, Sugarmen C, Ring A, Sinai J. Gas turbine solarization-modifications for solar/fuel hybrid operation. Journal of Solar Energy Engineering 2004;126:872–8.
[37] Bohn MS WTA, Price HW. Combined-cycle power tower. Proc ASME/JSME Int Solar Energy Conf. New York: ASME Press; 1995. p. 597–606.
[38] Pak PS, Hatikawa T, Suzuki Y. A hybrid power generation system utilizing solar thermal energy with CO2 recovery based on oxygen combustion method. Energy Conversion and Management1995; 36:823–6.

[39] Pak PS, Suzuki Y, Kosugi TA. CO2-capturing hybrid power-generation system with highly efficient use of solar thermal energy.Energy 1997; 22:295–9.

[40] Kolb GJ. Economic evaluation of solar-only and hybrid power towers using molten-salt technology.SolarEnergy1998; 62: 51–61.

[41] Horn M, Fuhring H, Rheinlander J. Economic analysis of integrated solar combined cycle power plants: a sample case: the economic feasibility of an ISCCS power plant in Egypt. Energy2004; 29: 935–45.

[42] Pierre Garcia, Alain Ferriere, Jean-Jacques Bezian. Codes for solar flux calculation dedicated to central receiver system applications: A comparative review. Solar Energy 2008; 82: 189–197

[43] James Spelling, Daniel Favrat, Andrew Martin, Germain Augsburger. Thermoeconomic optimization of a combined-cycle solar tower power plant.

[44] Price HW WDD, Beebe HI. SMUD Kokhala Power Tower Study. Proc of the 1996 international solar energy conference. San Antonio, Texas 1996.p.273–279.

CHAPTER III

Solar thermal power in Algeria

1. Introduction

The promotion of renewable energy is a major thrust of the Algerian energy and environmental policy, and the benefits of these energies have been recognized for the economic development of the country. Each of the channels of renewable energies in Algeria was examined, taking into account its potential for development, given the nature of the needs to be met and the resources (oil, sunlight, wind).

Algeria enjoys very important renewable, particularly solar energy resources. In light of the high economic and social stakes that these energy resources present, a national strategy for the promotion and development of renewable energy applications has been set up. Algeria has given a strategic and a priority character to renewable energy sources through a legislative framework enacted to this end. In order to implement the renewable energy strategy, various programs are underway. Besides the action on education and capacity building, efforts are made in research and development projects, and in scale demonstration and field testing projects. Commercial projects are also underway at the national, bilateral and regional level. In these programs, the largest share is dedicated to solar thermal power.

2. Algeria Energy Status

Algeria plays a central role in the energy world, as it is a major producer and exporter of oil and natural gas. In 2008, Algeria produced approximately 1.4 million barrels per day of crude oil, of which 85% was exported, and 86.5 billion cubic meters of natural gas, of which 70% was exported, mostly to Europe. Algeria was the fourth largest crude producer in Africa, and the sixth largest natural gas producer in the world. Oil and gas export revenues account for more than 95% of Algeria's total export revenues, around 70% of total fiscal revenues, and 40% of gross domestic product (GDP). Compared to other developing countries with a similar GDP, Algeria's energy consumption is high: 1.2 tons of oil equivalents and 840kWh of electricity per capita. However, these figures include self consumption and losses in the energy sector due to LNG exports. The share of oil in the country's overall consumption fell from 40% in 1990 to 34% in 2007; the share of gas increased from 57% to 64%. In industry, gas accounts for nearly 53% of final consumption. Gas consumption also increased substantially in the residential sector, and in 2007 accounted for 46% of final energy consumption. This evolution shows the progressive adequacy of offer structure to the structure of our present reserves, richer in natural gas [1,2] (Fig.3.1). Algeria's revenues come mainly from exporting fossil fuels. In spite of a clear progression of national consumption, exportations' share in energy commercial production remains determining (80%). It has passed from 56 million tons of oil equivalent in 1980 to 133 million tons of oil equivalent in 2003 and 142 million tons of oil equivalent in 2005. Reserves of oil announced in Algeria are 4.5 billion of tons of oil equivalent. Estimates of natural gas reserves, in 2004, were around $4.52\times10^{12}m^3$, which implies a lifetime of 62.2 years compared with an expected 61.9 years globally [3]. The national energy commercial consumption passed from 6 million tons of oil equivalent in 1970 to 32.7 million tons of oil equivalent in 2002, over 35.2 million tons of oil equivalent in 2003 and just under 40 million tons of oil equivalent in 2005. In unit terms, national consumption passed from 0.3 tons of oil equivalent /inhabitant in 1970 to 1 tons of oil equivalent /inhabitant in 2003 that is a tripling of the unit consumption in 30 years. The production of electricity in Algeria was 25.8 billion kWh in 2002 and 40.06 billion kWh in 2007 and the country

consumption is between 25 and 30 TWh/year [4]. As Algeria population grow many faster than the average 3%, the need for more and more energy is exacerbated. In Algeria, the consumption of energy at the national level is increasing year after year due to demographic and urban development, in addition to economic development in constant progression. As far as the resources are concerned, based essentially on oil and natural gas, they are not unlimited and are slowly being exhausted. Algeria generated, over the last 5 years, 185.8×10^9 kWh of electricity. Conventional thermal sources of which natural gas accounted for 94.5%, contributed almost all of Algeria's electricity, supplemented by a small amount of hydroelectricity (5%) and solar photovoltaic/wind (0.5%) [5]. Algeria is now positively disposed to the promotion of RES and views renewables as a way of promoting the development of small and local businesses in selected areas and diversifying supply patterns at the regional level. Algeria has developed national programmes and set national indicative targets for renewable: to pursue the development of alternative electricity sources, including solar and wind to achieve a share of renewable energy sources in primary energy supply of 5% by 2017 and 10% by 2020.

For Algeria, the development of solar thermal power is of paramount importance. Algeria enjoys qualitatively and quantitatively important solar energy resources. The exploitation of these resources opens new opportunities. First the development will strengthen the actions undertaken for regional balance and improvement of life conditions particularly in the rural and isolated area of the South. Second this permits the increase and the diversification of the national energy mix with all the implications that could have on the export opportunities and on the national revenue. Finally, the development of this energy addresses the world wide concern of the negative impacts on the environment using the conventional energy sources; and this could also stop or even reverse desertification and promote arid land development

3. Renewable energies potentials

The size of the Algerian Sahara could capture enough solar energy to meet the entire world's electricity needs, The assessed potentials (economic), by the German Space Centre (DLR), of renewable energy sources in Algeria are [6]:

• Thermal solar (TS): 169,440 TWh/year

• Photovoltaic (PV): 13.9 TWh/year

• Wind energy (WE): 35 TWh/year

Algeria is in urgent need of an adequate energy infrastructure so that it can achieve higher levels of economic development. This would allow all of its inhabitant's access to a quality energy supply, irrespective of their place of residence. Crucial objectives are targeted at substantially increasing and enhancing the contribution of renewable energies and favouring energy self-sufficiency. Pilot projects implemented in recent years justify the possibility to accelerate the use of indigenous energy resources, particularly for electricity supply.

The Government of Algeria has introduced a national program for integration of renewables with an objective to reach 5% of power generation by 2017 and a long-term target of achieving 20% renewable energy power by 2030. Further, the long-term goal is to be met primarily from the Concentrated Solar Power (CSP) (70% CSP, 20% wind and 10% PV) which would make it among the world's most ambitious CSP programs. Through a March 2004 decree, the Government also introduced incentives for electricity production from renewable energy plants, including a feed-in tariff

In the context of the implementation solar energy program adopted by Algeria, the evolution of the electrical energy production form CSP is reported in (Fig3.1).

This produced electrical power is meant not only for local consumption but also to export to Europe.

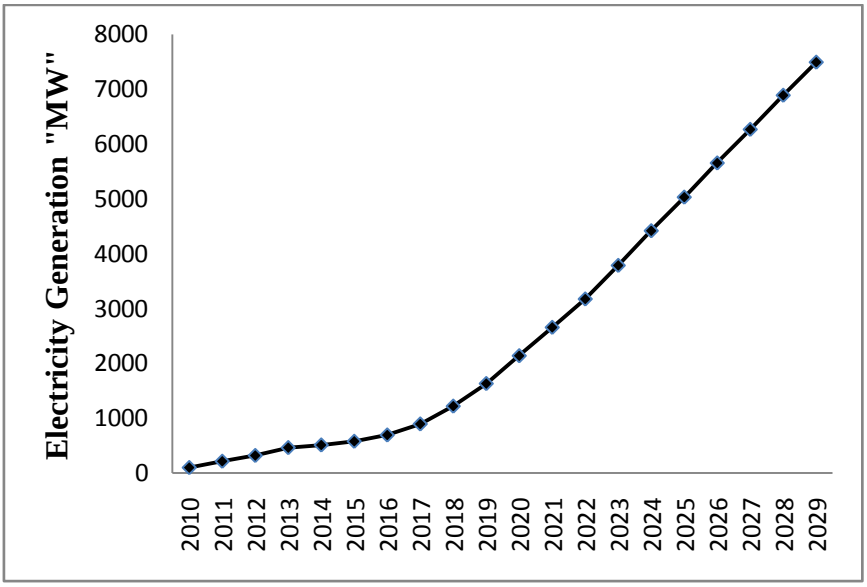

Fig.3.1. Evolution of energy generation in Algeria **[7]**

4. Solar energy characterization

Located in North-west Africa, Algeria covers an area in excess of 2 381 740 square kilometers. More than four fifth of its land is a desert. It lies at latitudes from 18° to 38 ° north and at longitudes from 9° west to 12° east. Its coast on the Mediterranean Sea extends over 1200 km. It stretches southward on 1800 km as far as the tropic of cancer. Solar radiation intensity in the regions selected for the study has been determined by the software Meteonorm for the period extending over the ten most recent years.

Algeria has the most important solar potential in the MENA region and one of the best in the world for both CSP and PV applications (Fig.3.2).

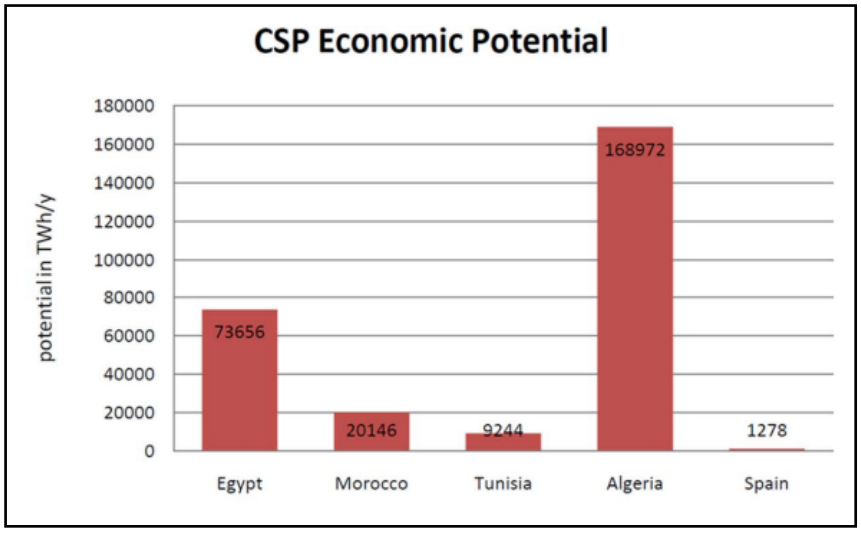

Fig.3.2. economic potential of most active countries in CSP in MENA

For the different climate conditions, three different sites representing the national climate conditions are chosen. As shown in (Fig.3.3) The chosen sites are Tamanrasset for the extreme southern Sahara desert, Hassi R'Mel for the northern Sahara and Algiers for the Mediterranean coastal area.

In our study we used The software Meteonorm it offers the possibility to create climate data for any location worldwide. Meteonorm calculations are based on the 10-year averages and give maximum radiation values under clear sky conditions. According to Meteonorm, comparisons of the measured solar radiations for longer periods show a discrepancy of less than 2% for all weather stations but computational models show less inaccuracy than the variation in measured total radiation between one year and the other. The objective of this work is to constitute a file containing the hourly data direct irradiation for the three sites selected over a year considered representative.

Fig.3.3..Algeria map showing the different locations

4.1.Temperature

Northern Algeria lies within the temperate zone, and its climate is similar to that of other Mediterranean countries, although the diversity of the relief provides sharp contrasts in temperature. The coastal region has a pleasant climate, with winter temperatures averaging from 10° to 12°C and average summer temperatures ranging from 24° to 26°C.

Farther inland, the climate changes; winters average 4° to 6° C , with considerable frost and occasional snow on the massifs; summers average 26° to 28° C . In this region, prevailing winds are westerly and northerly in winter and easterly and northeasterly in summer, resulting in a general increase in precipitation from September to December and a decrease from January to August; there is little or no rainfall in the summer months.

In the Sahara Desert, temperatures range from –10° to 34° C , with extreme highs of 49° C . There are daily variations of more than 44° C . Winds are frequent and violent.

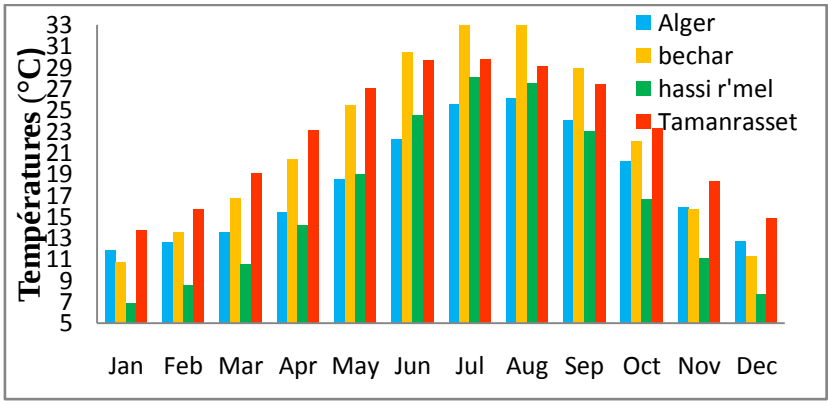

Fig3.4. Temperature variation in the various site

4.2.Sunshine duration

For the northern region, it can be seen from Fig. 3.5, that the average monthly of the daily sunshine duration is 5 hours/day in the winter. However it is much higher in the other seasons. In the summer it could be in excess of 11 hours/day. The yearly sunshine duration is on the average around 2850 hours.

Table.3.1. Monthly Sunshine duration in different locations (hour)

	Algiers	**Hassi R'mel**	**Adrar**	**Tamanrasset**
Jan	166	197	253	252
Feb	170	196	246	248
Mar	200	236	298	258
Apr	223	251	316	254
May	280	295	334	270
Jun	300	314	336	165
Jul	330	352	319	139
Aug	300	328	294	153
Sep	241	271	267	148
Oct	209	245	272	264
Nov	172	203	244	261
Dec	161	193	249	238
year	2752	3081	3428	2650

On the other side, the southern region enjoys a more important sunshine duration. The yearly sunshine duration is on the average 35 00 hours. As can be seen from [Table 3.1], the monthly average of the daily sunshine duration is all the time higher than 8 hours per day; it can peak at 12 hours per day.

Going from northern Algeria to Southern Algeria, sunshine duration increases. This due first to the fact the equator is closer and then to the influence of the climate conditions. Indeed going from north to south, the climate gets drier, meaning less clouds. Indeed, as can be seen from (Fig.3.5), the increase is more important in the winter. As example, it can be seen that the average monthly sunshine duration is about 5 hours/day in Algiers, around 6 hours/day in Hassi R'Mel and more than 8 hours/day for Adrar and Tamanrasset. However for the summer, the difference in sunshine duration between the different sites is no more than half an hour.

Tamanrasset, though located in the Sahara desert enjoys a specific climate and exhibit then a different sunshine duration more particularly in the summer season. Indeed, the summer season is the rainy season there. As a result of cloudy skies, this leads then to shorter sunshine duration by comparison to other sites in the Sahara. For example, the sunshine duration is more than twice longer in Adrar than it is in Tamanrasset for the months of June and July.

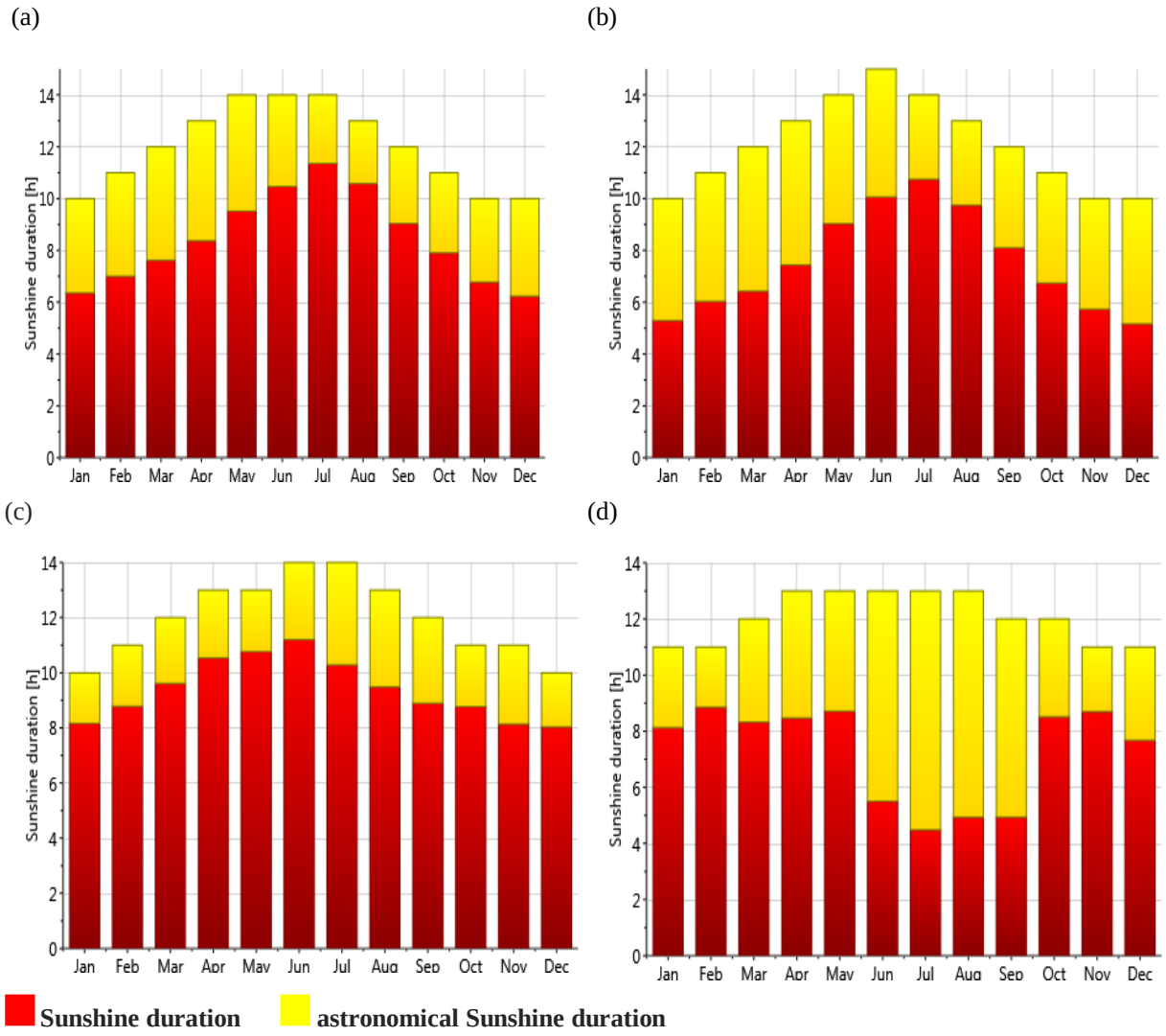

Fig.3.5. Average monthly of the daily sunshine duration: a) Hassi R'Mel b) Algiers c) Adrar d) Tamanrasset

4.3.Global irradiation

Algeria is located in the Sunbelt region. It is characterized by a high solar energy potential. (Fig. 3.6) presents the variation of the global irradiance over the year for the three sites under consideration, namely Algiers, Hassi R'mel and Tamanrasset. As can be seen in this figure, in northern region (Algiers), the global irradiation is all the time higher than 2.5 kWh/m² per day in winter and it can easily reach 7 kWh/m² per day in summer.

In the southern region, the global irradiation is even more important. The monthly average daily global irradiation is, all the time, in excess of 4.5 kWh/m² in winter and it peaks at about 8.5 kWh/m² in the summer

In the summer, the difference in global radiation between the different regions in Algeria is small. This difference is though more important in the winter. Indeed in the winter season the global radiation in Hassi R'mel is about twice that of Algiers and that of Tamanrasset about four times than about of Algiers.

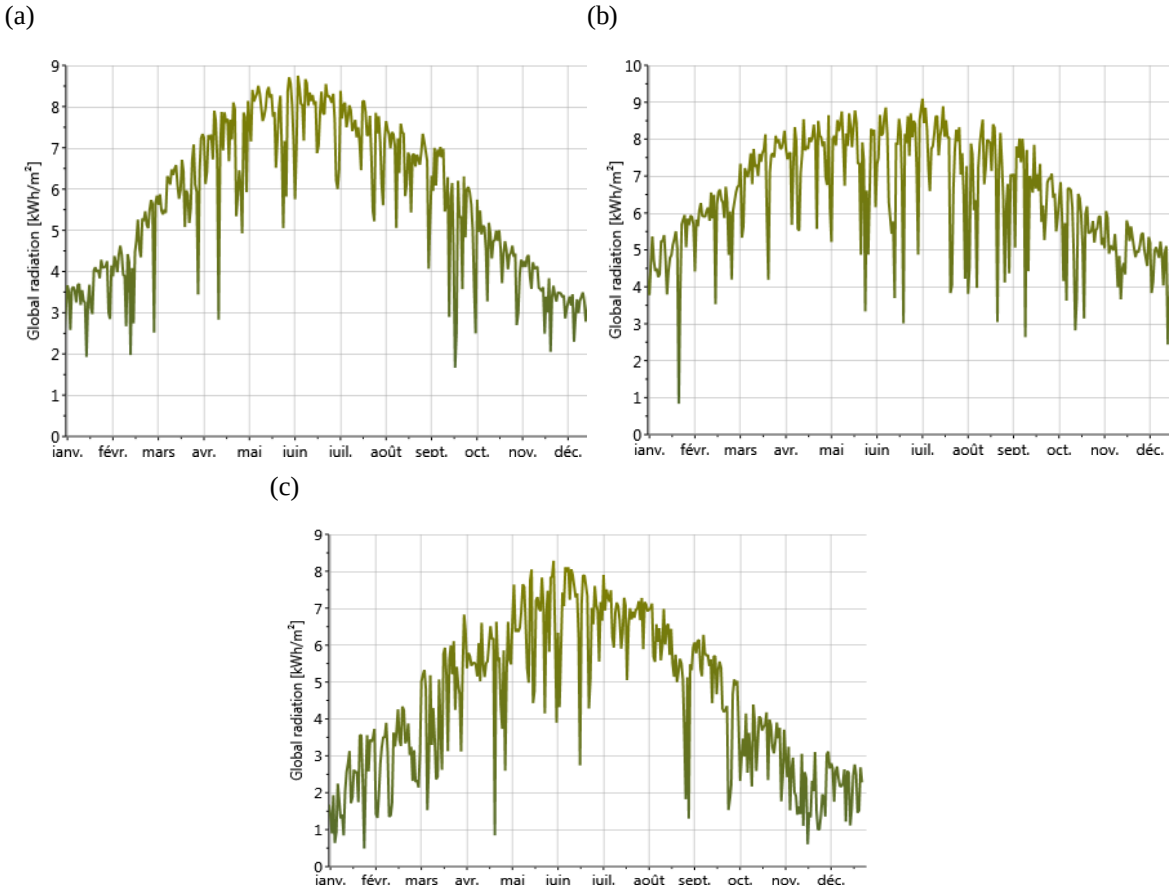

Fig.3.6. Daily global radiation a) Hassi R'Mel b) Tamanrasset c) Algiers

4.4.Direct Normal Irradiation

(Fig. 3.7) shows the evolution over the year of the monthly Direct Normal Irradiance (DNI) for different regions in Algeria. From this figure, it can be seen that Tamanrasset has the highest DNI. This DNI is at least equal 175 kWh/m²/month for the month of February, but it could be as high as 227 kWh/m²/month during the month of April. We

can also see that the DNI in Tamanrasset is the highest over each month of the year except for the month of August where it is slightly lower. For Algiers the DNI varies from 111 kWh/m²/month for December to 210 kWh/m²/month for August. For Hassi R'mel the value of the DNI is the same as that for Algiers for August and September, but it is higher for the other months.

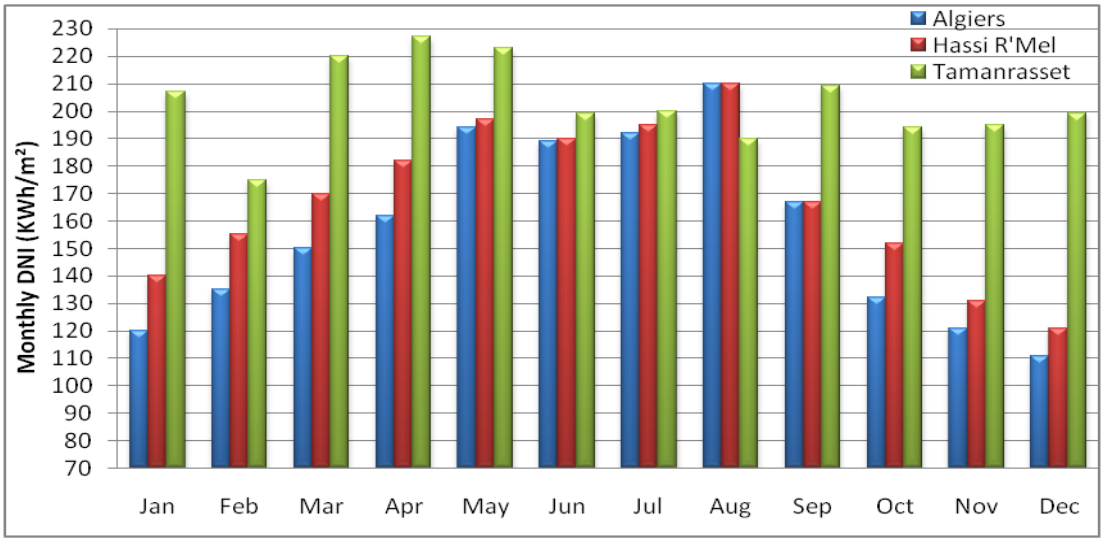

Fig.3.7. Evolution of Monthly DNI (KWh/m²) over the year for selected sites in Algeria

(Fig.3.8)shows the annual DNI for the three sites under consideration. For comparison, the range of DNI for CSP economical viability is also indicated. From this figure, it can be seen that the solar DNI received per year is higher than 1900 kWh/m². This is within the range of the recommended irradiation availability limit for an economical viable installation of CSP system. It has been recommended that the DNI should be in the range 1900 kWh/m² and 2100 kWh/m² [8]. It can be seen that the DNI received for Hassi R'mel and Tamanrasset is much higher than 1900 kWh/m²/year; for the case of Algiers the DNI received per year is though on the lower side of the range of the minimum value of the DNI necessary for a viable CSP installation. For the case of Tamanrasset the value of the DNI is even higher them the upper level of the range of CSP economical viability installation.

The selected locations in the present study clearly meet the above condition. For analyzing the thermal performance of solar thermal power plants, it is necessary to assess the solar radiation intensity.

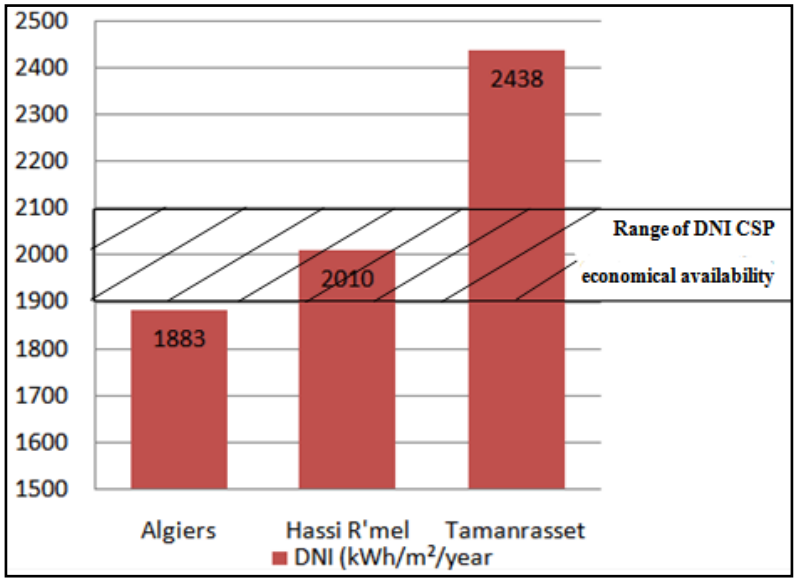

Fig.3.8. yearly DNI compared in the in different locations

To determine the performance of a CSP unit, there is the need for the hourly DNI reaching the heliostats at the chosen sites. To this end, this hourly DNI has been investigated for two periods, namely the winter period when the DNI is at its lowest value and the summer season when the DNI is at its highest value. (Fig. 3.9)&(Fig.3.10) shows the hourly DNI evolution over a typical day for both periods and for all the chosen sites. A typical day of January is taken as representative for the winter while a typical day of June is taken as representative for the summer.

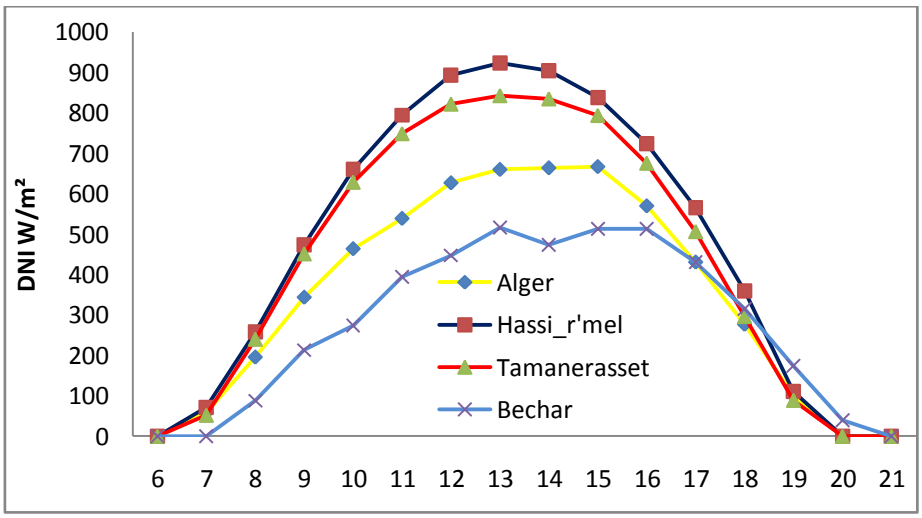

Fig.3.9.Direct normal irradiation at the 4th sites during the 2st June

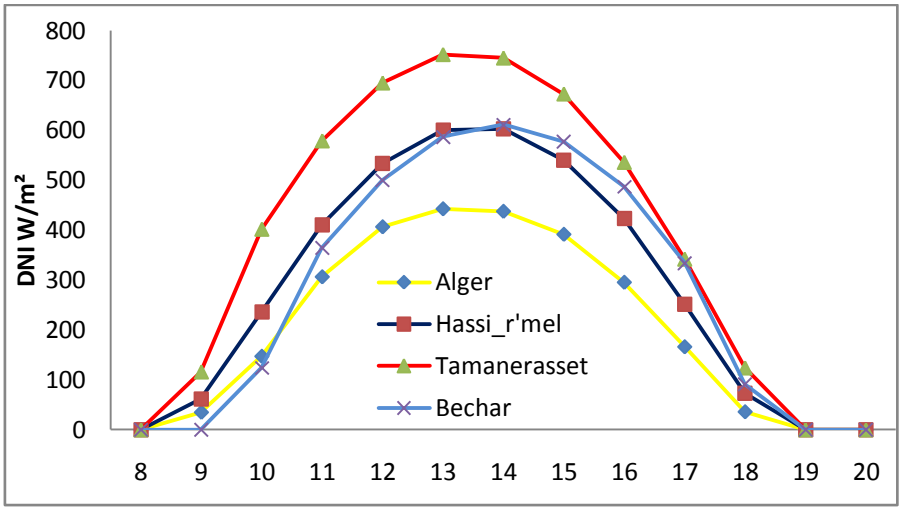

Fig.3.10. Direct normal irradiation at the 4th sites during January 29

it can be seen that the DNI exhibits a fast increase after sunrise. The rate of increase is up to 2000kJ/hr m² over the first two hours. The time when the DNI reaches its maximum depends on the season as well as the site.

Motre importantly, the maximum value reached by the DNI depends on the sites and on the season. This maximum varies from a high value of 2700 kJ/hr.m² for Tamanrasset to 1600 kJ/hr.m² for the winter season. For Hassi R'mel, it is 2200 kJ/hr.m². we can that there is a sizable difference between these maximum values. It can be seen that, by comparison to that of Algiers, this maximum is 37.5 % higher in Hassi R'mel and 68.75 % higher in Tamarasset.

However this is not the case for the summer season. Though the maximum increases for each site, the increase is not the same. This maimum is 2390 kJ/hr.m² for Algiers, 3323 kJ/hr.m² for Hassi R'mel and 3031 kJ/hr.m². In this case, it can be seen that the highest is in Hassi R'mel. The increase over the winter season is 49.37 % for the site of Algiers, 51.05 % for the site of Hassi R'mel and a mere 12.26 % for the site of Tamanrasset. This small increase could explained by the specific climat of Tamanrasset. Now, it can be also noticed from Fig. that the difference between the different maxima at each site is much smaller. Indeed, by comparison to that of Algiers, the maximum of Hassi R'mel is 39.04 % higher and 26.82 % higher in Tamanrasset.

5. Conclusion

The contribution of solar electricity to the domestic electricity consumption should reach 40% by the year 2030. The commitment is based on several favorable factors. There is a highly abundant solar insulation; the yearly DNI is much higher than the recommended level more particularly in the south. The unproductive and scarcely uninhabited lands could be used as heliostat fields. Moreover the existing gas pipe line network could be useful for system hybridization. Commitment to solar power technologies opens undeniable perspectives. First it permits the development of a source of energy, i.e., solar energy that has stayed untapped up to now. Second it allows the country not only to diversify and increase its energy mix but also to meet its local energy demand that are getting larger and larger. To meets these targets, increase in research funding and a stronger integration of fundamental and applied research, together with demonstration programmes and market incentives are required to speed up the innovation stage.Fundamental research on solar radiation assessment, solar subsystems, heat transfer fluids and storage technology are needed for taking some advanced CRS concepts from laboratory-scale prototype systems out to commercial scale applications.

Reference

[1] African Economic Outlook 2007-2008.
www.oecd.org/dev/publications/africanoutlook
[2] L'Actual n°81, July 2007. Les Nouvelles Revues Algérienne. www.actual-dz.com
[3] Cherigui A. et al, "Solar hydrogen energy: The Europeen-Maghreb connection. A new way of excellence for sustainable energy development »International Journal of hydrogen energy. Vol. 34, n° 11, pp 4934- 4940. 2009
[4]. Energy & Mines, review of the energy and mining sector. N° 08, Nov. 2008
[5] Energy & Mines, review of the energy and mining sector, 2009
[6]Energy & Mines Book 2007.www.mem-algeria.org

[7] Noureddine Yamani, Abdallah Khellaf, Kamal Mohammedi: Parametric Study of Tower Power Plant Performances for Its Implementation in Algeria. Chapter Progress in Clean Energy 2015, Volume 2 : 993-1003

[8] Omar Behar, Abdallah Khellaf, Kamal Mohammedi. Comparison of solar radiation models and their validation under Algerian climate – The case of direct irradiance. Energy Conversion and Management 98 (2015) 236–251

CHAPTER IV

Assessment of solar thermal tower technology under Algerian climate

1. Introduction

In order to determine the most promising solar tower technology in Algeria, an assessment of the performance of the different available solar tower technologies under the different Algerian climate conditions is carried out. For the technologies, the open air receiver technology for Brayton cycle and the tubular water/steam receiver technology for Rankine cycle are considered. As mentioned before, the climate conditions under consideration in Algeria are the Mediterranean climate of Algiers, the north Sahara climate of Hassi R'mel and the deep south Sahara climate of Tamanrasset. TRNSYS software has been used for the evaluation and the better understanding of the performance of the considered technologies under Algerian climate.

2. What is TRNSYS?

TRNSYS (TRaNsient Systems Simulation) [1] is a complete and extensible simulation environment for the transient simulation of systems, including multi-zone buildings. It is used by engineers and researchers around the world to validate new energy concepts, from simple domestic hot water systems to the design and simulation of buildings and their equipment, including control strategies, occupant behavior, alternative energy systems (wind, solar, photovoltaic, hydrogen systems), etc.One of the key factors in TRNSYS' success over the last 25 years is its open, modular structure.The source code of the kernel as well as the component models is delivered to the end users.This simplifies extending existing models to make them fit the user's specific needs.The

DLL-based architecture allows users and third-party developers to easily add custom component models, using all common programming languages (C, C++, PASCAL, FORTRAN, etc.). In addition, TRNSYS can be easily connected to many other applications, for pre- or postprocessing or through interactive calls during the simulation (e.g. Microsoft Excel, Matlab, COMIS, etc.). TRNSYS applications include:

- Solar systems (solar thermal and PV)
- Low energy buildings and HVAC systems with advanced design features (natural ventilation, slab heating/cooling, double façade, etc.)
- Renewable energy systems
- Cogeneration, fuel cells
- Anything that requires dynamic simulation!

3. Simulation and Parameters of the Installation

TRNSYS Simulation Studio is a complete simulation package containing several tools, from simulation engine programs and graphical connection programs to plotting and spreadsheet software. It is an integrated tool that can be used from the design of a project to its simulation. STEC (Solar Thermal Electric Components) [1] is a collection of TRNSYS models especially developed to simulate solar thermal power plants. It is a supplement to the standard TRNSYS routines featuring components from solar thermal power plants like CSP collectors, power conversion systems and high temperature thermal storage systems. It was developed as a SolarPACES package and is steadily used, updated and completed by users within the SolarPACES group. The STEC simulation models are intensively used in feasibility studies for solar thermal power projects as well as in research programs for new solar thermal power technologies

TRNSYS is a software platform that enables the user to model different transient systems using modular components. A component reads in a text-based input file and provides output through the solution of algebraic or differential equations. Components include weather data, solar thermal collectors, heat exchangers, power conversion cycles, etc

For the two considered configurations, namely the configuration based on the Brayton cycle and the configuration based on the Rankine cycle, the solar fields are identical. Then first the solar field parameters will be given, then the parameters for the Brayton

based configuration parameters will be reported and finally the Rankine based configuration parameters will be presented.

3.1.System configuration

A typical solar power tower consist mainly of a solar field for sun radiation concentration and reflection, a solar receiver placed on top of a tower for sun radiation energy transformation from electromagnetic energy to thermal energy and a power block where the thermal energy is used to generate power.

3.1.1. Solar field

The solar field consists of a large number of tracking mirrors, called heliostats. As its cost represents the largest part of the plant cost and as the plant efficiency depends on a large part on the optimal positioning of the heliostats, this solar field is considered the key element in the performance of solar power tower. In the solar field, each heliostat tracks the sun using a two-axis tracking system to minimize the cosine effect, and therefore maximize the solar energy collection by positioning its surface normal to the bisection of the angle subtended by sun and the solar receiver.

The number of mirrors depends on the plant nominal power. This number could reach thousands and the surface covered by the field many hectares. The position of the heliostat field depends also on the desired power and on the nature of the solar receiver. The heliostat could be positioned around the solar tower for large solar power plant. They could also be located on the north side of the tower for smaller power plants. In any case the positioning should be carried in such a way as to minimize the losses, more particularly the ones related to the cosine effect, the shading and the blocking effects and the spilling effect.

The field matrix of solar effectiveness used in this works [2] includes the reflectivity of the mirror(ρ_{Mirror}) the cosine effect(μ_{cosine}),, the shading and the blocking effects($\mu_{shad,block}$) and the spilling effect($\mu_{Atmosp\ hiric}$) :

$$(\mu_{field}) = (\rho_{Mirror}) \times (\mu_{cosine}) \times (\mu_{shad,block}) \times (\mu_{Atmosp\ hiric}) \quad (1)$$

$$\mu_{cosine} = \frac{\sqrt{2}}{2}\sqrt{[\sin(\alpha)\cos(\lambda) - cos(\theta_H - A)cos(\alpha)sin(\lambda) + 1]} \quad (2)$$

$$(\mu_{Atmosp\ hiric}) = \begin{cases} 9932.10^{-4} - 1176.10^{-8} \times S_0 + 197.10^{-9} \times S_0^2 (S_0 \leq 1000m) \\ e^{-1106.10^{-8} \times S_0} \quad (S_0 > 1000m) \end{cases} \quad (3)$$

Where, S_0 is the distance between the heliostat and the receiver (Fig.4.1)

$\mu_{shad,block}$ Depends on the positioning of the mirrors. It depends strongly on the field lay out and could then usually determined using lay out software such as HFLD (Heliostat Field Layout Design)

The power to the receiver generated by the heliostat filed evaluated by

$$\dot{Q}_{rec} = A_{field} \times \rho_{Mirror} \times I \times \mu_{field} \times \Gamma \quad (4)$$

with ;

A_{field} : Reflective field Area

ρ_{Mirror} :reflectivity of the mirror

I: direct normal irradiation DNI

Γ : control parameter for describing the fraction of the field in track.

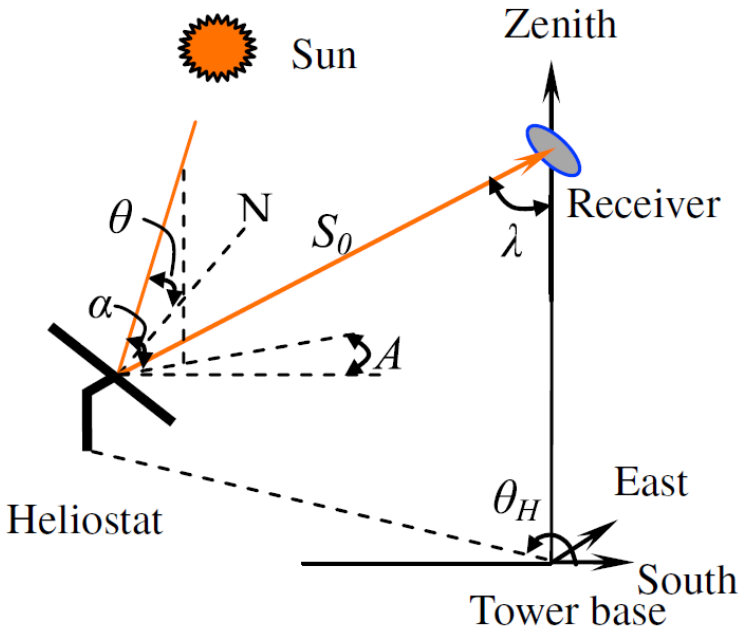

Fig.4.1. Heliostat field coordinate in relation to the sun and the receiver position [3]

In the present study, the heliostat field of the selected plant consists of 700 heliostats for a total reflective surface of 28 000 m². Each heliostat is a mobile 40 m² curved reflective surface mirror that concentrates solar radiation on a receiver placed on top of an 80 m

tower. For this purpose, every heliostat is spherically curved so its focal point is at a distance equal to the slant range to the receiver. All the solar fields are similar for all the different configurations considered in the study.

The heliostat field model deals with the lay-out of the heliostat field taking into account the reflectivity of the mirrors and the DNI incident available at the site. In this model, the object is to determine the power flux reaching the central receiver. This power is determined taking into account The total surface of the mirror as well as its reflectivity, the solar DNI and the solar field efficiency. As reported earlier, the solar field efficiency depends on the optimum positioning of the mirrors in such a way as to minimize the different losses. The model includes also the electrical parasitic for tracking, start-up and shut-down. Moreover, a parameter taking into account the fraction of the field in track is also included in the model.

Figs.10&11 shows the TRNSYS simulation model presentation. In this presentation, the DNI is included in the weather data reading and processing "weather data" which is linked to the component of the heliostat field efficiency model, namely "FEffMatx". This component uses the DNI from the data reader, the solar zenith and azimuth angle from the radiation processor to determine power flux that is fed to the central receiver.

The parameters of the solar filed are given in Table.4.1

Table.4.1 Heliostats field input parameters

Parameters	**Value**
No of zenith angle data points	7
No of azimuth angle data	9
No of concentrator units	700
Mirror surface area	40 m²
reflectivity	0.85

3.1.2. Solar receiver

The solar receiver is the heat exchanger where the solar radiation is absorbed and transformed into the thermal energy that is necessary for the power block operation. There are different solar receivers, depending on the nature of the absorber material and of the heat transfer fluid as well as on the geometrical configuration. The solar receiver should mimic a blackbody by minimizing radiation losses. To do so cavities, black-painted tube panels or porous absorbers capable of trapping incident photons, are used. In most designs, the solar receiver is a single unit that centralizes all the energy collected by the large mirror field, and therefore high availabilities and durability are a must. a typical receiver operating temperatures are between 500°C and 1200°C and incident flux covers a wide range going from 300 kW/m² to over 1000 kW/m². In the present study we have chosen the open air volumetric receiver for Rankine cycle and the water/steam receiver for the Brayton cycle

a. Open air volumetric receiver

The open air volumetric receiver consists of porous wires of either metal or ceramic. The open air receiver, developed by DLR [4], is an open loop system that uses air as heat transfer fluid. A good volumetric receiver produces the so-called volumetric effect, which means that the irradiated side of the absorber is at a lower temperature than the medium leaving the absorber. In this type of receiver, air, circulating through the porous structure that acts as a convective heat exchanger, absorbs the incident solar irradiance by heat transfer mode [5]. Typical characteristics of the open air receiver are reported in Table.4.2. These characteristics correspond to those of the receiver of the central receiver power plant erected in Jülich, Germany [6].

Tabale.4.2 Reported Receiver characteristics of Power Plant Jülich (DLR)

Process parameters	Pressure	ambiant
	Return air	120°C
	Receiver air outlet	680°C
material load	max. temp	1100°C
parameters	max. load	1000kW/m²
	temp. gradient	100K/cm
	average mass flow	0.55 kg/m²-s

The thermal power received $\dot{Q}_c$ in the cavity of receiver is written:

$$\dot{Q}_c = \mu_{field}\, I_c S_c \tag{5}$$

S_c : the sensor surface of heliostats

The cavity of the volumetric receiver loses a fraction of this power by reflection, natural convection and radiation , the power transmitted ($\dot{Q}_r$) by the cavity of the receiver is given by:

$$\dot{Q}_r = \dot{Q}_c - h_{cv} A_r (T_r - T_0) - \sigma \varepsilon A_r (T_t^4 - T_0^4) \tag{6}$$

Where

h_{cv} : Coefficient of convection transfer.

A_r : Receiver area

σ : Stefan Boltzmann constant

ε: Absorber emissivity.

T_r: Temperature external of receiver

T_0: Temperature interior of receiver

b. water/steam Tubular receiver

The receiver consists of tube panels through which water circulates in order to absorb the heat resulting from the conversion of solar radiation energy into thermal energy. This type of receiver is capable of withstanding high pressures. This allows direct production of high pressure superheated steam (up to 185 bars) and avoids then the need for dangerously flammable and polluting HTFs that are widely used in parabolic trough plants. Typical characteristics of this kind of receiver are reported in Table.4.3.

Table.4.3 Reported water/steam Receiver characteristics

Inlet temperature	330°C
Outlet temperature	800°C
Pressure	100Bar

In this model, the conductive losses are neglected in the calculation of the net absorbed power. The net thermal collected power is given by:

$$\dot{Q}_{net} = \alpha \dot{Q}_{incident} - \dot{Q}_{convection} - \dot{Q}_{radiation} \quad (7)$$

Where: $\dot{Q}_{incident}$ is the incident power, $\dot{Q}_{convection}$ the power losses due to convection and $\dot{Q}_{radiation}$ the power losses due to radiation.

The radiative power losses $\dot{Q}_{radiation}$ and the convective power losses $\dot{Q}_{convection}$ can usually be represented by third order polynomials respectively of rate of incident radiation $\dot{Q}_{incident}$ and of wind speed V [7]. We have then:

$$\dot{Q}_{radiation} = R_0 + R_1 \dot{Q}_{incident} + R_2 Q_{incident}^2 + R_3 Q_{incident}^3 \quad (8)$$

$$\dot{Q}_{convection} = C_0 + C_1 V + C_2 V^2 + C_3 V^3 \quad (9)$$

3.1.3. The power block

In the power block, the thermal energy produced at the receiver is used to generate superheated vapor. This vapor is used to set in motion the turbine and the generator to produce electricity.

In the present study, both the Rankine and the Brayton cycles are considered. The aim is to carry a comparison of the performance of these two technologies.

3.1.3.1.Brayton cycle

a. Description

The Brayton cycle, considered in the present study, is coupled to a volumetric air receiver. The gas turbine is usually installed close to the receiver in order to reduce any other energy losses at the compressor outlet and the combustor inlet. The case of a hybrid system is also considered. As shown in Fig.4.2, the power block includes a combustion chamber, a gas turbine and a generator. The concentrated solar radiation in

the receiver heats up to about 700 °C the air coming at pressure up to 100 bars from the compressor of a gas turbine. This air is fed to the combustion chamber of the gas turbine, which increases the temperature of this air to more than 1000°C. The main advantages of this technology are a greater efficiency due to the high operating temperature and a reliable hybridization.

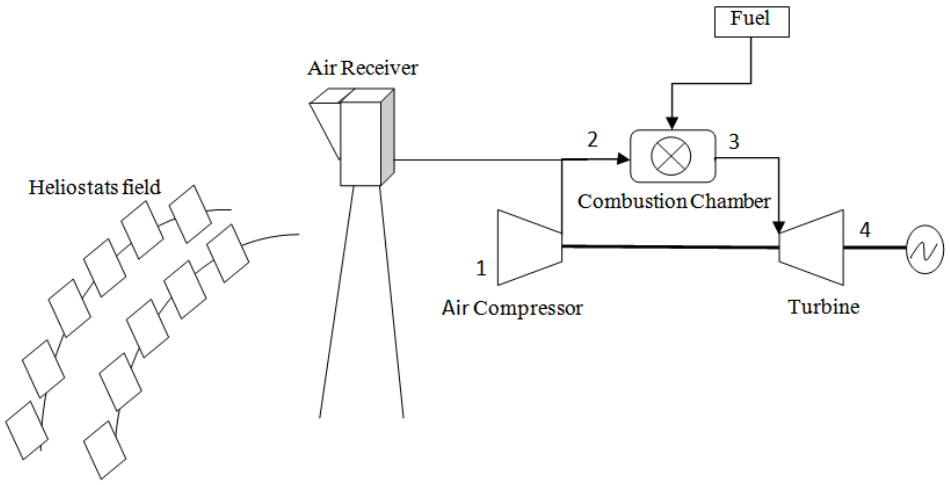

Fig.4.2.Design of solar power tower with Brayton configuration

The air compressor (AC) input power is given by:

$$\dot{Q}_{AC} = \dot{m}_{air}\, C_{Pair}\, (T_2 - T_1) \tag{10}$$

With:

$$T_2 = T_1\left(1 + \frac{1}{\mu_{AC}}\left(\frac{P_2}{P_1}^{\frac{\gamma_{air}-1}{\gamma_{air}}} - 1\right)\right) \tag{11}$$

$$\mu_{AC} = (h_2^s - h_1)/(h_2 - h_1) \tag{12}$$

γ_{air} is the specific heat ratio.

C_{Pair} specific heat

μ_{AC} The compressor efficiency

h_2^senthalpy isotropic

In the combustion chamber, the gas is injected and burned with the pressurized air according to the following chemical reaction

$$C_n H_m O_j + \left(n + \frac{m}{4} - \frac{j}{2}\right)[O_2 + 3.76N_2] \rightarrow (n)CO_2 + \left(\frac{m}{2}\right)H_2O + 3.76\left(n + \frac{m}{4} - \frac{j}{2}\right)N_2$$

The gas turbine output power is expressed by:

$$\dot{Q}_T = \dot{m}_{gaz}\, C_{Pgaz}\, (T_4 - T_3) \tag{13}$$

$$\text{With } T_4 = T_3 \left(1 - \mu_T (1 - \left(\frac{P_4}{P_3}\right)^{\frac{1-\gamma\, gaz}{\gamma\, gaz}}\right) \tag{14}$$

Fig4.3 illustrates the TRNSYS model for simulation of solar power tower in the case of the Brayton based configuration. As shown in this figure, the hot air coming from the receiver is fed to the combustion chamber where it is heated to the desired temperature. The amount of fuel to be added to the combustion chamber in order to raise the air to the desired temperature depends on the temperature of the air coming from the central receiver which in turn depends on the DNI The air is then compressed before being fed to the turbine that drives the generator.

More details could be found in [1]. The most important parameters are reported in Table .4.4

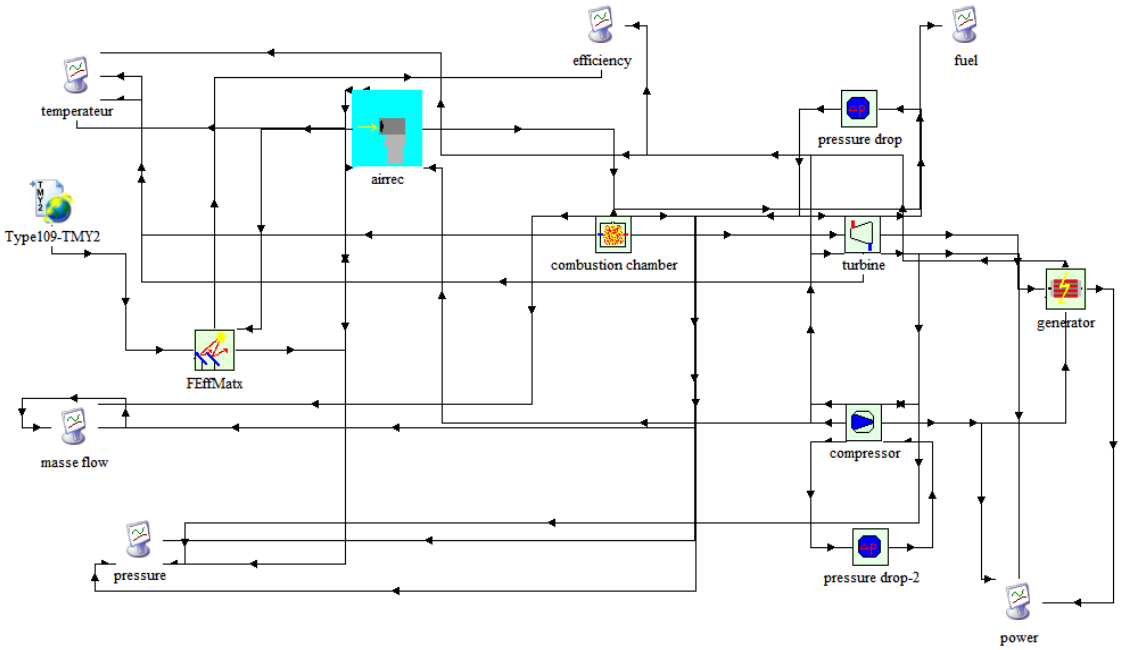

Fig.4.3.TRNSYS model for simulation of solar power tower Brayton based configuration case

Table4.4 Input parameters value of SPT with air receiver

Parameters		**Value**
Volumetric Receiver	Optical efficiency	0.95
	Emissivity of absorber	0.8
	Receiver aperture	25m²
	surface area of piping	1m²
	design inlet pressure	15 BAR
	design inlet temperature	450°C
	design inlet mass flow	75000 kg/hr
Combustion Chamber	lower calorific value	47600 kJ/kg
	C mass ratio	0.7318
	H2 mass ratio	0.2341
	N2 mass ratio	0.0159
	O2 mass ratio	0.0182
	relative pressure drop_design	0.02
Compressor	compression ratio	15
	mechanical efficiency	1
	ISO inlet mass flow_design	75000kg/hr
Turbine	mechanical efficiency	1
	maximum inlet temperature w/o cooling	900 °C
	ambient pressure	1.013 BAR
	maximum inlet temperature with cooling	1200

b. Main modules used

Air Receiver (type 422): This type can be used for steady state simulation of an air receiver. The receiver outlet temperature, pressure and enthalpy is calculated depending on inlet conditions of the air flow and the radiation input. A simple black body radiation model is included to calculate the receiver efficiency. Receiver body and piping heat losses as well as receiver cooling losses can be calculated. The pressure loss depending on temperature, pressure and mass flow can be calculated.

Combustion chamber (type 426): This model describes an adiabatic combustion chamber for different liquid or gaseous fuels. The user has to define the fuel by the lower heating value and the mass ratio of the fuel elements: C, H_2, S, O_2, N_2, H_2O, ashes and air nitrogen given in the organic analysis. The model allows two different operating modes- in the first case for a given outlet temperature the required fuel mass flow is calculated, in the other way the reached temperature results from the fuel flow used. Beside that a pressure loss is evaluated, based on a user specified reference value as a function of inlet conditions.

Compressor (type 424): This compressor model calculates the outlet conditions from the inlet state by using an isentropic efficiency which can be specified by the user as a function of the flow rate using a variable curve. In this way, the model calculates for a given compressor ratio the outlet-temperature $T_{out,is}$ and enthalpy $h_{out,is}$ for an isentropic compression by calling the Gas routine (call Gas with the inputs P_{out} and $S_{out,\ is} = S_{in}$). The real outlet conditions are then calculated by using the isentropic efficiency and a new call of the Gas routine (call Gas with the inputs P_2 and h_2).

$$\Delta h = \frac{h_{out\ ,is} - h_{in}}{\mu_{is}} \tag{15}$$

$$h_{out} = h_{in} - \Delta h \tag{16}$$

$$P(compressor) = \frac{m_{out} \times \Delta h}{\mu_{mec\ h}} \tag{17}$$

Gas turbine (type427): This gas turbine model calculates the outlet conditions from the inlet state by using an isentropic efficiency which can be specified by the user. In this way, the model calculates for a given ambient pressure and therfore known turbine outlet pressure first the outlet- temperature $T_{out,\ is}$ and enthalpy $h_{out,\ is}$ for an isentropic expansion by calling the Gas routine (call Gas with the mixture of the combustion air and the inputs pout and $S_{out,\ is} = S_{in}$). The real outlet conditions are then calculated by using the isentropic efficiency and a new call of the Gas routine (call Gas with the mixture of the combustion air and the inputs P_2 and h_2). For the inlet state the model considers the merge of the combustion and cooling air by computation new inlet conditions for the mixture.

$$\Delta h = \frac{h_{in} - h_{out,is}}{\mu_{is}} \quad (18)$$

$$h_{out} = h_{in} - \Delta h \quad (19)$$

$$P(turbine) = m_{in} \times \Delta h \times \mu_{mec\,h} \quad (20)$$

Pressure drop (type 429): This model describes a pressure loss with consideration of the actual load condition.

Electric Generator (type 428): calculates net electric output and GT thermal efficiency.

3.1.3.2.Rankine cycle

a. Description

the Rankine cycle is a model that is used to predict the performance of steam turbine systems including feed-water heating with a cavity receiver on top of tower.As shown in Fig.4.4, the block includes a Heat Recovery Steam Generator, a steam turbine, a generator, a cooling system and a deaerator. In the Heat Recovery Steam Generator, we have water evaporation, steam superheating, combined evaporation and superheating, steam reheating, air preheating, and combined air preheating and feed-water heating. The steam temperature can reach 300 °C.

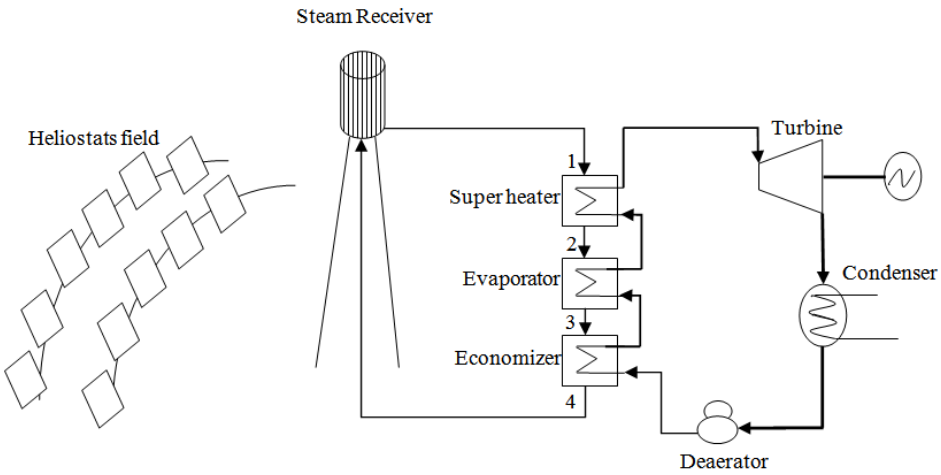

Fig.4.4. Design of solar power tower with a Rankine configuration

In order to determine the HRSG performance, the energy and mass balances between the hot and cold streams on the HRSG different heat exchangers are needed [8]. To this

end, the different parameters are reported in Fig.3.These parameters are the flow rate, temperature, pressure of superheated steam and outlet temperature.

The energy balance of the HRSG can be expressed by the following equation :

$$\dot{Q} = \dot{Q}_{sup} + \dot{Q}_{eva} + \dot{Q}_{eco} \quad (21)$$

Where:

$$\dot{Q}_{sup} = \dot{m}.C_P(T_1 - T_2) \quad (22)$$

$$\dot{Q}_{eva} = \dot{m}.C_P(T_2 - T_3) \quad (23)$$

$$\dot{Q}_{eco} = \dot{m}.C_P(T_3 - T_4) \quad (24)$$

The turbine output power is expressed by:

$$\dot{Q} = \dot{m} \times (h_{out} - h_{in}) \quad (25)$$

The isentropic efficiency is calculated from:

$$\mu = (h_{in} - h_{out})/(h_{in} - h^s_{out}) \quad (26)$$

The TRNSYS model for simulation of solar power tower in the case of the Rankine based configuration is visualized in Fig.4.5. As can be seen from this figure, a heat recovery steam generator (HRSG) is used. The HRSG section consists of an economizer heat exchanger, an evaporator heat exchanger and a superheater heat exchanger. The heat transfer fluid (HTF), coming from the receiver, is used in the HRSG to generate steam.

Steam quality and enthalpy are used instead of temperature in the turbine model. These quantities depends on the HTF flow direction. A steam turbine with two extraction lines is selected. The final turbine stage is connected to a condenser. The two extraction splitters are linked to the deaerator and the feedwater heater. A condensing preheater and a subcooler and a feedwater pump are part of the system. All parameters of deferent used components are shown in Table.4.5

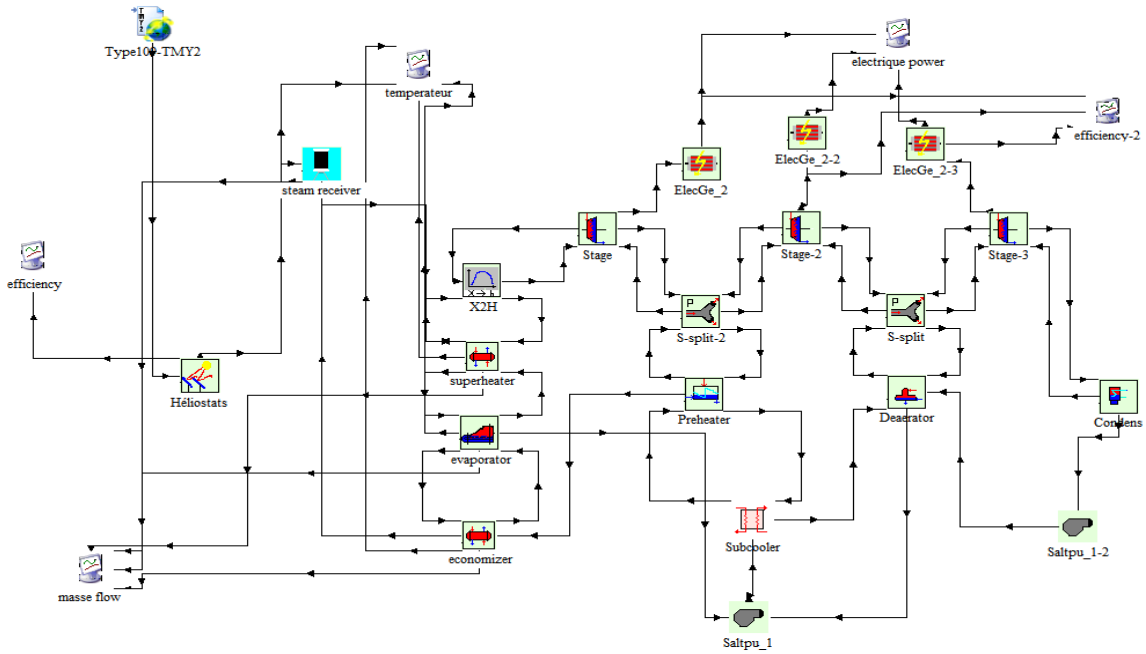

Fig.4.5.TRNSYS model for simulation of solar power tower Steam Rankine case

Table.4.5 Input parameters value of SPT with water/steam receiver

Parameters		**Value**
Steam	Effciency	0.8
Receiver	Fluid inlet temperature	100 °C
	Fluid inlet flow rate	576000 kg/hr
	Temperature set point	350 °C
	Fluid Specific Heat	4.18 kJ/kg.K
HRSG	Superheater overall heat transfer coefficient of exchanger	1008000 kJ/hr.K
	Evaporator overall heat transfer factor	9720000 kJ/hr.K
	Economizer Overall heat transfer coefficient of exchanger	2520000 kJ/hr.K
	Preheater overall heat transfer factor	186840 kJ/hr.K
Turbine	design inlet pressure	100 BAR
	design flow rate	144000 kg/hr
	design inner efficiency	0.8
	generator efficiency	0.98

b. Main modules used

Steam receiver (Type 395): The receiver model it provides as output the flow rate required to achieve the outlet temperature set point. Since our initial heliostat field model is based upon a simple field efficiency table interpolation, only the total power to the receiver is calculated. To find the detailed flux distribution on the receiver, a complex numerical convolution, or ray-trace optical model, must be used. Without detailed flux information, an empirical receiver heat loss model is more appropriate than one based on heat transfer relations at the receiver's surface. In this model, the conductive losses are neglected in the calculation of the net absorbed power

Economizer, Superheater for Water/ Steam heated (type 315): A zero capacitance sensible heat exchanger is modelled in counter flow mode. The cold side input is assumed to be water/steam depending on the quality. The respective specific heat of the cold side fluid is calculated from water/steam property data. The effectiveness is calculated by using the overall heat transfer coefficient

Steam evaporator (type 316): This model simulates a water evaporator, giving outlet temperatures and flow rates of hot and cold streams as well as demanding for a certain water inlet flow rate to obtain total evaporation. The cold side is assumed to be water/steam depending on the quality. Water/Steam conditions are given by temperature, pressure and quality. The effectiveness method is used to describe the heat transfer using an overall heat transfer factor

Turbine stage (type 318): This turbine stage model calculates the inlet pressure of the turbine stage from the outlet pressure, the steam mass flow rate and reference values of inlet and outlet pressure and mass flow rate using Stodolas law of the ellipse. It evaluates the outlet enthalpy from the inlet enthalpy and inlet and outlet pressure using an isentropic efficiency.

Controlled Splitter (type 389): The turbine stage can be combined with a controlled splitter in order to assemble an extraction turbine.

3.2.Results and discussion

In the present section, the results of the simulation using TRNSYS are presented for the two configurations. It should be kept in mind that the solar field lay-out is chosen to be the same for both cases. The results concerning the central receivers are included in the power block cycle. In our study, we considered the performance over the summer season and the winter season. To this end, the day of January 29 is taken as the representative of the winter season.

From the curves representing the results reported below, some undesirable patterns are visible. These patterns could be found in most locations and time. They seem to happen at high azimuth angles and angles of incidence that relate to the input file weather data. Evolution of the azimutal and zenith angles are reported in Fig.4.6& Fig.4.7 for both seasons. The values of these angles high affect the collected solar power and the collect duration. This is going of course to affect the HTF temperature evolution and the plant performance.

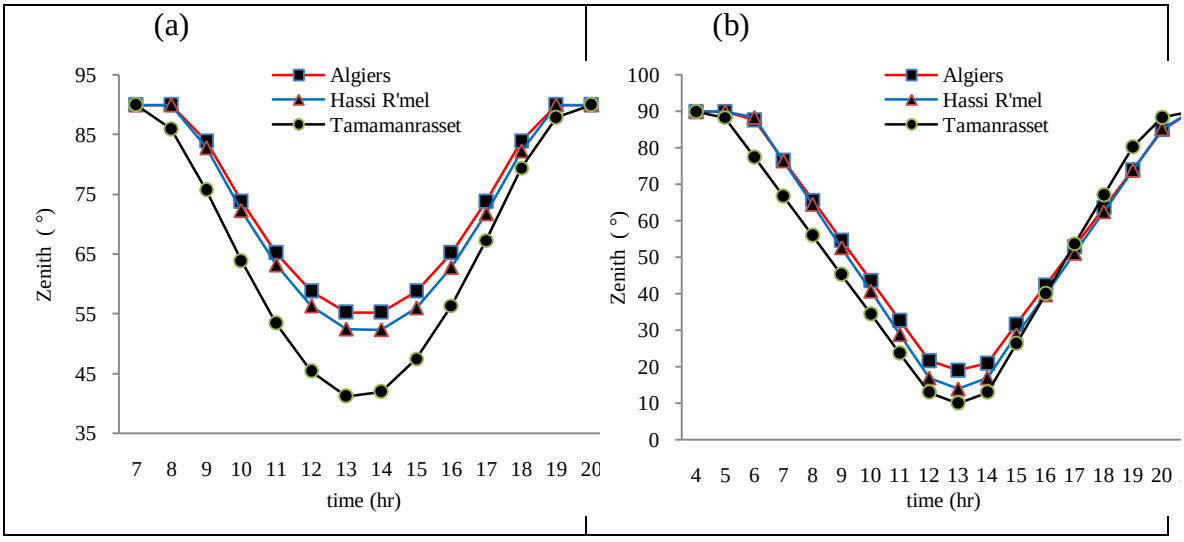

Fig.4.6. Zenith angle a) case of January 29; b) case of June 2

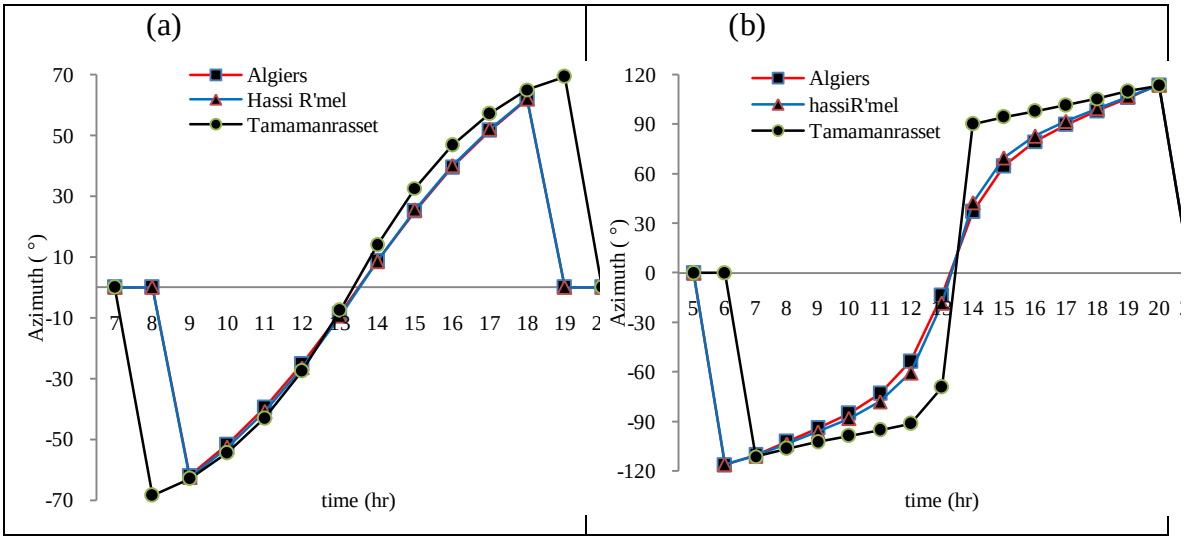

Fig.4.7. Azimuth angle a) case of January 29; b) case of June 2

3.2.1. Solar field

The power flux reflected by the solar field onto the receiver is reported in Fig.4.8. From this figure, it can be seen that the largest power incident on the receiver are obtained in the summer season with the largest at Tamanrasset with a power of 15.810 MW. This is to be expected as we have higher DNI in the summer season.

Moreover, it can be noticed that the difference between the peak values of the different sites are smaller in the month of June, i.e., the summer season. It is much larger for the

month of January. In this last case, the peak values of Tamanrasset and Hassi R'mel are respectively 77.6 % and 37 % higher than that of Algiers.

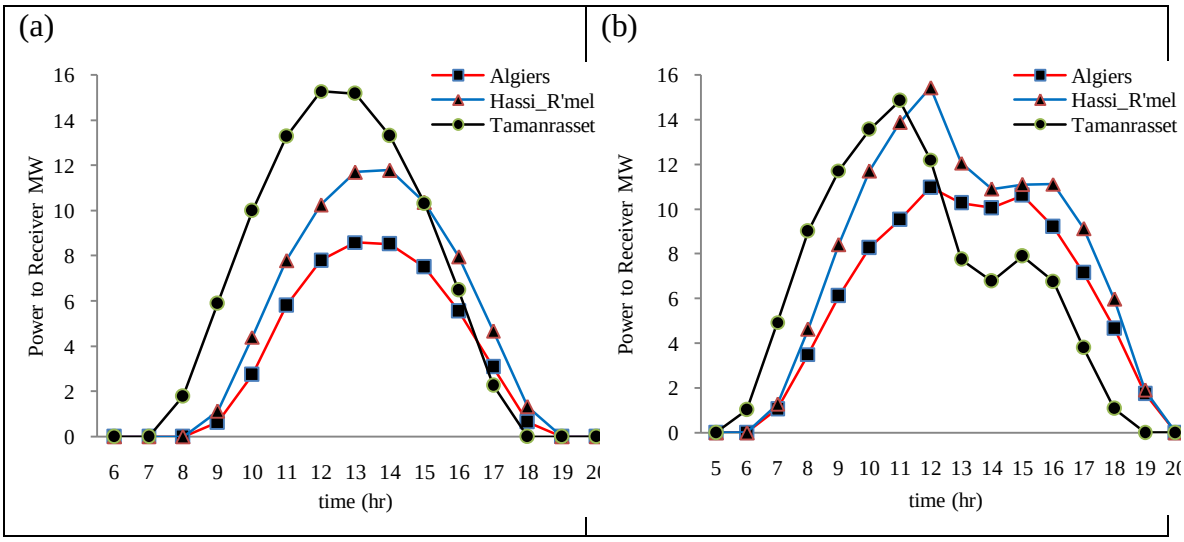

Fig.4.8. the incident power flux a) case of January 29; b) case of June 2

The values of solar energy reflected over the whole day are represented for the three locations and both days in Fig.4.9 . It can be seen that the summer season offers a much higher collected solar energy than the winter season. In Algiers, the summer energy collected is 70 % higher than that collected in the winter season. For Tamanrasset and Hassi R'mel, these values are respectively 49 % and 52 %.

From this figure, it could also be seen that the energy collected in Algiers in the lowest. Indeed, for winter it represents only 66 % of that of Tamanrasset and 71.3 % of that of Hassi R'mel. For the summer these values are 76 % and 79.8 % respectively. The difference in energy collected in Tamanrasset and Hassi R'mel is relatively small. It is a mere 4 % in summer and 6.5 % in winter.

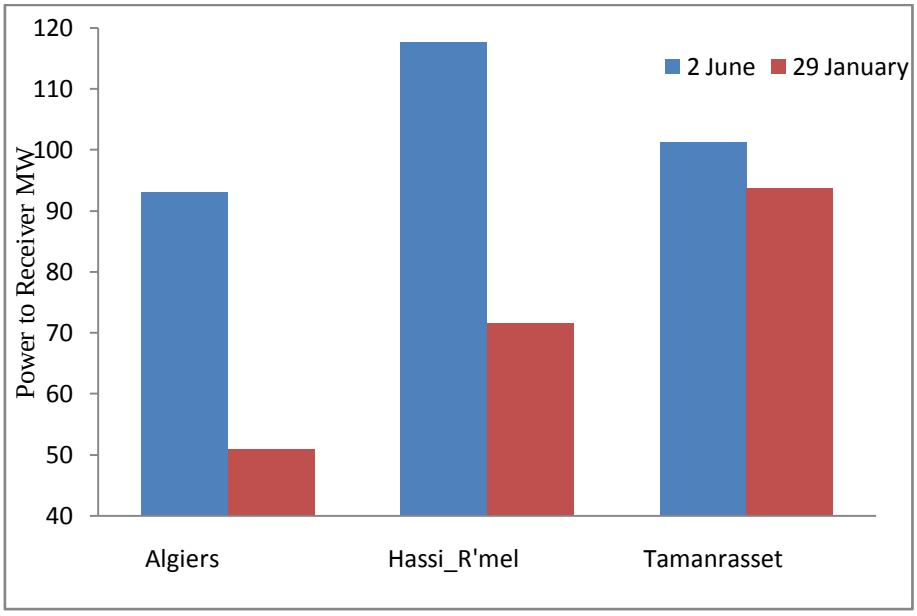

Fig.4.9. Daily incident power flux

3.2.2. First configuration: Brayton cycle with volumetric air receiver

To evaluate the performance of this configuration, the study is concentrated on the receiver parameters, mainly its efficiency and the temperature achieved at its output. Based on the temperature of the HTF, the fuel needs to reach the temperature for an optimal performance of the Brayton cycle, i.e., 1000 °C are determined.

a. Receiver

First, the results of the HTF temperatures reached at the receivers are discussed. Fig.4.10 shows the evolution of the HTF temperature over the day for the summer season. As shown in this figure, the operating temperature is time as well as site dependant.

For the month of January, i.e., the winter season, the temperature peaks up around 1000 °C. for the other two sites, it is much lower. It is around 750 °C in Algiers and around 880 °C for Hassi R'mel. For the month of June, it is 1020 °c in Hassi R'mel almost 1000 °C and 850 °C in Algiers. It should though be noted that the 1000 °C temperature is reached only at the peak time. This is a very short time. Moreover, it is most of the time much lower than the required 1000°C. This is not enough to insure a sufficient performance of the power plant. There is then the need for another source of energy to raise the temperature to 1000 °C.

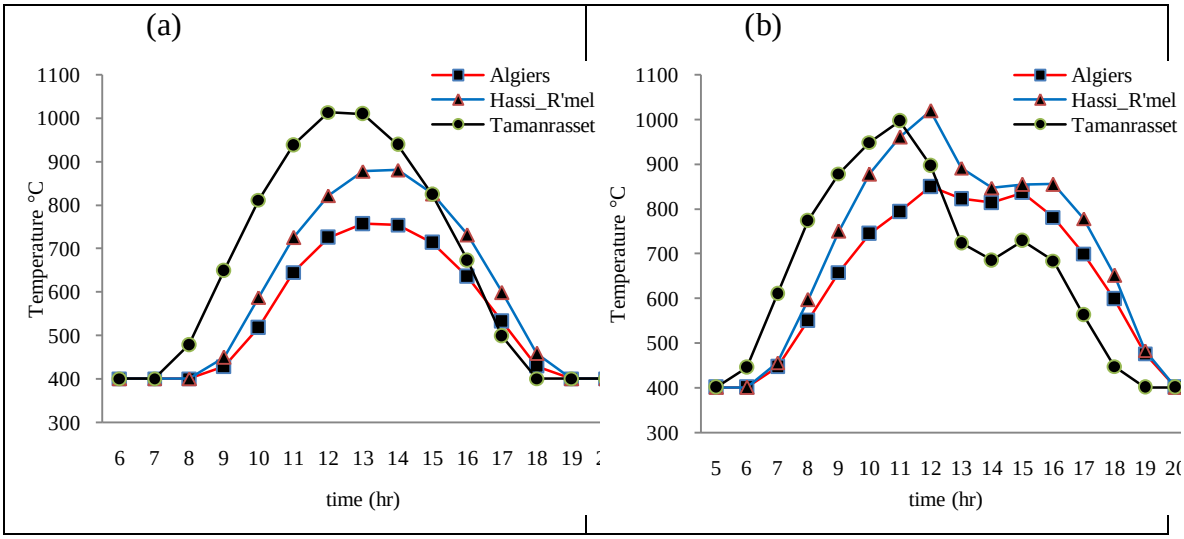

Fig.4.10. Variation of Receiver temperature a) case of January 29; b) case of June 2

The receiver outlet temperature, pressure and enthalpy are estimated using the inlet conditions of the air flow and the solar radiation intensity. For the receiver efficiency, a simple black body radiation model is used. The results are reported in Fig.4.11. From this figure, it can be seen that the efficiency is is really good. It is within the range of 87 % to 88 %. This value is of course dependant on the sunshine radiation. Only within this time interval could we obtain such a value.

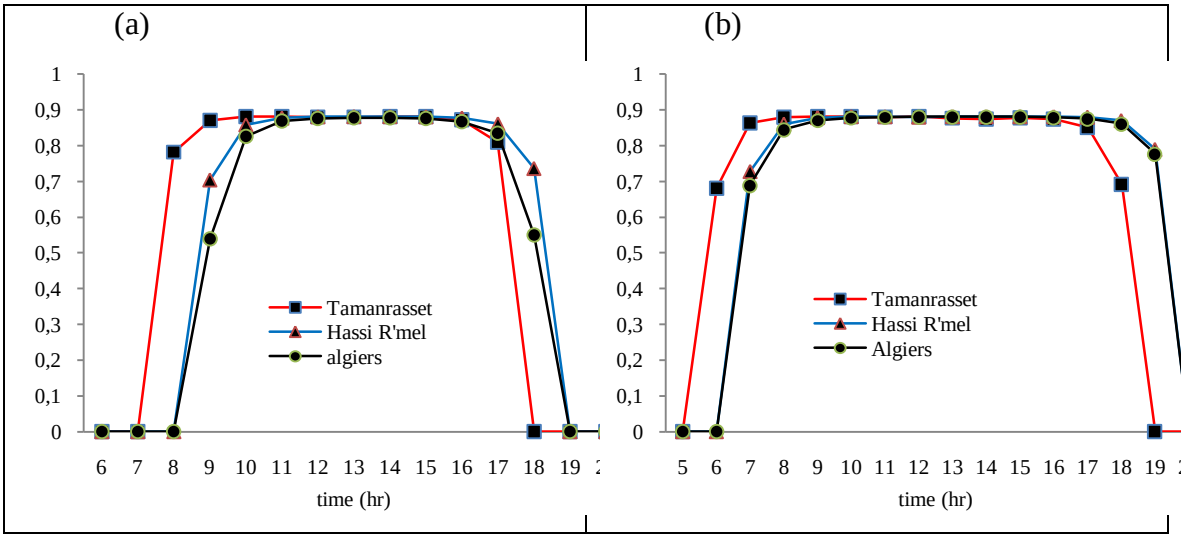

Fig.4.11. receiver thermal efficiency a) case of January 29; b) case of June 2

b. Combustion chamber fuel

for this configuration, the desired output electrical power is fixed to 5.1 MW. This could be achieved by a gas turbine operating at 1000 °C. As shown above and as the maximum temperature reached with the solar system is most of the time less than 1000 °C, it is then necessary to use a combustion chamber to bring the air temperature to 1000 °C. The amount of fuel need to fire the combustion chamber depends on the temperature of the air flowing in. Moreover, as this temperature is variable, the amount of needed fuel is also variable. At maximum, i.e., when there is no solar radiation, it is 1100kg/hr.

Taking into account the inlet temperature of the air and the thermophysical properties of the fuel, the amount of fuel needed to reach a temperature of 1000 °C is determined.

Fig.4.12 shows the hourly evolution of the fuel needs for the different sites for both days. The needs for energy are of course covered at night by the fuel as there is no solar energy. During the day, the extra energy needed to bring the gas temperature to 1000 °C are covered by the fuel burned in the combustion chamber. This extra energy depends on the power collected by the mirror at the receiver and the duration of collection. As expected the needs are higher for the month of January for all sites. For both days the fuel needs are the highest in Algiers. It should be noted that for the case of Hassi R'mel, the fuel needs are the lowest in the month of June.

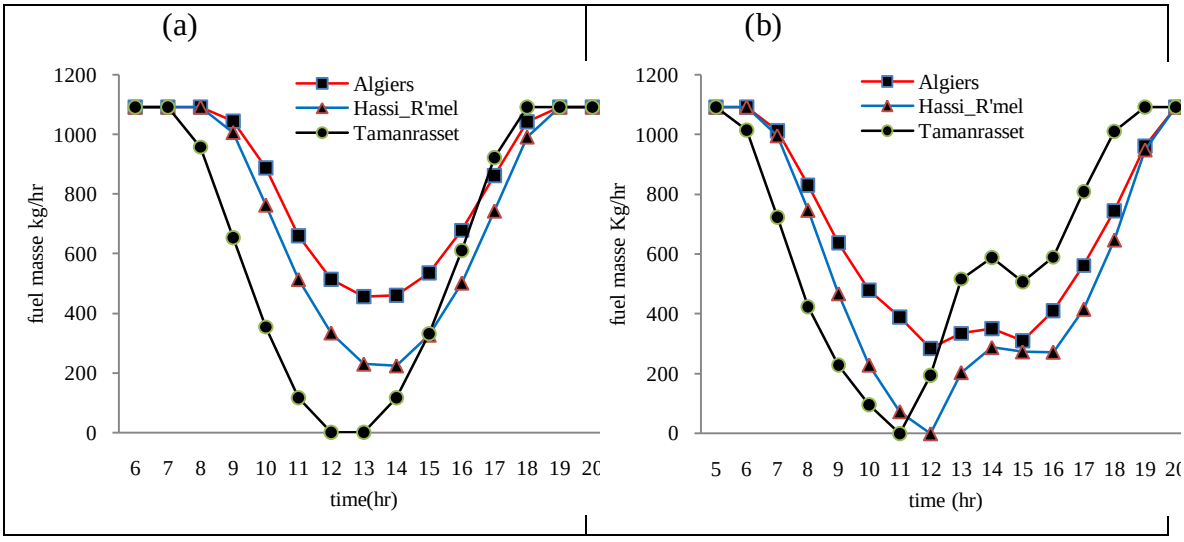

Fig.4.12. Hourly fuel needs for the combustion chamber a) case of January 29; b) case of June 2

Fig.4.13 shows the daily needs for fuel to be burned in the combustion chamber to bring the gas temperature to 1000 °C. This shows clearly that the needs for June are the lowest for all the sites. Indeed by comparison to the fuel needs for the month f June, the daily fuel needs of January are 16 % higher in Algiers, 19% in Hassi R'mel and 3 % in Tamanrasset. The low change in Tamanrasset could be explained by its specific climate. It could also be noticed that if for the month of January, the fuel needs are the lowest at Tamanrasset, these fuel needs are at the lowest at Hassi R'mel. By comparion to Tamanrasset, the fuel needs in Algiers are3 % higher in the month of June and 16% higher in the month of January. For the case of Hassi R'mel, the fuel needs are 10 % in the month of June and 7 % in the month of January.

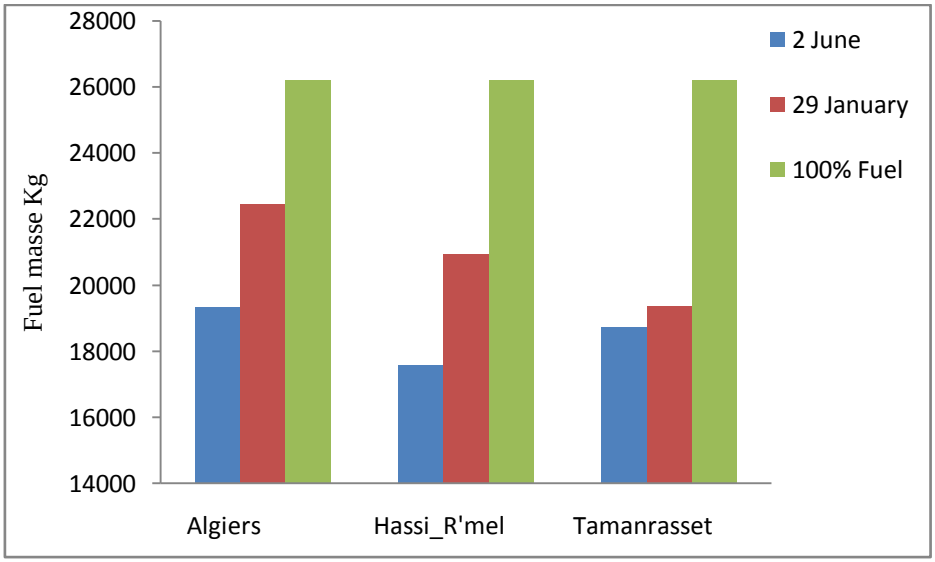

Fig.4.13. Daily fuel needs for the combustion chamber a) case of January 29; b) case of June 2

3.2.3. Second configuration : Rankine cycle with water/steam receiver

In this case the working temperature is lower than the case of the Brayton cycle configuration and a heat recovery steam generator (HRSG) is used in conjunction with the steam turbine. The heat necessary to generate steam in the HRSG is obtained by using reflectors that concentrate solar radiation onto a receiver placed on top of the tower. The heat is delivered to the HRSG by means of an HTF circulating through the receiver. The HTF is usually water. In this part, the performances of the reicer, the HRSG and the turbine are presented.

a. Receiver

The solar field and the receiver are designed in such a way that the receiver outlet temperature is 350 °C. To reach the desired temperature, the HTF flow rate in the three considered sites and for the months of June and January is determined. The results are reported in Fig.4.14 . First it can be noted that the mass flow rate in the HRSG depends on the intensity of solar radiation, the higher the solar radiation the higher is the mass flow rate. From the figure, it can be seen that for the month of January, the difference between the flow rates for the different sites is fairly large with that of Tamanrasset peaking at about 70369kg/hr. Indeed the flow rate peak values of Tamanrasset and of

Hassi R'mel are respectively about 95 % and 44 % higher than that of Algiers. The flow rate peak value of Tamanrasset is about 35.5 % higher than that of Hassi R'mel. For the month of June, the largest flow rate peak value is that of Hassi R'mel. However for this month, the difference between the flow rates of the different sites is smaller. By comparison to the flow rate peak value of Algiers, that of Tamanrasset is about 42 % higher and that of Hassi R'mel 49 % higher. It can be noted that the flow peak value of Hassi R'mel is a mere 4 % higher than that of Tamanrasset.

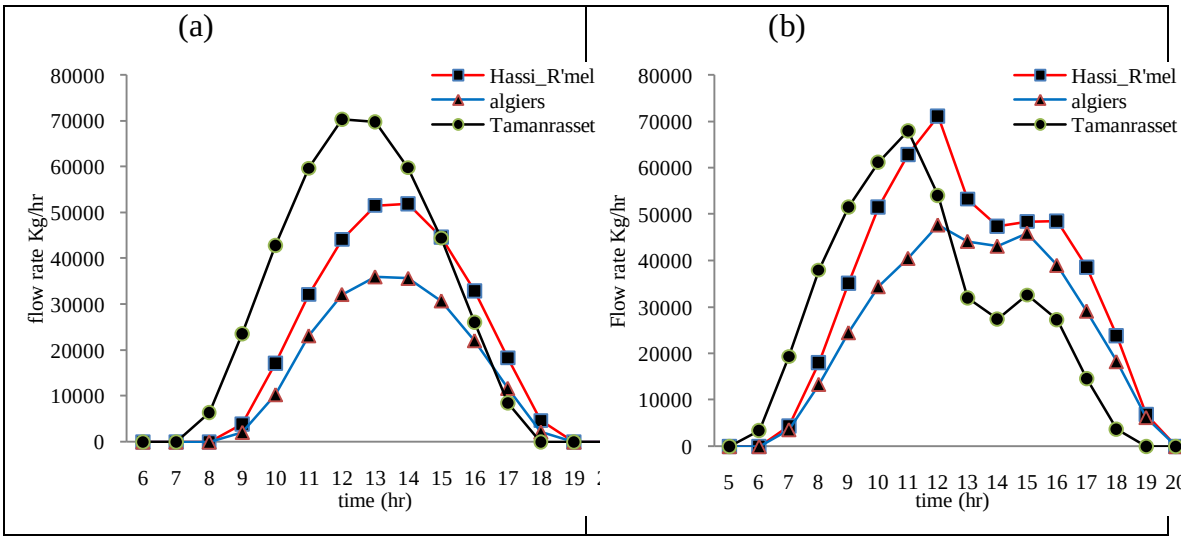

Fig.4.14. Variation of the flow rate in Receiver a) case of January 29; b) case of June 2

b. Heat recovery steam generator performance

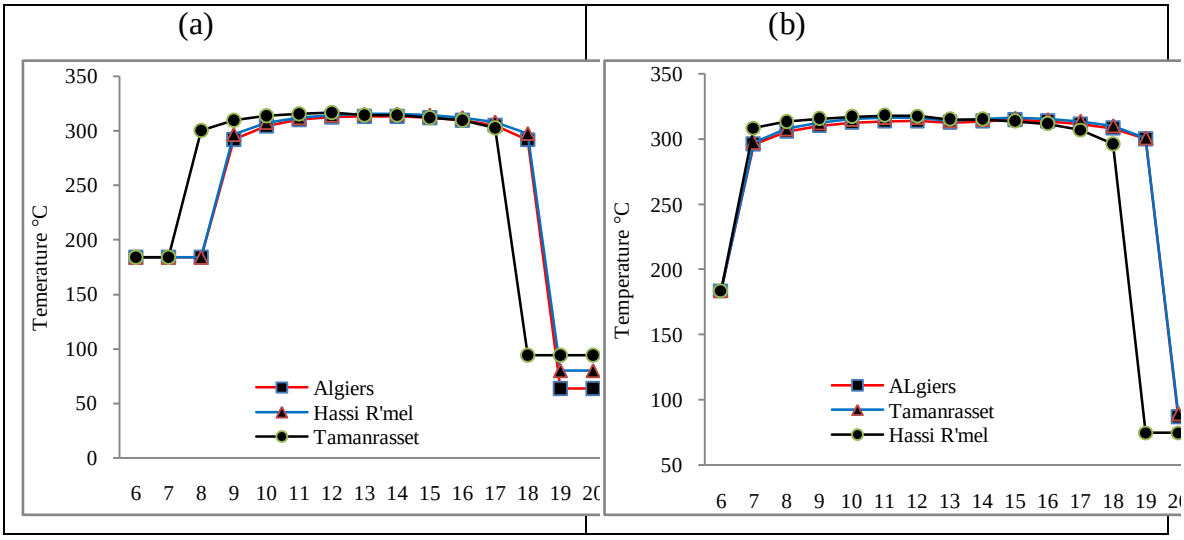

Fig.4.15. Variation of temperature in the super heater a) case of January 29; b) case of June 2

From sunrise to sunset of the selected day, air receiver offers higher temperatures and therefore better performance for the power conversion system. The difference between the three zones is the sunshine duration, At midday, the super heater(fig4.15) can reach up to 320°C for 10 hour average in January for hassi r'mel and tamanrasset and 8 hour for Algiers while Much more than in summer she can be reach 13 hours which is very acceptable The same thing for evaporator (fig4.16)but with a lower temperature about 160°C Finally, the economizer a provides low temperature 140°C (fig.4.17) it lower stack temperatures which may cause condensation of acidic combustion gases and serious equipment corrosion damage if care is not taken in their design and material selection.

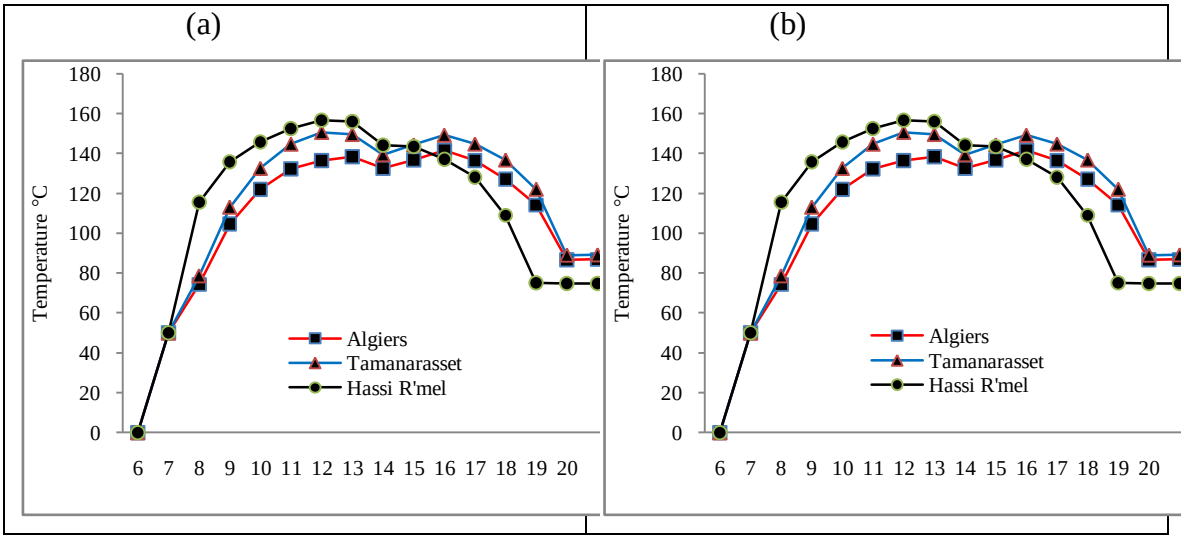

Fig.4.16. Variation of temperature in the evaporator a) case of January 29; b) case of June 2

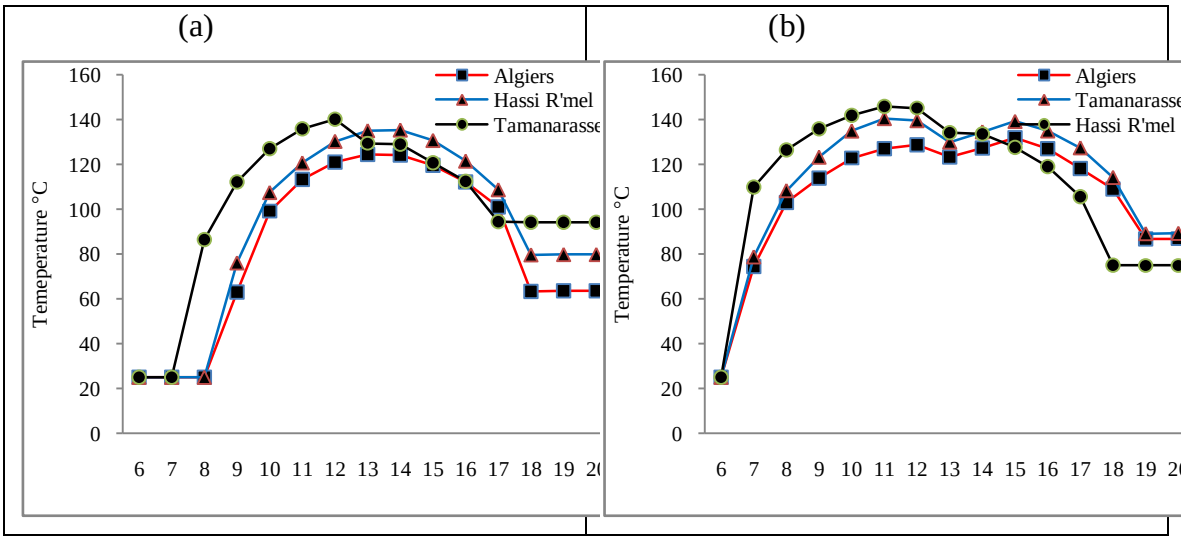

Fig.4.17. Variation of temperature in the economizer a) case of January 29; b) case of June 2

In order to assess the performance of the HRSG, the enthalpy at its outlet is estimated for three sites and for both the months of January and June. This HRSG outlet enthalpy represents the inlet enthalpy of the turbine. The enthalpy depends on the month as well as on the site. It is minimum value is the lowest in Tamanrasset for the month of January. For June, the difference between the different values of the enthalpy, more particularly between the site of Tamanrasset and Hassi R'mel is very small fig.4.18.

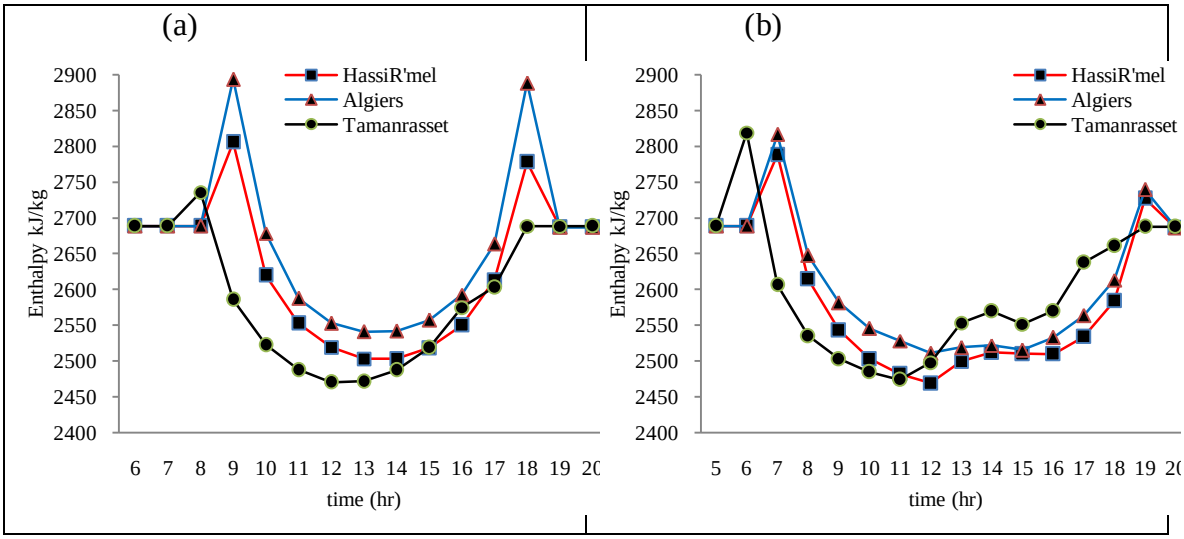

Fig.4.18.variation of the turbine inlet enthalpy a) case of January 29; b) case of June 2

c. Turbine

in order to assess the turbine performance, an analysis of its outlet enthalpy as well as its power output and efficiency is necessary.

The turbine outlet enthalpy for the different sites and for both months is reported in Fig.4.19. It can also be notice that the difference between the outlet enthalpy of the different sites is more important in January than it is in June.

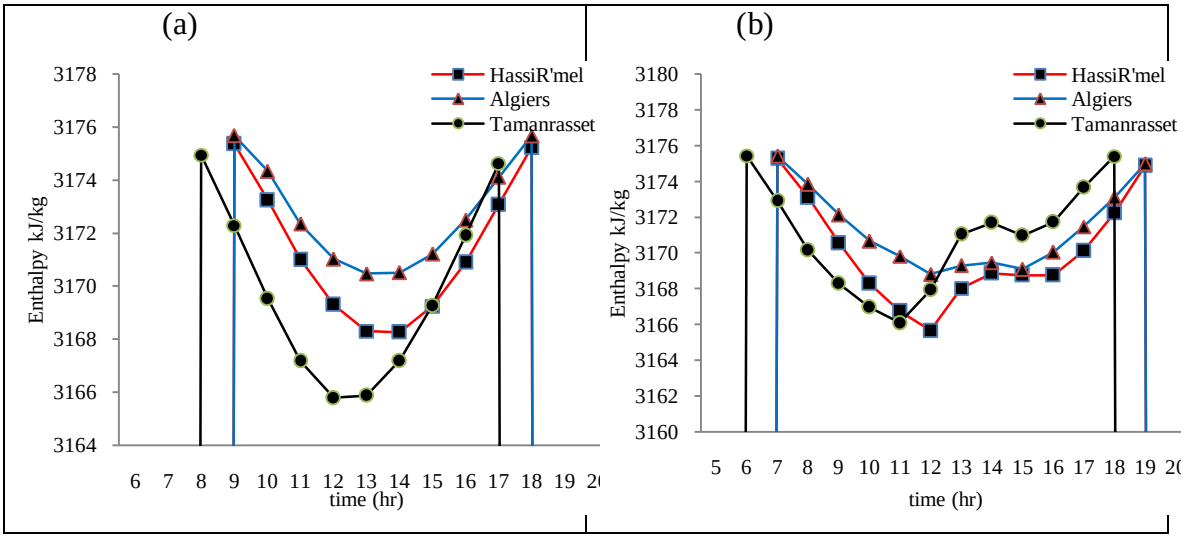

Fig.4.19.variation of the turbine outlet enthalpy a) case of January 29; b) case of June 2

Moreover, as we can seen in Fig.4.20, the difference between the turbine outlet and inlet enthalpy is more important most of the time for the month f or the site of Tamanrasset. This is an indication of higher performance.

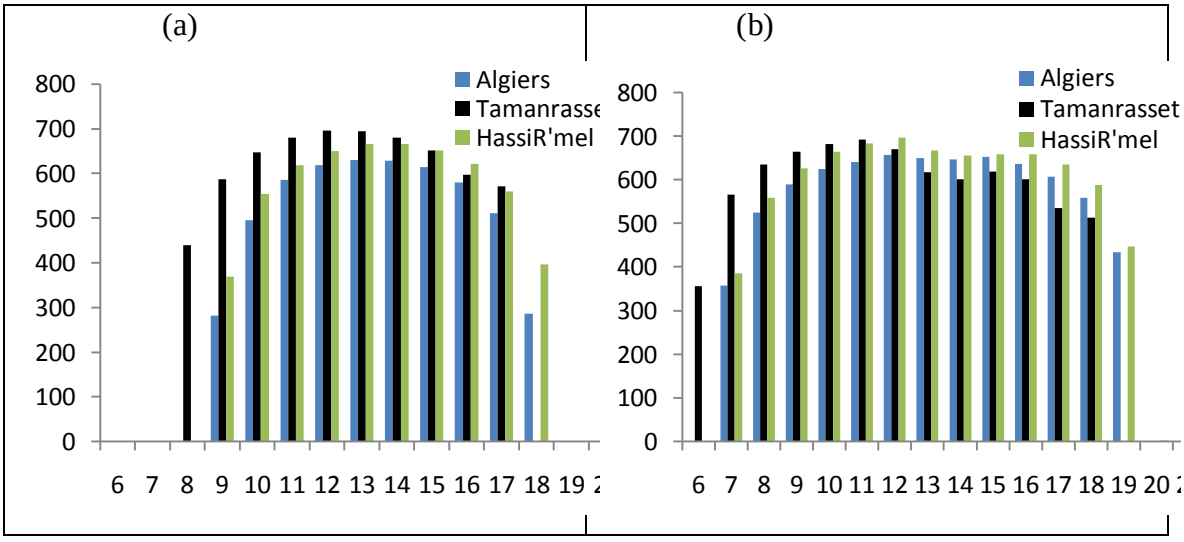

Fig.4.20.variation of , the difference between enthalpy $h_{out} - h_{in}$ a) case of January 29; b) case of June 2

The turbine generated power is shown in Fig.4.21 . From this figure, it can be seen, as expected from the higher DNI, that the generated power is more important in June. In January, the largest maximum turbine generated power is obtained in Tamanrasset with a value of 2.92 MW. For June the maximum turbine generated power is obtained in Hassi R'mel with a value of 2.96 MW. Moreover the difference in generated power is more important in January than it is in June. By comparison to Algiers, the generated maximum power is 43 % higher in Tamanrasset and 55 % higher in Hassi R'mel.

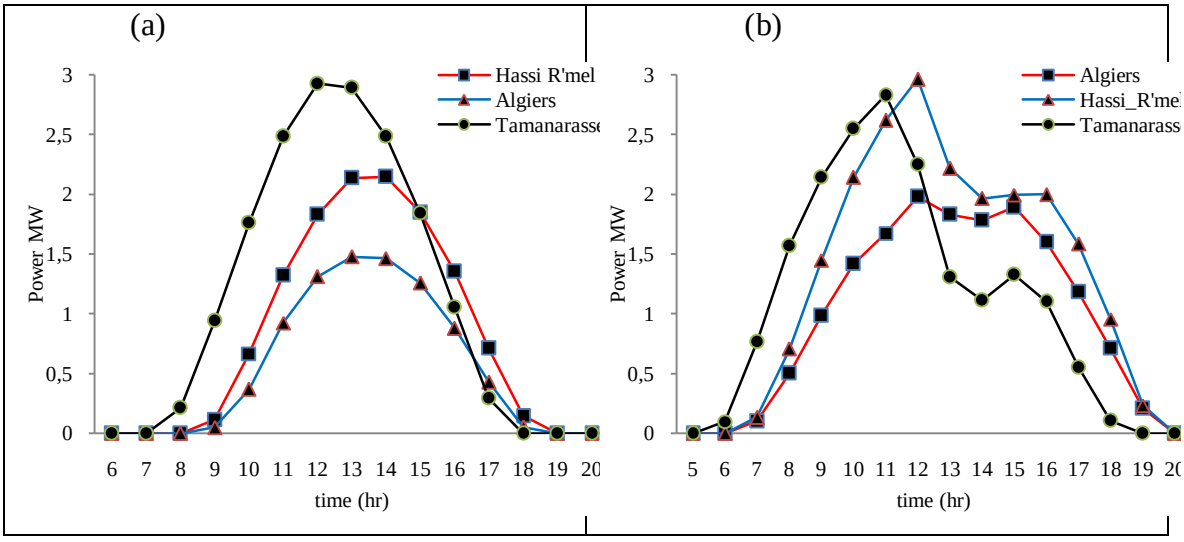

Fig.4.21. Variation of turbine power a) case of January 29; b) case of June 2

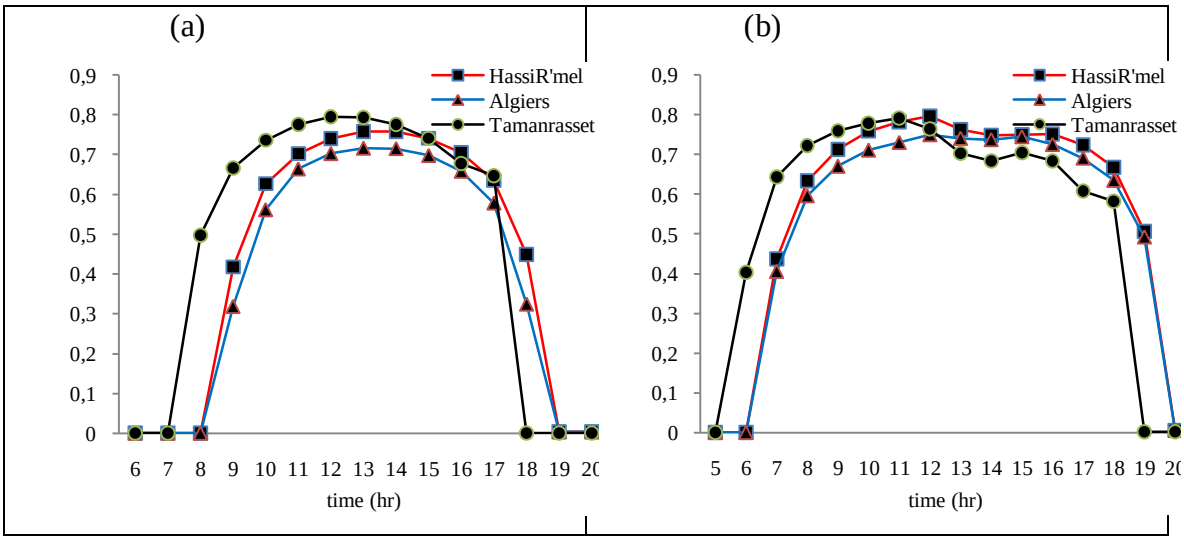

Fig.4.22.Steam turbine Efficiency a) case of January 29; b) case of June 2

To keep the power generation constant over the operation time, a thermal storage unit is used. Fig.4.23 shows the system configuration. The simulation results for the most favorable day and the most unfavorable day are shown in Fig.4.24.From this figure, it can be seen that the power output is constant during all the system operation. This is the aim sought by the storage unit.

This model describes a concrete thermal storage for single phase fluid (HTF, water). It consists of parallel equally spaced tubes in concrete with HTF flowing through in two possible directions:

- flow down (normally charge flow entering hot)
- flow up (normally discharge flow entering cold).

The model includes thermal capacity of concrete mass, thermal capacity of HTF and thermal loss of concrete to environment. It does not include thermal capacity of (steel) pipe in concrete. Convective and conductive heat transfer perpendicular to flow direction are considered. Axial conduction are not included. The number of nodes in flow direction can be chosen deliberately (10 nodes are normally sufficient).

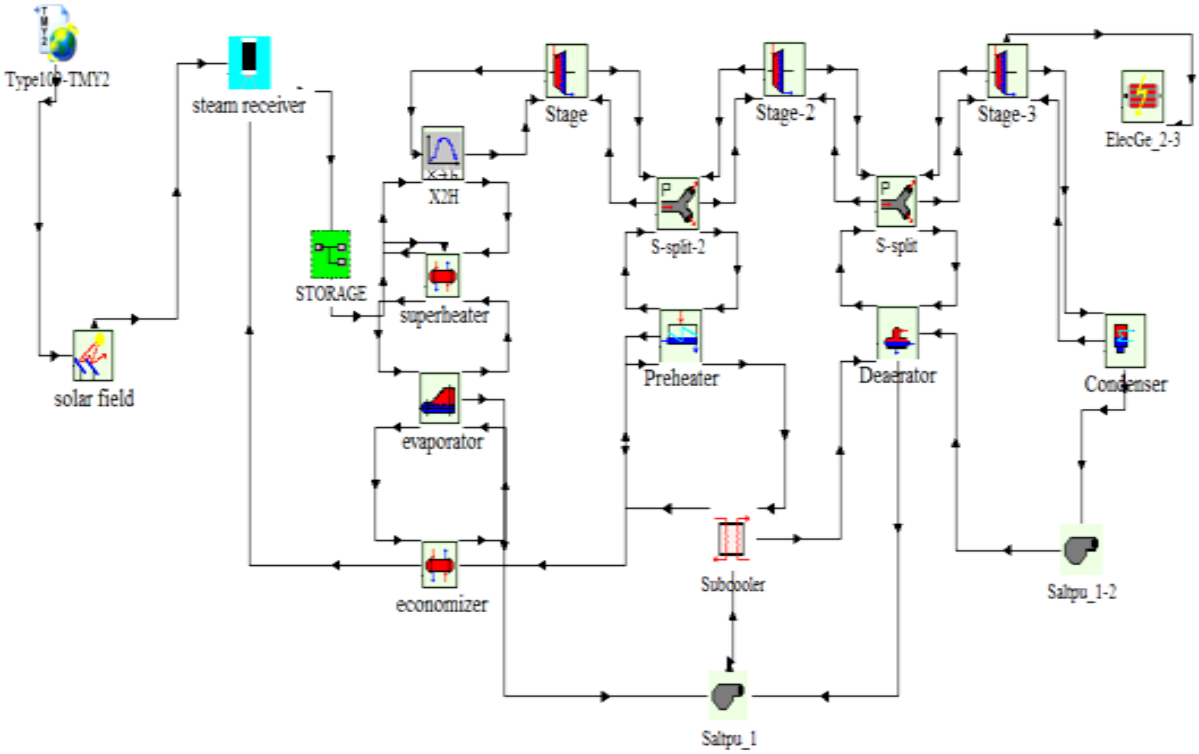

Fig.4.23.TRNSYS model for simulation of solar power tower Steam Rankine case with thermal storage

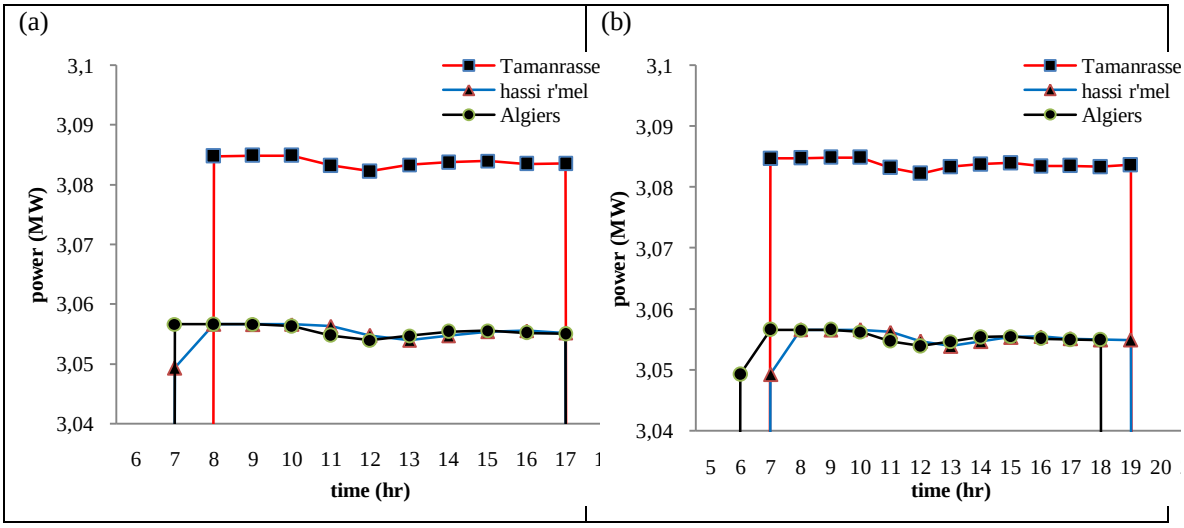

Fig.4.24. Variation of turbine power a) case of January 29; b) case of June 2

4. Economic assessment

In electrical power generation, the distinct ways of generating electricity incur significantly different costs. Calculations of these costs at the point of connection to a load or to the electricity grid can be made. The cost is typically given per kilowatt-hour or megawatt-hour. It includes the initial capital, discount rate, as well as the costs of continuous operation, fuel, and maintenance. This type of calculation assists policy makers, researchers and others to guide discussions and decision making.

The levelised cost of electricity (LCOE) is a measure of a power source which attempts to compare different methods of electricity generation on a consistent basis. It is an economic assessment of the average total cost to build and operate a power-generating asset over its lifetime divided by the total energy output of the asset over that lifetime. The LCOE can also be regarded as the minimum cost at which electricity must be sold in order to break-even over the lifetime of the project generally given by :

$$\text{LCOE} = \frac{\text{sum of costs over lifetime}}{\text{sum of electrical energy produced over lifetime}}$$

A technical study shows that the Rankin cycle system is more efficient than a Brayton cycle. In this part, the economic performance of the two technologies at all the sites under consideration is investigated. The model used in this investigation is based on the one used by Carapullecci [9-10]. However in the present work, the cost of CO2

emission cost is included in the cost of electricity production. The LCOE production is given by:

$$LCOE = \frac{TCR\ .CCF}{Q\ h_{eq}} + \frac{O\&M}{h_{eq}} + c_{fuel}\,.\,q_{fuel} + SC\_CO2.q_{CO2} \quad (27)$$

4.1.The Total Capital Requirement

Was determined by adding pre-production cost and inventory capital, The general TCR determination procedure is illustrated in Table.4.6& table.4.7

Table.4.6. Available Gross Costs of power Rankine generation

TCR estimate summary	**U.S $**
Civil/Structural	820 000
Steam turbine	1 600 000
HRSG	300 000
Electrical	472 000
piping	320 000
Indirect Costs	460 000
Engineering and home office Costs	626 000
heliostat field cost	170 $/m²
	4760000
Tower and receiver cost	754.3 $/m²
	565725
Total plant cost	**9 923 725**

Table4.7. Available Gross Costs of power Brayton generation

TCR estimate summary	**U.S $**
Civil/Structural	400 000
Gas Turbine	3 860 000
Electrical	550 000
piping	140 000
Indirect Costs	280 000
Engineering and home office Costs	630 000
heliostat field cost	170 $/m²
	4760000
Tower and receiver cost	754.3 $/m²
	565 725
Total plant cost	**1022000**

4.2.Operation and Maintenance Cost

The O&M cost was calculated next its includes fixed and variable components.

Fixed O&M cost incorporates:

- Operating labor
- Maintenance labor and materials
- Administration and support labor

Variable O&M cost is composed of:

- Reagent
- Disposal(by-product credit given)
- Steam
- Electrical energy

Operating and maintenance costs, O&M in equation (27), include fixed costs, variable costs and insurances. The fixed O&M cost components were estimated as 20 $/kW-yr, They are evaluated on the basis of assumptions summarized in Table4.8.

4.3.Fuel price

Fuel costs can be calculated considering the specific fuel consumption, q_{fuel} in equation (27) and the fuel price, c_{fuel} . The first is a result of the thermodynamic simulation of the air configuration plant carried out through the GateCycle model; the second is an input related to the natural gas market. The natural gas price has fluctuated substantially during the last two decades, ranging from about 2 to 8 $/GJ. In the following analysis, the natural gas price is assumed to be 5 $/GJ in the base case; however, effects of lower or greater fuel prices (in the range 2-8 $/GJ) on the optimization of air configurations will be also investigated.

4.4.Capital charge factor

The capital charge factor CCF referred to as annuity present worth factor and given as :

$$CCF = \frac{i(1+i)^n}{(1+i)^n - 1} \quad (28)$$

Where:

(n) Is the number of periods

(i) The interest rate

The choice of interest or discount rate (i) is crucial it depends on:

- the relative values of equity and debt financing
- whether the debt financing is less than the life of the plant
- tax rates and tax allowances (which vary from one country to another)
- inflation rates

4.5.Results

The different parameters used in this study are reported in Table.4.8.

Table.4.8. Main features economic parameters

Design parameter		**Value**
Life of plant (years)		25
Operating hours (h/year)		6000
Specific investment cost for solar field ($/m²)		130
Specific investment cost for tower with receiver ($/m²)		500
discount rate ($)		0.1
CCF ($)		0.11
Steam Configuration	HRSG ($/m²)	170
	Steam turbine ($/kWh)	340
	Storage ($/kWht)	30
	Civil/Structural ($/kWh)	273
	Engineering and home office Costs($/kWh)	208
	Indirect Costs($/kWh)	417
	O&M($/year)	20
Air configuration	Gas Turbine($/kWh)	772
	Civil/Structural($/kWh)	80
	Engineering and home office Costs($/kWh)	126
	Indirect Costs($/kWh)	194
	O&M($/year)	60
	c_{fuel} ($/GJ)	5
	SC-CO_2 ($/ton)	30

The results are reported in Fig.4.25 for both technologies and for all the sites under consideration. For the steam technology, as shown in Fig4.25, the LCOE is the higher for the production at Tamanrasset and the lowest at Hasssi R'mel.

By comparison to Hassi R'mel, the cost of electricity production is about 12 % higher in Algiers and 16.3% higher in tamanarasset . The cost of electricity in Tamanrasset is about 3.9% higher than that of Algiers

Concerning the Air technology and as shown in the same figure, the LCOE is the lowest at Hassi R'mel . By comparison to Hassi R'mel the cost of electricity production using this technology is about 3.1% more expensive in Algiers but only 0.7% more expensive in Tamanarasset. The LCOE is about 2.4% higher in Algiers by comparison to Tamanrasset.

Now, carrying a comparison between the two technologies, it can be seen from Fig.24 that the cost of electricity production using steam technology is how more expensive. The cost in the steam technology is higher due mainly to the much lower capacity factor of the system. However, indications are that the steam technology will be competitive with the air technology with improvement in technology and as a result of the learning curve process [11].

It can also be noticed that the difference in electricity production cost between the two technologies depends on the site. It can be noted that this difference is only 3.4% for the site of Hassi R'mel. But it is much higher for the two other sites. It is about 11% in Algiers and 16.4% in Tamanrasset. This could be explained by the highest DNI and the largest sunshine duration that Hassi R'mel enjoys.

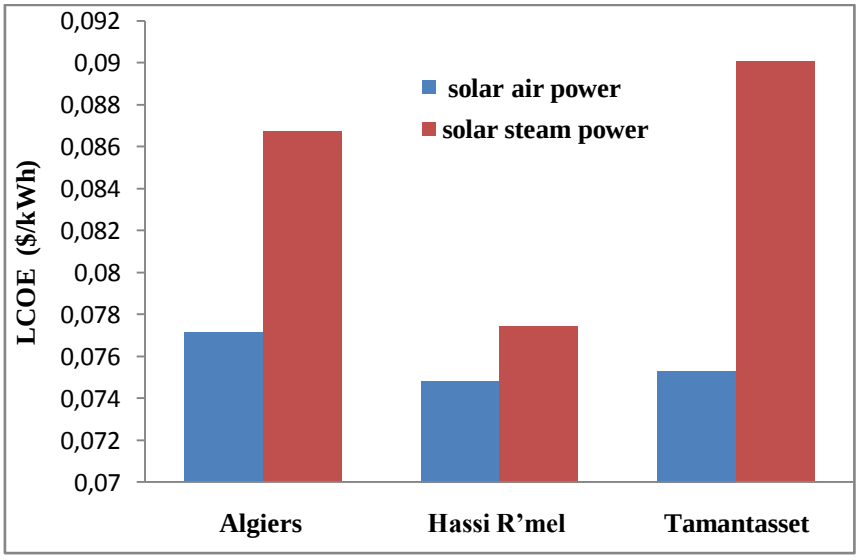

Fig.4.25. the deferent value of the LCOE

5. Conclusion

Using TRNSYS-STEC, we have simulated the performance of a solar power tower with two receiver configurations, namely, a water/steam receiver and a volumetric air receiver. We have investigated the performances of the solar power tower under Algerian climate in order to determine and select the most suitable technology that should be implanted in the future solar power plants.

The study has pointed out that the volumetric air technology is more suitable for Algeria than the state-of-the-art water/steam technology when it is coupled to a Rankine cycle.

The simulation of annual performance has shown that the overall efficiency and the solar electricity ratio could reach 32 % and 85 %, respectively. Moreover, such a hybrid concept is capable of saving about 2,000 T/year of fossil fuel.

Algeria is making concerted efforts to harness its renewable energy potential despite being a hydrocarbon-rich nation; Algeria's renewable energy program is one of the most comprehensive in the MENA region, and the concerned authorities are determined to secure investments and reliable technology partners for the ongoing and the upcoming projects.

Reference

[1] Peter Schwarzbözl. A TRNSYS Model Library for Solar Thermal Electric Components (STEC) A Reference Manual, Release 3.0, 2006.

[2] Hu, Eric, Baziotopoulos, Con and Li, Yuncang 2002, Solar aided power generation from coal fired power stations: THERMSOLV software. in AUPEC 2002 : conference proceedings, Monash University, Melbourne, Vic., pp. 1-7.

[3] F.M.F. Siala, M.E. Elayeb. Mathematical formulation of a graphical method for a no-blocking heliostat field layout. Renewable Energy 23 (2001) 77–92

[4] Zhihao Yao, Zhifeng Wang, Zhenwu Lu, Xiudong Wei. Modeling and simulation of the pioneer 1 MW solar thermal central receiver system in China. Renewable Energy 34 (2009) 2437–2446

[5] Nils Ahlbrink, Boris Belhomme, Robert Pitz-Paal. Modeling and Simulation of a Solar Tower Power Plant with OpenVolumetric Air Receiver. Proceedings 7th Modelica Conference, Como, Italy, Sep. 20-22, 2009

[6] Peter Heller, Markus Pfander , Thorsten Denk , Felix Tellez, Antonio Valverde, Jesu´s Fernandez, Arik Ring. Test and evaluation of a solar powered gas turbine system. Solar Energy 80 (2006) 1225–1230

[7] Mark Schmitz, Peter Schwarzbozl, Reiner Buck, Robert Pitz-Paal. Assessment of the potential improvement due to multiple apertures in central receiver systems with secondary concentrators. Solar Energy Solar Energy 80 (2006) 111–120.

[8] T. Fend, R.-P. Paal, O. Reutter, J. Bauer, B. Hoffschmidt. Two novel high-porosity materials as volumetric receivers for concentrated solar radiation. Solar Energy Materials & Solar Cells 84 (2004) 291–304

[9] Roberto Carapellucci and Lorena Giordano. A Genetic Algorithm for Optimizing Heat Recovery Steam Generators of Combined Cycle Power Plants. Proceedings of the ASME 2011 International Mechanical Engineering Congress & Exposition. IMECE2011-63703

[10] Roberto Carapellucci, Lorena Giordano. A comparison between exergetic and economic criteria for optimizing the heat recovery steam generators of gas-steam power plants. Energy 58 (2013) 458-472

[10] Peng Zou , Qixin Chen, Yang Yu, Qing Xia, Chongqing Kang. Electricity markets evolution with the changing generation mix: An empirical analysis based on China 2050 High Renewable Energy Penetration Roadmap. Applied Energy 185 (2017) 56–67.

Conclusion

A detailed thermal performance comparison between the most mature central receiver solar power technologies has been carried out under Algerian climate. These two technologies are the Brayton cycle based configuration with an open air receiver and the Rankine cycle based configuration with a water/steam receiver. Meteonorm has been very helpful to get precise information about climate data in particular solar radiation intensity.

The modeling of the two configurations has been carried out using the software TRNSYS-STEC This concerns the solar field as well the steam turbine with the water/steam tubular receiver in the case of the Rankine cycle based configuration and the gas turbine with volumetric air receiver in the case of Brayton cycle the has been presented and results analyzed.

An analysis of the solar radiation indicates that, as shown from the data for the representative sites of the different climate conditions in Algeria, the irradiance level is higher than the minimum level required for a viable exploitation of concentrating solar plant.

The modeling results of the solar field show that the site of Tamanrasset, though exhibiting the largest collected solar irradiance, has a collected irradiance that does not increase as much as the other two sites. This is due to the specific climate of the Tamanrasset region. Indeed, it is characterized by dry winters and somehow humid summer. Nonetheless, it has been found that the central receiver solar thermal power plants are strongly affected by the solar radiation intensity.

Concerning the receiver, the modeling results show that it is possible to reach much higher temperature with the open air receiver than with the water/steam receiver. For the case of the water/steam receiver the temperature is 350 °C. On the other hand for the

case of open air receiver., the temperature peaks at 1000 °C around the solar noon in January in Tamanrasset and in June in Tamanrasset and Hassi R'mel. But this temperature remains most of the time below the needed temperature of 1000°C for an optimal performance of a Brayton cyle. A back up energy source is then necessary. In the present case, a combustion chamber is considered. An analysis of the fuel needed to bring the temperature to 1000 °C indicates that these needs are less important for Tamanrasset and Hassi R'mel than in Algiers. The fuel contribution is fairly sizable in January in Algiers.

In the case of gas turbine with volumetric receiver, results indicate that the higher the DNI the higher the performance of the gas turbine. In the case of steam turbine with water/ steam receiver, operating with relatively lower temperature, could achieve higher thermal efficiency.

In the present case, the modeling results have shown that the steam turbine with water/steam receiver is more suitable than the gas turbine with volumetric receiver especially under lower solar radiation intensity. The gas turbine requires higher operating temperatures which are usually difficult to reach throughout the year.